

UNCLASSIFIED

AD 416309

DEFENSE DOCUMENTATION CENTER

FOR

SCIENTIFIC AND TECHNICAL INFORMATION

CAMERON STATION, ALEXANDRIA, VIRGINIA



UNCLASSIFIED

NOTICE: When government or other drawings, specifications or other data are used for any purpose other than in connection with a definitely related government procurement operation, the U. S. Government thereby incurs no responsibility, nor any obligation whatsoever; and the fact that the Government may have formulated, furnished, or in any way supplied the said drawings, specifications, or other data is not to be regarded by implication or otherwise as in any manner licensing the holder or any other person or corporation, or conveying any rights or permission to manufacture, use or sell any patented invention that may in any way be related thereto.

N-63-4-6

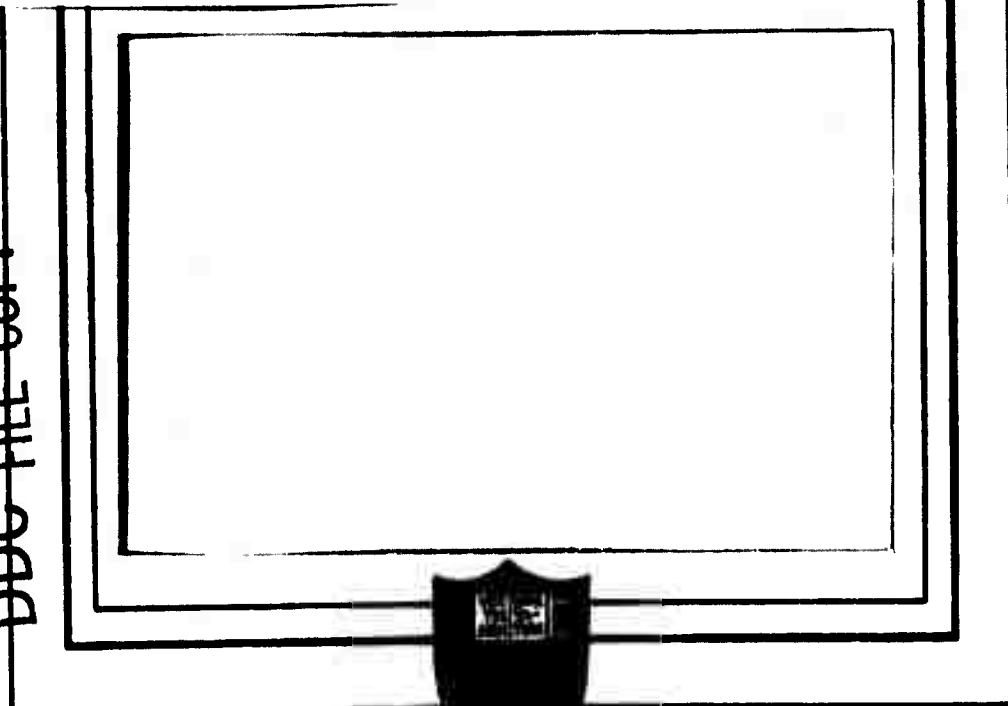
5716 300

0

AD NO. 416309

416309

DDC FILE COPY



DDC
FORMED
SEP 13 1963
TISIA B

PRINCETON UNIVERSITY

11 10.10

⑤ 716 300

④ \$10.10

⑦-⑧-⑨ NA

⑫ 113 p.

⑬ NA

⑭-⑮ NA

⑯-⑰ NA

⑱-⑲ NA

⑳ W

⑥ THE EFFECT OF VACUUM ON
THE SHEARING RESISTANCE
OF IDEAL GRANULAR SYSTEMS,

⑩ by
Gerald D. Sjaastad.
Captain,
~~United States Army~~

⑪ NA Submitted in partial fulfillment of the requirements
for the degree of Doctor of Philosophy from
Princeton University, June 1963

Gerald D. Sjaastad Author

Hans F. Kirkuborn Advisor

⑫
Submitted June 1963,

PREFACE

This thesis describes the initial phase of a research program on the frictional behavior of granular systems being conducted in the Department of Civil Engineering at Princeton University. This initial phase was carried out by the writer of this thesis during the period 1961-1963 under the supervision of Dr. Hans F. Winterkorn, Professor of Civil Engineering at Princeton University. The work was generally motivated by the apparent absence of a definitive approach to the lunar soils engineering problem. This aspect is emphasized, therefore, throughout the thesis. ~~Because~~ of the ~~vast~~ uncertainty regarding the nature of the moon's surface material this research is aimed primarily at learning more about the frictional behavior of ideal individual particle media. It is expected that results obtained will be applicable to natural lunar soils or to handling of materials on the moon's surface. If this does not prove to be the case, the study should still contribute to the knowledge of the behavior of granular soils.

In this respect the program on the frictional behavior of granular media is coordinated with the continuing research in non-cohesive soils (macromeritics) being conducted by Professor Winterkorn.

ACKNOWLEDGEMENTS

The author wishes to express sincere appreciation for the confidence shown and for the guidance given throughout the past two years by Professor Hans F. Winterkorn.

The author is grateful to Professor Norman J. Sollenberger for the active interest shown and for the support given to this research project. The efforts of Professor Gregory P. Tschebotarioff in reviewing and commenting on early outlines of this work and in acting as a reader of the thesis are appreciated. The author wishes to thank Professor Werner E. Schmid for reviewing the draft and for serving as a reader of the thesis.

Special appreciation is expressed to Dr. Ahmet S. Cakmak for his keen interest in the work and for specific help on many problems.

Acknowledgement is made to: Mr. Robert Stevenson for the patient performance of numerous tasks in direct support of this thesis.

The United States Air Force for allowing the author to pursue study and research at Princeton University.

My wife, Barbara, for her continuing help, including the typing of this dissertation.

TABLE OF CONTENTS

	<u>Page</u>
PREFACE	11
ACKNOWLEDGEMENTS	111
TABLE OF CONTENTS	iv
LIST OF FIGURES, TABLES AND PLATE	viii
 CHAPTER I: Introduction	 1
Lunar Soils - The General Problem	1
Previous Experimental Lunar Soil Studies	3
A Basic Approach To Lunar Soils Research	6
Model Materials	8
Properties	9
Lunar Effects	9
Princeton Research Program in Frictional Behavior of Granular Systems	13
Initial Phase	13
Specific Objectives	13
Method of Testing	14
Later Phases	16
 CHAPTER II: The Relationship Between Shear Strength And Interparticle Friction	 17
General	17
Brief Resume of Existing Analytic Solutions	18

	<u>Page</u>
Solutions Not Allowing for Changes in Porosity	18
Caquot's Solution	18
Bishop's Solution	19
Dantu's Solution	20
Scott's Solution	20
Solutions Allowing For Changes in Porosity	22
Idel's Solution	22
Wittke's Solution	23
Spencer's Solution	24
Other Solutions	24
A Simplified Solution for the Tan ϕ Versus f Relationship	24
Assumptions	25
Solution	27
Most Dense Packing	27
Loosest Packing	35
Values at Intermediate Porosities	36
Review of Existing Data	37
 CHAPTER III: The Effect of Particle Size on the Strength of Granular Materials	 40
The Significance of Particle Size in the Argument of This Thesis	40
Existing Beliefs Concerning the Relationship Between Grain Size and Shear Strength	41

	<u>Page</u>
Review of Existing Data Favoring a Particle Size Effect	42
Review of Data Supporting Independence of Strength from Particle Size	47
Particle Size Experiments Performed as a Part of This Research Project	49
First Series of Tests	50
Materials and Apparatus	50
Performance of Tests	52
Discussion of Results	54
Second Series of Tests	56
Effect of Gradation on Shear Strength of Granular Materials	58
Summary	64
 CHAPTER IV: Apparatus, Tests and Results of Experimental Program	 66
Apparatus	66
Load Cell	68
Heating and Heat Control Equipment	72
Vacuum Equipment	73
Modifications	75
Materials	76
Tests and Test Results	77
Tests on Glass Spheres	77
Tests on Nickel Shot	84
Tests in Atmosphere	86
Test on Mineral Friction	87

	<u>Page</u>
CHAPTER V: Summary and Conclusions	89
Conclusions	90
CHAPTER VI: Additional Considerations and Suggestions for Further Study	92
Soil Cohesion in the Lunar Environment	92
Porosity	94
Particle Shape	96
Gradation	97
Theoretical Method for Determining the Stress-Strain Diagram for Granular Materials	97
Conductivity Relationships	100
Behavior of Flocculated or Dendritic Structures	102
ADDENDUM	104
VITA	106
BIBLIOGRAPHY	107

LIST OF FIGURES, TABLES AND PLATE

<u>Figure</u>	<u>Following Page</u>
1 Tan ϕ vs f Relationships Which do not Consider Porosity	19
2 Idel's Solution, tan ϕ vs f	23
3 Wittke's Solution, tan ϕ vs f	23
4 Spencer's Solution, tan ϕ vs f	24
5 Geometry of Failure Path I	28
6 Geometry of Failure Path II	31
7 Tan ϕ vs f Relationships for Extreme Failure Paths	33
8 Tan ϕ vs f, Based on Equal Probability and Relative Density	34
9 Tan ϕ vs f, Based on Equal Partition of Energy and Relative Density	35
10 Sample Calculations	36
11 Tan ϕ vs f, Based on Equal Probability and Macromeritic Equation	36
12 Comparison of Existing Data with Equal Partition Solution	37
13 Size and Strength Relationships for Glass Spheres	54
14 Grain Size Analysis, 1.1 and 2.6 mm. Glass Spheres	56
15 Density, CBR Relationships, Siedek and Voss	62
16 Schematic Diagram of Apparatus	66
17 Detail of Shear Device	67
18 Results of Vacuum Tests on Glass Spheres	83
19 Results of Vacuum Tests on Nickel Spheres	85

<u>Figure</u>	<u>Following Page</u>
20 Shearing Resistance <u>vs</u> Porosity	95
21 Extended Equal Partition Solution	95
22 $\tan \phi$ <u>vs</u> f Relationship for Plate-like Particles	96
23 Load Deformation Diagrams	98
24 Development of Stress-Strain Curve	99

<u>Table</u>	<u>Page</u>
1 Extract of Size and Strength Data, Wu	44
2 Size, Uniformity and Strength Data, Zeller and Wullimann	45
3 Results of Direct Shear Tests, Kjellman and Jakobson	46
4 Results of Direct Shear Tests on Glass Shot	55
5 Strength and Uniformity Data on River Sands and Gravels, Bishop	60
6 Strength and Uniformity Data on Natural Aggregates, Chen	61
7 Results of Direct Shear Tests on Glass Spheres in Vacuum	79
8 Comparison of f and $\tan \phi$ Values for Glass	83

<u>Plate</u>	<u>Following Page</u>
1 Photograph of Apparatus	66

CHAPTER I

INTRODUCTION

LUNAR SOILS- THE GENERAL PROBLEM

While future experience may reveal as many varied problems with the surface materials of the moon as we have today with terrestrial soils the paramount question seen now is that of the lunar dust. The term "dust" as here applied refers generally to a granular material and will not be restricted to those with very fine particle size. The existence of soil forming agents that would favor granular over cohesive surface materials has been argued by several writers, and a general agreement prevails regarding the presence of some dust on the moon. While opinion varies in the extreme as to the amount of dust actually present on the lunar surface (25, 64, 66)*, it seems reasonable to expect local accumulations of some magnitude. In addition to the observed mountainous macrorelief it has been postulated since the time of Galileo that a rough microrelief is also prevalent (69). Based on this assumption one might logically expect considerable lateral variation in the quantities of dust on the moon's surface.

Allowing the presence of such local deposits three basic engineering problems can be foreseen.

Stability of such material for space craft operations and lunar base support is open to question. Here again speculation

* Numbers in parenthesis refer to similarly numbered references in the bibliography.

varies regarding the probable performance of lunar dust as a foundation soil. One school of thought (34) regards the dust layer as possibly extremely unstable with little or no bearing capacity. Some of the earlier experimental data (10) aimed specifically at the lunar problem seemed to lend support to this conclusion. Others (56, 85) favor the idea of a surface strong enough to allow normal operations.

Excavation and handling characteristics of lunar surface materials may prove to be a more formidable problem than stability. The possibility of subsurface placement of future lunar bases seems high in view of resulting attenuation of temperature and radiation extremes (64, 72, 90). Energy for accomplishment of required excavation and soil placement can be expected to be in short supply. It would seem then that dust deposits might be sought out as possible soft ground for location of subsurface lunar construction.

Construction materials for initial lunar bases will be extremely critical. Possible modification of unconsolidated dust for this use must be considered. Some ideas concerning possible utilization of local materials for construction have been advanced (22, 90).

So it seems that serious study of the lunar dust is of basic importance regardless which theory of its abundance and distribution is accepted. Once this is established as a primary problem, the question of method of study arises. Many speculative accounts based on indirect though logical evidence appear in the recent literature. While these are of fundamental importance, particularly

in the initial stages of the problem, it seems further development along these lines is strictly limited. The overall question of the surface, environment and difficulties of operation have been well summarized by many writers. Several discerning papers concerning probable behavior of lunar soils have been presented (36, 63, 83). Existing knowledge of soil science has been applied to a more specific review of the lunar surface material and possible methods of stabilization (91). Little purpose can be served by further pursuing this approach, nor is it the object of this thesis to report these conjectures in detail as they are well recorded in recent literature.

The conclusion then is that fundamental experimental data is the quantity most needed at this time. This lack of data is cited with due regard for optical, radar and other scientific studies which have placed the problem in perspective. Due note must be taken also of the several previous experimental works aimed explicitly at learning more about possible engineering behavior of lunar soils. These are briefly reviewed in the next section.

PREVIOUS EXPERIMENTAL LUNAR SOILS STUDIES

While a large volume of speculative literature concerning probable lunar soil conditions has been written, only a minor effort in experimental research has been reported. An attempt will be made to present a brief review of such experimental work as is known.

The account here offered may not be complete due to the failure of such reports to appear in the more widely read engi-

neering and scientific journals. It seems that no report has appeared in the standard soil mechanics or civil engineering literature. While this to a degree signifies a lack of interest on the part of civil engineers it is noted that very little is given on this subject in other journals. Beyond a doubt additional interesting work has been completed with the results remaining unavailable to the generally interested reader.

One of the earliest known efforts was that of Dr. Dwain Bowen of North American Aviation (9). His work consisted of comparing the penetration of a falling steel ball into fine (0.2 micron) alundum powder under atmospheric and vacuum conditions. He reported that the ball penetrated to the bottom of the dust in air, but was stopped at the surface in the vacuum test. The difference was attributed to lubricating action of the air. Since further details of the test were not reported, very little can be concluded from Dr. Bowen's results. This is particularly true in view of opposite results found in similar tests by Professor G. Kennedy, of the University of California at Los Angeles. Ryan (63) reports that Professor Kennedy found no difference in penetration between air and vacuum conditions.

The first widely known formally reported results are those concerning tests conducted at the University of Michigan (10). These tests again attempted to compare the dynamic penetration resistance of granular materials under normal atmosphere and vacuum conditions. A definite increase in penetration (decrease in strength) was found under vacuum conditions. These results are also impossible to evaluate without additional data on the

testing program. A soft vacuum (estimated at less than 1 mm. Hg.) was used indicating that the major effect was probably the removal of entrapped air. No data on void ratio or porosity were reported although this is well known as a major factor in determining the resistance of granular materials.

A series of dynamic penetration tests on various lunar dust models was run at Wright-Patterson Air Force Base, Ohio, in 1961 (32). These tests were also nonconclusive. The trend of data indicated an increase in penetration depth and crater diameter with decreasing pressure (to 10^{-5} mm. Hg.). Because of the large number of unknown factors (for instance void ratio or porosity which was not reported) it is impossible to evaluate the above reported results. Such items as failure to bake-out, unknown air displacement effects, and very large particle surface areas with resulting small diameter pores undoubtedly contributed to the failure to achieve definite results. One interesting result indicated a consistently smaller penetration when using an ambient atmosphere of carbon dioxide-hydrogen in place of the air-helium mixture used in most of the tests. On the other hand this might have been due to a slight difference in porosity in the various tests. It is a factor, however, that should be investigated further.

Partial results of static penetration tests at Grumman Aircraft Engineering Corporation, have been recently reported (36). These tests were performed on a fine (2-100 micron) commercial pumice. In this case an increase in penetration resistance with decrease in pressure was evident. While details on soil density were not given it seems that reasonably comparable void ratios

were established by a uniform shaking after each test. A long prebake (300°F- 2 weeks) undoubtedly contributed to the general effect. Minimum pressures were 10^{-6} and 10^{-8} mm. Hg.

Static and dynamic penetration tests performed at Armour Research Foundation, confirmed the results cited above (62). These tests were performed on a white silica flour with 85% of the particles in the 2-40 micron range. Void ratios (1.02-2.45) were controlled and reported as an integral part of all results thereby introducing basic soil mechanics into the lunar surface materials problem. As in the Grumman tests a prebake (110°C- 18 hours) facilitated the pumping (to 10^{-7} mm. Hg.). Very significant increase in static penetration resistance was noted at pressures below 10^{-5} mm. Hg.. Dynamic penetration resistance increased more gradually and changes were at higher pressures. The effect of vacuum on dynamic penetration resistance was significantly greater at higher densities. For some unknown reason this was not evident in the static tests. As will be pointed out in Chapter VI this result should be expected for static tests in particular.

An attempt has been made to list these works in a chronological order. A favorable trend in approach and results can be seen. This will help to clarify one of the disadvantages of being active early in a new field of study*.

A BASIC APPROACH TO LUNAR SOILS RESEARCH

The experimental efforts reviewed in the preceding section represent the pioneer work in a new field of civil engineering. The deficiencies in the methods used are perhaps more apparent

* See Addendum.

now that some actual experimental work has been carried out than at the time these studies were formulated.

If further effort in this direction is to be profitably applied, however, a more fundamental study with definite, meaningful objectives is in order. One approach to such a fundamental study is now offered. It is not suggested as the only possible method, or even the most favored, but it seems to follow directly once the previously outlined general lunar soils problem is accepted.

Because of the rather primitive state of knowledge in the area under consideration and because results of any single individual project can be expected to be modest, the following criteria must govern the study under consideration:

1. It must be basic and sufficiently fundamental to apply regardless of the actual detailed condition that might be encountered.
2. It should be of a nature such that it may fit into any existing or future overall coordinated effort in the field.
3. It should be sufficiently specific so that results of value can be reasonably expected.

The basic approach outlined herein and the specific program reported in this thesis are formulated in accordance with these criteria. In determining more specifically the nature of a basic experimental lunar soils study three questions must be answered:

1. What material should be used as a laboratory model?
2. Which properties should be studied?

3. Which effects or variables of the lunar environment should be considered?

MODEL MATERIALS

Tendencies to date seem to center on speculation of the most probable lunar soil with regard to composition and grain size distribution. Though a sampling of opinion may indicate a general trend of agreement toward siliceous material ranging in size from sub-micron to about a millimeter*, this approach is rejected at this time. This is done primarily because such a premise would serve by its nature, to defeat the previously outlined criteria. At least four of the five basic soil forming factors identified by Jenny (46) are active on the lunar surface. These are; time, climate, parent material and topography. There is no reason for expecting a uniformity in the effect of each of these factors over the moon's surface. One should anticipate, on the other hand, considerable variation in soil forming factors from one lunar location to another and hence, non-homogeneity of surface materials. Rather than restrict ourselves then to a particular model of the lunar soil it seems more sound to recognize that our interest is in the behavior of granular media in general under expected lunar conditions. Accordingly, an ideal material is proposed for initial studies. This serves to eliminate some of the variables and hence reduce the indeterminacy of the problem. Further, this should allow

* An argument is also offered for a rigid surface of porous, sintered metallic dust (82), another for a surface of large, sharp edged fragmented rock (1, 54).

application of the results, at least in a qualitative manner, to a wider range of possible lunar materials.

PROPERTIES

While all characteristics of the lunar soil will eventually be of interest to the engineer a logical choice for initial study is shear strength. This is the property that will govern its stability and to a large degree its excavation and handling characteristics. Shear strength is recognized as a basic factor in trafficability (2). Further, it is a property with which engineers are familiar and are able to apply directly to evaluation and design problems.

LUNAR EFFECTS

Possibly four differences between terrestrial and lunar conditions might be mentioned as predominant:

- 1. Atmosphere
- 2. Gravity
- 3. Radiation
- 4. Temperature

Effect of atmosphere is selected for this study as one which satisfies all of the following criteria:

- 1. There is justification to expect significant effects on shear strength.
- 2. Such effects do not lend themselves to reasonably accurate analytic solutions.
- 3. Required laboratory equipment is relatively modest.

A pointed review of prevalent shear strength theory for granular soils will bring out the reasons why one may expect a significant change in this property with changing atmosphere. The shear strength of a granular material may be expressed as (77):

$$S = N \tan \phi$$

where

N = the normal force on the shear plane,

ϕ = the angle of internal friction or angle of shearing resistance of the aggregate..

ϕ is known to be a function of several variables, especially:

1. The coefficient of friction between individual grains.
2. Particle shape and size distribution.
3. Void ratio* or packing factor of the aggregate.

If, in keeping with the previously mentioned concept of an ideal material, particle size, shape, size distribution and void ratio are fixed, then ϕ becomes essentially a function of the coefficient of friction between individual grains.

The distinction between $\tan \phi$ which is a property of the aggregation or system of particles and the coefficient of friction between individual grains must be made clear. The coefficient of friction acting between individual grains will be designated as f and is the ratio of tangential force to applied normal force necessary to cause sliding between two surfaces in contact. It is the elementary (Amontons or Coulomb) friction described in any elementary physics text. It might be termed "friction without interlock" as it is characterized

* The ratio; volume of void space: volume of solids.

by absence of any visible interlock between the two surfaces.

In fact, however, interlock on the microscopic scale is known to exist and herein lies the basis for expecting a change in f , hence in $\tan \phi$, with atmosphere in a granular system. Without reviewing in detail the recent excellent work on friction which is well covered elsewhere* a brief physical picture will be offered. Any apparently flat smooth surface is known to be, on the microscopic and sub-microscopic scales, in actuality very rough. Consequently the gross area in common between two touching flat smooth surfaces is an apparent area of contact only. The real contact area is much less and involves only the tips of the asperities or peaks of the two surfaces. Resistance to sliding can be related to the yield strength of the materials and the true area of contact (7, 39). Within limits, the true area of contact will vary with normal load and thus the gross, empirical laws of elementary friction continue to be satisfied. These elementary concepts of friction then can still be applied as macroscopic phenomena valid within the limits of observation. One should recognize, however, that the true nature of friction is more involved than might be supposed from the elementary Coulomb laws.

With the concepts given above and the application of basic physical chemistry one is able to complete the picture of friction as a function of atmosphere. A clean solid surface, as a boundary between phases, possesses a free energy. In accordance with the Second Law of Thermodynamics this

* See References 7, 8 and 39.

free energy is reduced through adsorption of available molecules by the surface, forming in general a multi-molecular boundary layer. Between two smooth surfaces in apparent contact then these boundary layers act to influence frictional behavior by controlling the degree of true contact or interlock between the asperities of the surfaces. Partial or complete removal of the layers of adsorbed molecules, or their substitution by other kinds of molecules can be expected to, and in fact does*, alter the frictional behavior and change the value of the elementary coefficient of friction.

It seems logical then that changes in ambient atmosphere can be expected to alter the coefficient of friction and hence the shear strength of granular materials. This thinking is not novel but rather the logical consequence of considering as a whole the previously distinct fields of soil mechanics and low pressure physics. This concept has been generally considered in at least two previously published lunar soil studies (36, 62), and was recognized in the previously cited papers by Ryan (63) and Weil (83).

In summary then, one approach to the problem is to study the effect of atmosphere on the shear strength** of an ideal granular material.

* Numerous measurements have been made to substantiate this, especially in the case of metals. See References 6, 7, and 39.

** Throughout this thesis "shear strength" will be used in a broad sense. It is recognized that actual measured quantities will be $\tan \phi$ or the tangent of the angle of internal friction, or of the angle of shearing resistance, depending upon terminology preferred.

PRINCETON RESEARCH PROGRAM IN FRICTIONAL BEHAVIOR OF GRANULAR SYSTEMS

Within the criteria and framework outlined in the preceding section a small scale research project in frictional behavior of soils has been initiated in the Department of Civil Engineering at Princeton University. The general objective of this study is to determine more about the frictional behavior of granular soils with particular emphasis on the effect of atmosphere. It should be stressed that this project is limited in its scope and objectives. The atmospheric effects on the shear strength of a granular mass are the objects of immediate concern. Such phenomena as meteoroid impact, sputtering, dust bombardment and others are recognized as probably greatly modifying any results that may pertain to the lunar soils problem. The basic study of frictional behavior, however, is important in itself both from a lunar and a terrestrial standpoint. It is, therefore, taken as the subject of this research project.

INITIAL PHASE

The initial phase of this project is the subject of this thesis and is described below with regard to specific objectives and method of test.

SPECIFIC OBJECTIVES

There are five primary objectives in the initial phase of this project. These are:

1. To test the general validity of the assertion upon which this research project is based. That is, that

shear strength of a granular material is a function of atmosphere. Specifically, it is asserted that outgassing of the adsorbed surface layers of individual particles at very low pressures will cause a change in intergranular friction and hence shear strength.

2. To determine whether or not there exists an analytical relationship between interparticle friction and shearing resistance that may be verified in more or less idealized granular materials.
3. To determine whether or not certain possible lunar surface materials* significantly alter their frictional coefficient at low pressure.
4. To determine which factors (such as particle size, shape, gradation and porosity) can be expected to enter directly into the frictional behavior of granular systems and to determine which of these factors require further research.
5. To develop apparatus and techniques for application to further experimental work in this and related areas.

METHOD OF TESTING

In selecting a method of test two criteria were considered paramount. First, the data must be relatable to shear strength; and second, the testing technique must be relatively simple.

The direct or box shear method was selected from those available as best fitting the criteria under the expected test conditions. The problems inherent in the

* Primarily non-metals, the case seems well established for metals.

direct shear apparatus (14) are considered to be less than those imposed by other testing methods.

Measurement of viscosity was considered first as being simple to obtain and related by definition to shear strength. This property is particularly interesting as a possible link in the analogy existing between loose particle assemblies and true liquids (88). Preliminary flow experiments with a fine (0.01 micron) powder of silica spheres, however, were completely unsuccessful. At near atmospheric pressures the observed phenomena were obviously largely due to displacement of entrapped air. At lower pressures electrostatic attraction and possibly vacuum spot welding caused clinging and poorly defined flow behavior. The viscosity approach was abandoned. This might have been premature, however since the problems were mainly due to the extreme dimensions of the particles.

Static penetration methods were considered and eliminated because of the lack of a firm correlation with shear strength. Another problem involved the relationships between the requirements for a small sample volume*, for a possible variation in particle size and for a plunger diameter significantly greater than the largest particle size but similarly smaller than the sample diameter.

Dynamic penetration or impact studies offer the same difficulties as given above for static penetration. In addition, at atmospheric and low vacuum pressures a

* The object being to reduce load on the vacuum pumping system.

majority of the applied energy must be dissipated in compression and displacement of entrapped air. This was anticipated from the viscosity results previously mentioned, and possibly illustrated in some of the previously reported impact testing programs. Another very important factor is that of applied normal stress. At a depth of an inch or two the normal stress in a granular material is negligible. Measurement of shear strength at this depth is impossible therefore without an applied normal load. Application of such a load without interfering with impact results would present a problem. It is emphasized that the foregoing comments apply to the use of impact tests for determining shear strength and are not to imply a general failure of such methods for other purposes.

Triaxial or cell testing would depend heavily upon membrane outgassing at low pressure and high temperature. This procedure will undoubtedly be used in the future but may require some delay in finding suitable membrane materials.

LATER PHASES

Details of later phases of the Princeton Research Program will be dependent upon the developments and needs in the study of lunar soil mechanics, macromeritics and frictional behavior of granular systems. Some specific areas contemplated for future study in this Program are listed in Chapter VI.

CHAPTER II

THE RELATIONSHIP BETWEEN SHEAR STRENGTH
AND INTERPARTICLE FRICTIONGENERAL

The concept that the angle of shearing resistance of a granular material is a function of the coefficient of friction acting between individual particles has been accepted with little if any opposition. The actual nature of this relationship, however, remains unclear. While a general augmentation of shearing resistance with rising friction seems obvious, this increase is not always pronounced, or even measureable. Leonards (52) refers to the well established significant dependence of friction of some minerals on moisture and the failure of this influence to manifest itself in the angle of shearing resistance. Specifically, quartz experiences a several fold increase in friction in going from a surface dry to wet condition (41, 58, 79). This increase is not reflected in the shearing behavior of granular materials made up of quartz particles.

On the other hand the experience reported by Jakobson (45) indicates that a small change in average friction can significantly alter shearing resistance of granular materials. In this case the angle of shearing resistance of two apparently near identical sands differed considerably (34° and 40.5°). The only discernible difference was a polish, unobserved by the naked eye, of some of the grains of the material with the lower shearing resistance.

In this Chapter existing knowledge and theories on the role of interparticle friction in the shearing resistance of granular media will be reviewed, a new solution will be developed and existing experimental data will be compared with the various analytic solutions.

BRIEF RESUME OF EXISTING ANALYTIC SOLUTIONS

Density or porosity, relative or absolute, is one of the major factors governing the behavior of granular materials. For this reason, and because density is easily defined and measured and further because porosity- friction relationships may be especially important in the lunar environment, the existing solutions are separated in regard to whether they do or do not have provisions for changes in porosity.

SOLUTIONS NOT ALLOWING FOR CHANGES IN POROSITY

CAQUOT'S SOLUTION

The earliest well known relationship between coefficient of friction and shearing strength was offered by Caquot in 1934 (15). Caquot considered each tangent sliding plane between touching grains as an individual surface element of a semi-sphere. This is, as was pointed out by Caquot, more or less precise depending upon the number of such tangent planes (grain to grain contacts) in a given failure surface and the probability of preferred orientation. Integrating over the surface of the semi-sphere he obtained expressions for the resultant shear

and normal forces. Taking the ratio of one to the other then gives the desired relationship,

$$\tan \phi = \frac{\pi}{2} f,$$

which is plotted in Figure 1. Because of the nature of the analysis, treating the mass as a continuous medium, no restrictions are expressed with regard to porosity, grain shape and size distribution or gradation. In fact, it is known that all of these factors greatly influence shear behavior. The implication that shear strength should be zero in the case of a frictionless material overlooks the work done on or by the normal forces at any but the critical voids ratio (77).

BISHOP'S SOLUTION

Bishop (4), without presenting details of his analysis gives a pair of expressions relating $\sin \phi$ to f .

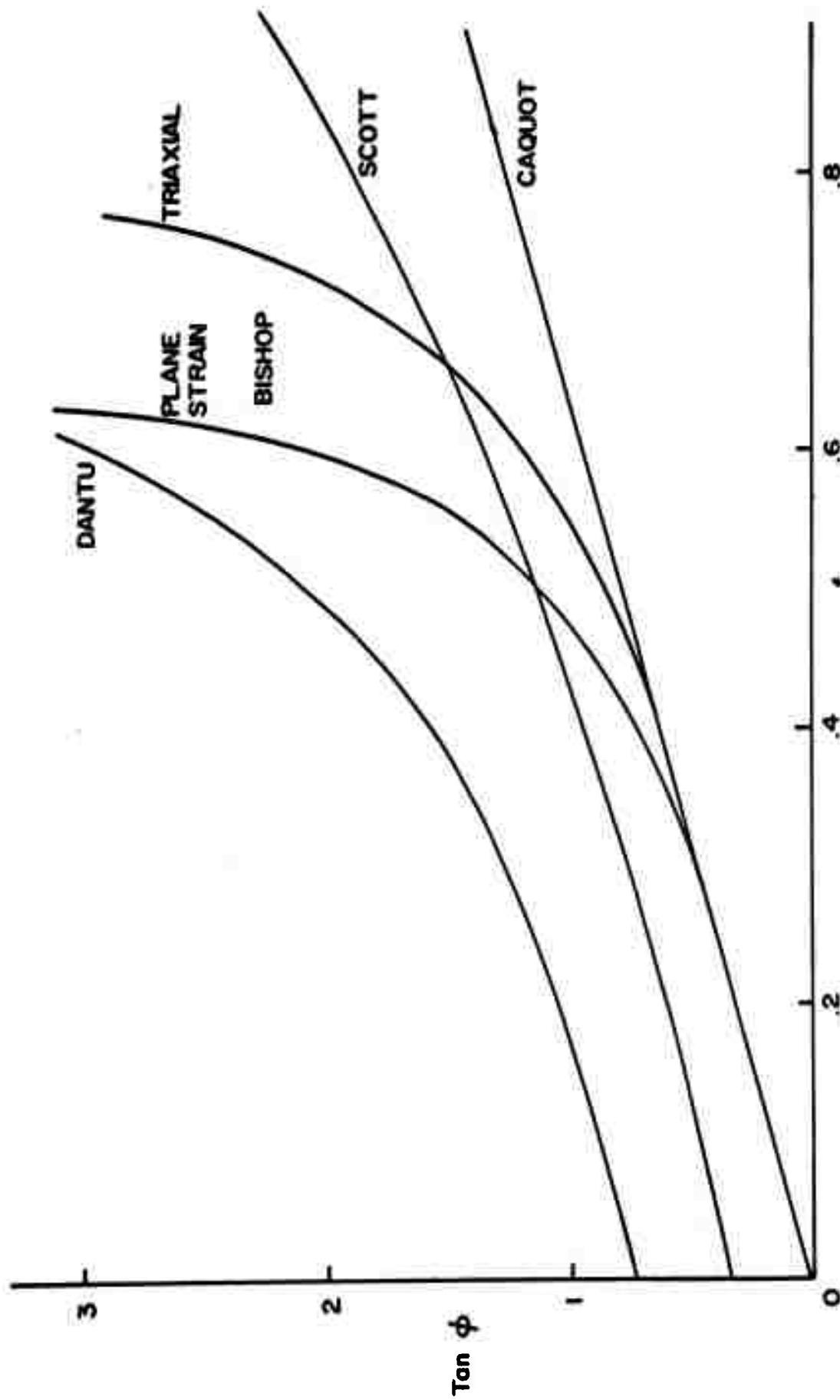
For the triaxial case:

$$\sin \phi = \frac{15f}{10 + 3f}$$

For plane strain:

$$\sin \phi = \frac{3}{2} f .$$

Both these expressions give values of shearing resistance very close to that of Caquot up to a coefficient of friction of about 0.4. They indicate also an absence



Tan ϕ vs f Relationships Which Do Not Consider Porosity

Figure 1

of all shearing resistance in the case of a frictionless material. Contrary to Caquot, however, both of these expressions imply a rapid increase of strength as the f exceeds 0.4 as shown in Figure 1.

DANTU'S SOLUTION

Dantu (19) approached the problem by considering a mass of perfect spheres in rhombohedral (hexagonal) packing*. In summing forces on a unit surface in each of three mutually perpendicular directions he determines the forces acting between spheres in terms of the applied normal stresses. The form of the resulting expressions and the assumption that the forces between spheres must not be negative (i.e. tension not possible) allows Dantu to establish the following formula:

$$\sin \phi = 3 \frac{\sqrt{2} + 2f}{5\sqrt{2} + 2f} .$$

This relationship, also plotted in Figure 1, gives a value for $\tan \phi$ of 0.750 (36.9°) in the case of frictionless spheres. A coefficient of friction of 0.707 corresponds to a ϕ of 90° , hence a theoretically infinite shearing resistance.

SCOTT'S SOLUTION

In considering a face centered cubic arrangement**

* One of the variations of most dense packings of equal spheres (porosity 0.26). Each sphere is in contact with six spheres in its own layer and three each in the adjacent upper and lower layers. For a discussion of the various packings of equal spheres see Reference 21 or 30.

** The face centered cubic arrangement is identical with the rhombohedral (hexagonal) packing as viewed from a different orientation.

of equal spheres Thurston and Deresiewicz (78) established a failure criterion for triaxial compression of a granular column. In this case a load (stress difference) is added to the regular array of spheres held by a confining isotropic stress. The applied load is directed normal to the unit face centered cube while failure is assumed to occur between parallel adjacent hexagonal planes. These parallel hexagonal planes make an angle of 54.8° with the horizontal. If each sphere in the face-centered cubic arrangement is considered with respect to the hexagonal orientation it is found to be in contact with six spheres in its own plane and three each in the adjacent upper and lower planes (see note on page 20). A given ball then is assumed to slide through the valley formed by two of the three underlying spheres. Resolution of the forces acting on a given sphere allowed Thurston and Deresiewicz to derive an equilibrium (incipient failure) expression relating the stresses and the interparticle coefficient of friction. The solution is generalized to allow variation in the orientation of the applied stress difference.

This generalized solution has been extended by Scott (68) who considers the ratio of tangential to normal stresses on the assumed failure surface and so is able to express the shearing resistance as

$$\tan \phi = \frac{\sqrt{3} + 4\sqrt{2} f}{2(\sqrt{6} - f)}$$

This solution is also shown in Figure 1.

SOLUTIONS ALLOWING FOR CHANGES IN POROSITY

IDEL'S SOLUTION

Idel (43) has introduced the very important concept of porosity into the $\tan \phi$ versus f relationship. He begins by taking the hexagonal packing of equal spheres as the basis for his analysis. This packing is briefly described in the note on page 20. More specifically he considers the tetrahedron formed by the lines joining the centers of four adjacent spheres. These can be considered as any single sphere and the three of the next lower layer which form the hollow into which it fits. Such a tetrahedron is shown in Figure 6. The angle formed by the line joining the centers of the single sphere and any one of the other three spheres, and its projection in the plane of the three spheres is fundamental to the analysis and is designated "j". This angle is shown in Figure 6. In the ideal case of most dense (rhombohedral) packing j is the octohedral angle (54.8°). Since the volume of the tetrahedron and that portion of the volume of the four spheres lying within the tetrahedron can be expressed in terms of j , the porosity, n , is written as a function of j :

$$n = 1 - \frac{0.202}{\cos^2 j \sin j}$$

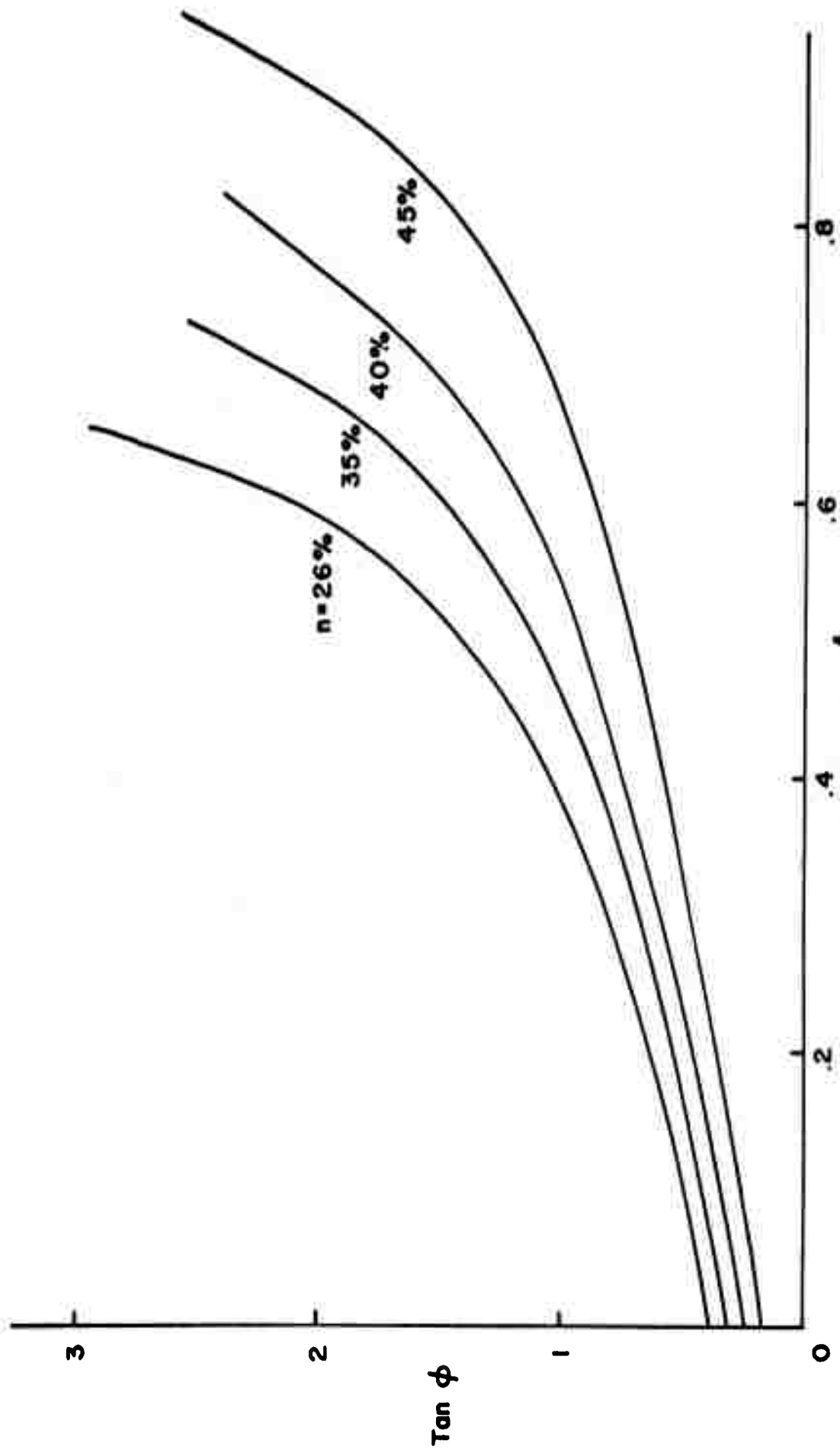
Idel then considers three spheres, one from each of three successive layers, and forms the force polygon resulting from the application of a normal and a shearing load. This allows the derivation of an expression relating the normal and shearing forces with the angle j and with ρ , the angle whose tangent is the coefficient of intergranular friction. Straight application of the Mohr diagram (77) results in the following formula:

$$\sin \phi = \frac{1.5 \tan (\rho + j) - 1}{1.5 \tan (\rho + j) + 1} .$$

This relationship, together with that relating j and porosity allows one to establish the $\tan \phi$ versus f relationship shown in Figure 2.

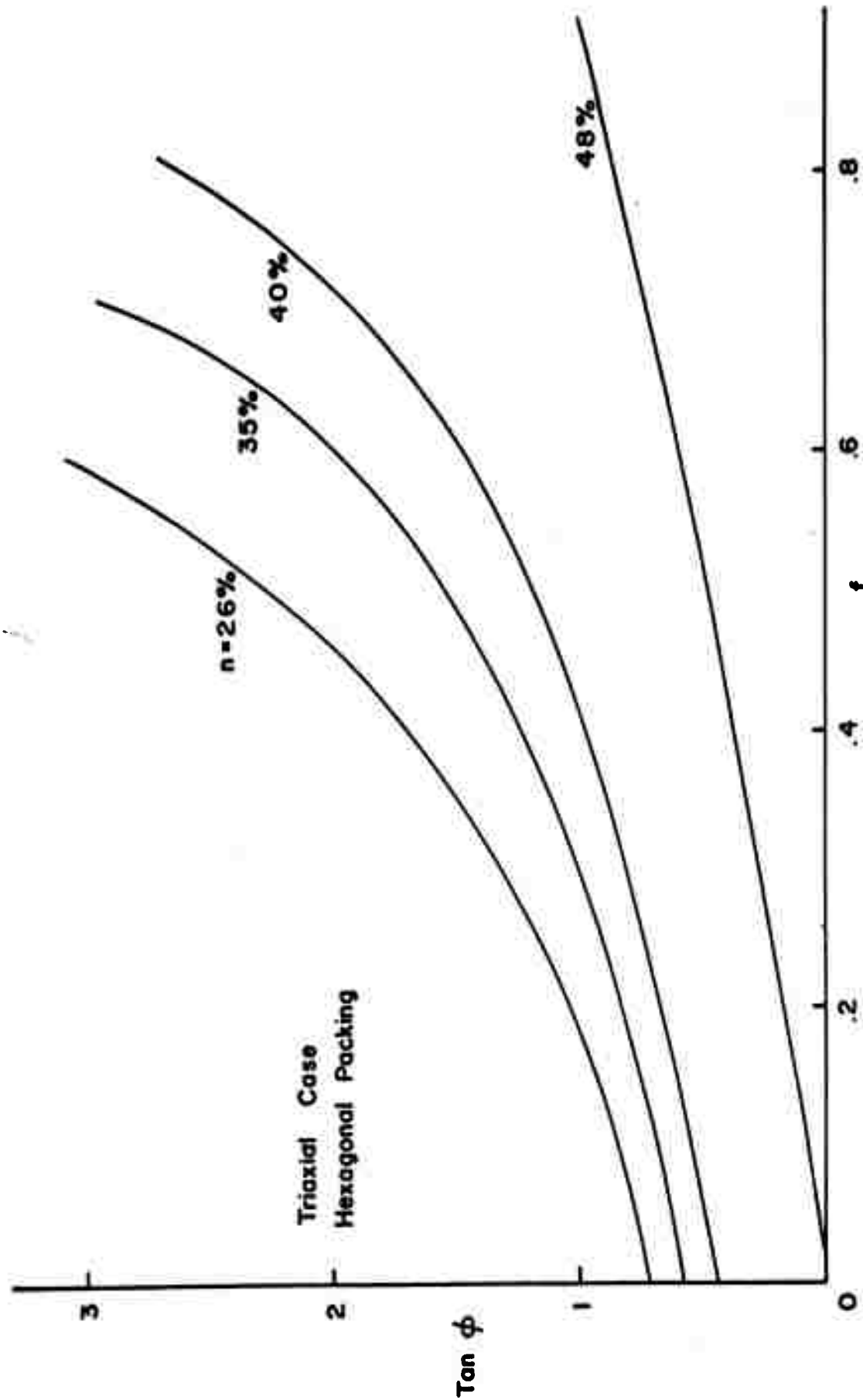
WITTKE'S SOLUTION

Wittke (92) has attempted to improve on Idel's solution in two specific ways. First, he considers three different orientations of the most dense or rhombohedral packing. These are two slight variations of the previously discussed hexagonal packing and the quadratic or face centered cube. Secondly, he rejects Idel's force polygon approach and solves the problem in terms of applied stresses considering separately the triaxial and plane strain cases. While significant differences exist between the various solutions only the case of hexagonal packing in a triaxial state of stress will be given here (see Figure 3) for comparison. Wittke concludes that in this case,



IDEAL'S SOLUTION, $\tan \phi$ vs f

Figure 2



WITTKE'S SOLUTION, $\tan \phi$ vs f

Figure 3

$$\tan^2 \left(45 + \frac{\phi}{2} \right) = 2 \tan j \cdot \tan (j + \rho)$$

where j and ρ are as defined in the discussion of Idel's work.

SPENCER'S SOLUTION

In an apparently similar* manner Spencer (76) derived a relationship between porosity, angle of external friction ($\arctan f$) and ϕ . This is shown in Figure 4 which was constructed through calculations based on points taken from a small scale plot of Spencer's relationship. It is thus subject to some degree of inaccuracy.

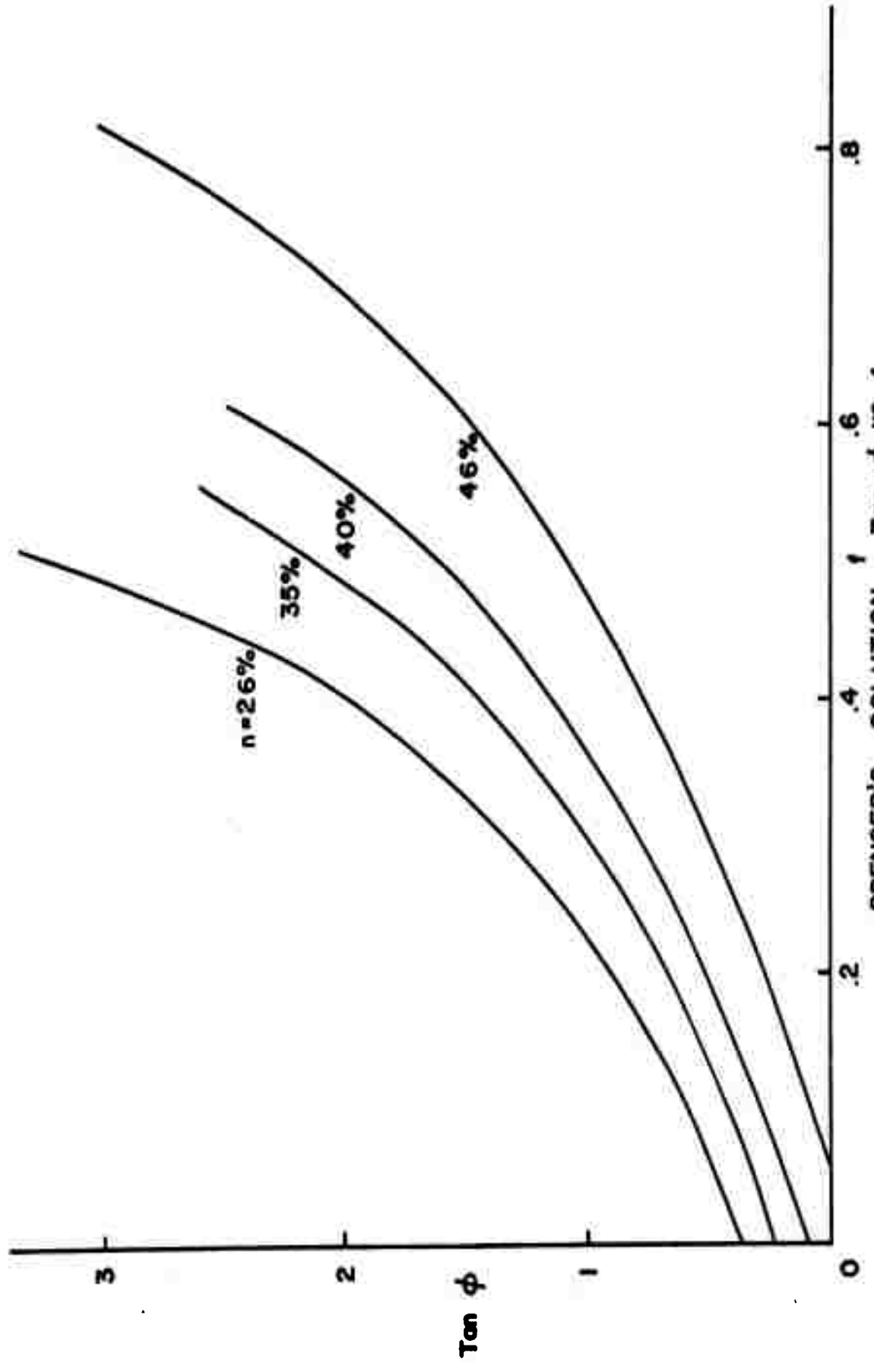
OTHER SOLUTIONS

Other solutions, express and implied, may have been developed for the $\tan \phi$ versus f relationship. It is believed, however, that all of the more explicit solutions have been briefly reviewed above. A few of these solutions are mentioned by Wikramaratna (87) in a discussion of Reference 19.

A SIMPLIFIED SOLUTION FOR THE TAN ϕ VERSUS f RELATIONSHIP

A new solution for the $\tan \phi$ versus f relationship has been developed and will be outlined in the following paragraphs. This solution is somewhat simplified and lacks the rigor which is attached to some of the solutions reported earlier in this Chapter.

* Only a brief review of this work has been published with a note that full details have been submitted to Geotechnique.



SPENCER'S SOLUTION, $\tan \phi$ vs f

Figure 4

In view of the gross assumptions in applying any analytic solution to other than a perfectly ideal material the simplifications used here are considered justified. This solution has the advantage that the assumed failure mechanism, which is a mean of several limit cases, can be easily visualized. In addition, it is asserted that this solution fits the applicable observed data as well as or better than other published analytic relationships.

ASSUMPTIONS

This solution, which is intended for applicability to granular materials composed of equal sized spheres, is based upon several fundamental assumptions that will be discussed below.

As in all other such relationships it is implicitly assumed that the macroscopic or traditional view of sliding friction is applicable. This allows the validity of the resulting solution for nearly all normal situations. It may negate the solution under certain extreme conditions such as a perfect vacuum where the Amontons (8) concepts are open to question. It will be shown, however, that the extreme situation of vacuum welding is satisfied by the solution, and in fact by nearly all similar solutions. It is applicable to the wide range of conditions in which a definite coefficient of sliding friction, as traditionally defined, can be measured.

The widest latitude is taken by the assumption that failure occurs with one distinct layer of spheres, together with all those above it, sliding over the layer immediately

below, which, together with all others remains fixed. The existence of such layers in any but the ideal packings is open to serious question, and such a failure mechanism is only an approximation at best. Such an assumption is necessary, however, to make the formulation of a simple analytic solution feasible.

It is generally held that rolling friction as well as sliding friction enters into the determination of the shearing resistance of granular materials. At least one writer (52) attributes a majority of shearing resistance to rolling friction and interlock rather than sliding friction. In this analysis rolling friction is discounted as an important factor in the shear behavior of granular systems. It is difficult to picture a significant amount of rolling in view of the large number of contacts each sphere has with others. In the most dense ideal packing there are twelve contacts for each sphere while the loosest cubic packing gives six contacts. It has been experimentally verified that these values give the approximate limits for random packings of equal spheres (74). A loose packing of equal spheres with a porosity of 45%, for instance, has been shown to have an average of seven contacts per particle. It seems then that the assumption of sliding friction only will not induce a large error.

Another basic assumption is that the concept of relative density* can be applied to systems of uniform equal spheres,

*
$$\text{Relative Density} = \frac{e_{\max} - e}{e_{\max} - e_{\min}} \cdot 100$$
, where e_{\max} is the void ratio at loosest packing, e_{\min} is the void ratio at densest packing, and e is the void ratio of the packing under consideration. For a complete discussion of this concept see Reference 13.

and that the ideal rhombohedral and cubic packings can be considered as giving the minimum and maximum void ratios. It has been shown that in general the angle of shearing resistance of a granular soil varies directly as the relative density. This is particularly true in the case of rather uniform grain size (13).

Elastic deformation of the particles is considered a second order effect and is ignored.

Other minor assumptions used are mentioned as they are applied in the solution.

SOLUTION

MOST DENSE PACKING

The hexagonal (rhombohedral) packing is the densest arrangement of equal sized spheres. This packing has been briefly discussed in the footnote on page 20. Since there is an equal number of spheres in each layer the problem can be further simplified by considering only a single sphere in the lowest sliding plane and the three in the next lower layer upon which it rests. Except for the shear force, the loads applied by means of the other adjacent nine spheres and by the weight of the sphere in question can be regarded as a single exterior verticle force P , and a couple C , adequate to resist rotation. Upon application of a horizontal shearing force component S , parallel to the assumed failure plane, the sphere under consideration has two extreme paths it may take.

One path being directly over one of the three underlying spheres, the other path lying in the cleavage of any two of these underlying spheres as shown in Figure 5a which pictures the four spheres involved in this discussion. Applying the method of virtual work or simply the laws of statics to each failure path one obtains four separate relationships between $\tan \phi$ and f ; one for each path for the coefficient of static friction f_s , and for the coefficient of kinetic friction f_k . In view of the very small difference between static and kinetic coefficient of friction of minerals (41) no distinction will be made between the two. Consequently, the subscripts s and k will not be used.

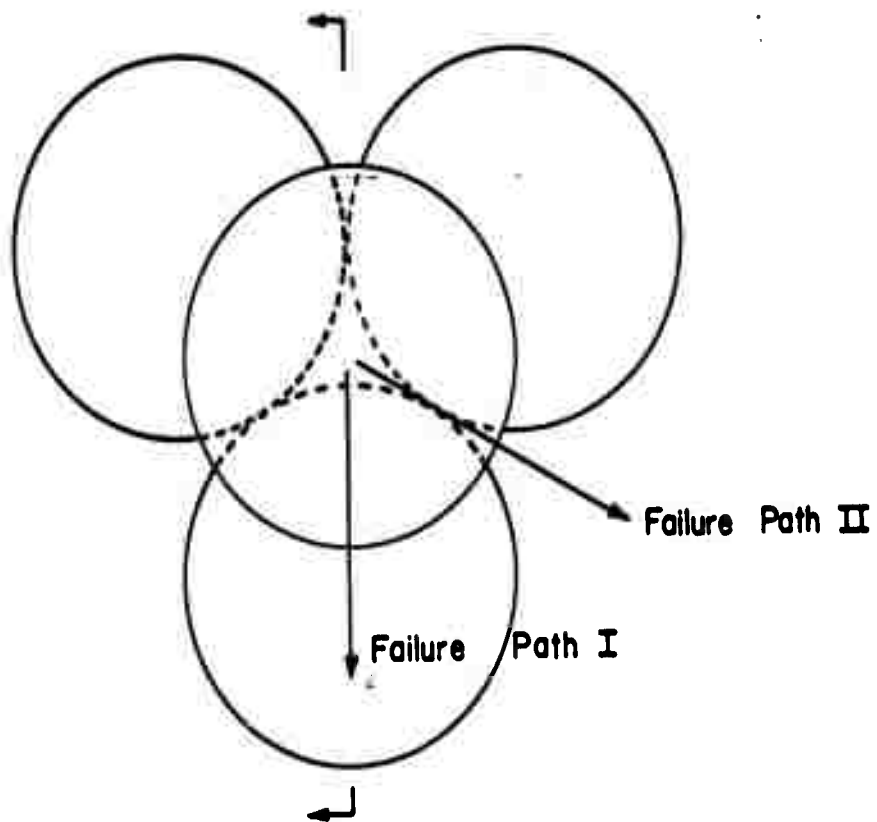
FAILURE PATH I, STATIC CASE:

If one assumes equilibrium of verticle forces acting on the top sphere before application of the shear load component the normal force N , between spheres can be computed as

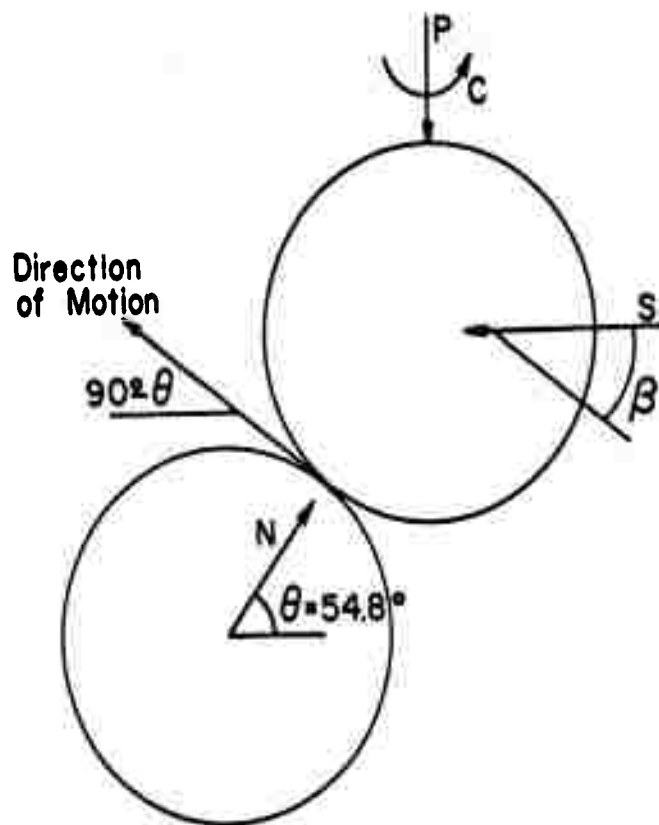
$$P = 3N(\sin \theta + f \cos \theta),$$

$$N = \frac{P}{3(\sin \theta + f \cos \theta)} \quad (1)$$

Upon application of the shear force, assuming superposition, a summation of forces in the direction of initial motion (making an angle of $90^\circ - \theta$ with the horizontal as shown in Figure 5b) allows



a. Plan View Showing Extreme Failure Paths



b. Section Containing Failure Path I
Geometry of Failure Path I

Figure 5

formulation of the shear force S , in terms of the exterior vertical load P :

$$S \sin \theta = f (N + S \cos \theta) + P \cos \theta .$$

Substituting for N from equation (1) and rearranging, one obtains

$$S(\sin \theta - f \cos \theta) = P \left[\frac{f}{3(\sin \theta + f \cos \theta)} + \cos \theta \right] .$$

Since P is normal to the assumed failure plane for the mass of spheres, and S is the shear component parallel to failure plane, one may express the shearing resistance as the ratio of S to P :

$$\tan \phi = \frac{1}{\sin \theta - f \cos \theta} \left[\cos \theta + \frac{f}{3(\sin \theta + f \cos \theta)} \right] \quad (2)$$

Since θ is known to be the octahedral angle, 54.8° , one can compute $\tan \phi$ for various values of f by means of equation (2).

The same result can be obtained by the method of virtual work. Allowing a virtual displacement, $Rd\theta$, in the direction $90^\circ - \theta$, where R is the radius of the sphere, one can express the work as;

Work done by shear force, S :

$$W_s = SR \sin \theta d\theta ,$$

Work done against normal load, P :

$$W_p = PR \cos \theta d\theta ,$$

Work done against friction:

$$W_f = \frac{f PR d\theta}{3(\sin\theta + f \cos\theta)} \int f R S \cos\theta d\theta .$$

Since

$$W_s = W_p + W_f$$

one obtains, upon simplification, equation (2) as before.

FAILURE PATH I, KINETIC CASE:

Again taking the external vertical load alone, without the shear force, one is able to compute the normal force between spheres after motion has begun. In this case the sliding sphere will be in contact with only one of the three spheres of the lower layer. Summation of forces in a vertical direction gives

$$N = \frac{P}{\sin\theta - f \cos\theta} . \quad (3)$$

Note that this value of N is not reduced by a factor of 3 as in equation (1), and further, that the friction force now acts downward resulting in a sign change in the denominator. Application of the shear force, summation of forces in a horizontal direction and simplification allows one to express $\tan\phi$ as before

$$\tan\phi = \frac{S}{P} = \frac{\cos\theta + f \sin\theta}{\sin\theta - f \cos\theta} . \quad (4)$$

FAILURE PATH II, STATIC CASE:

This case differs from the previous ones in that initial motion takes another direction and is resisted by two frictional contacts. Consider the upper sphere 1, the three spheres upon which it rests, 2, 3 and 4, and the tetrahedron 1-2-3-4 formed by joining their centers as shown in Figure 6a. If it is assumed that sphere 1 slides through the cleavage of spheres 2 and 3, one can determine the true direction of initial motion by obtaining an edge view of the plane 1-2-3, as shown in Figure 6b.

The normal force N , acting between the spheres and due only to the applied exterior load will be given by equation (1) as before.

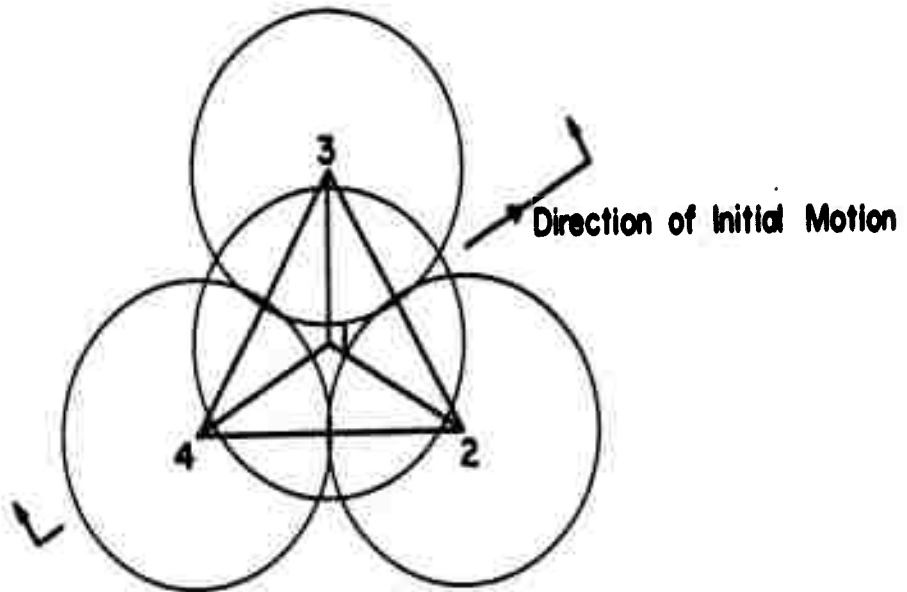
Upon application of the shear load S , one can identify its component in the 1-2-3 plane as

$$S \sin \alpha$$

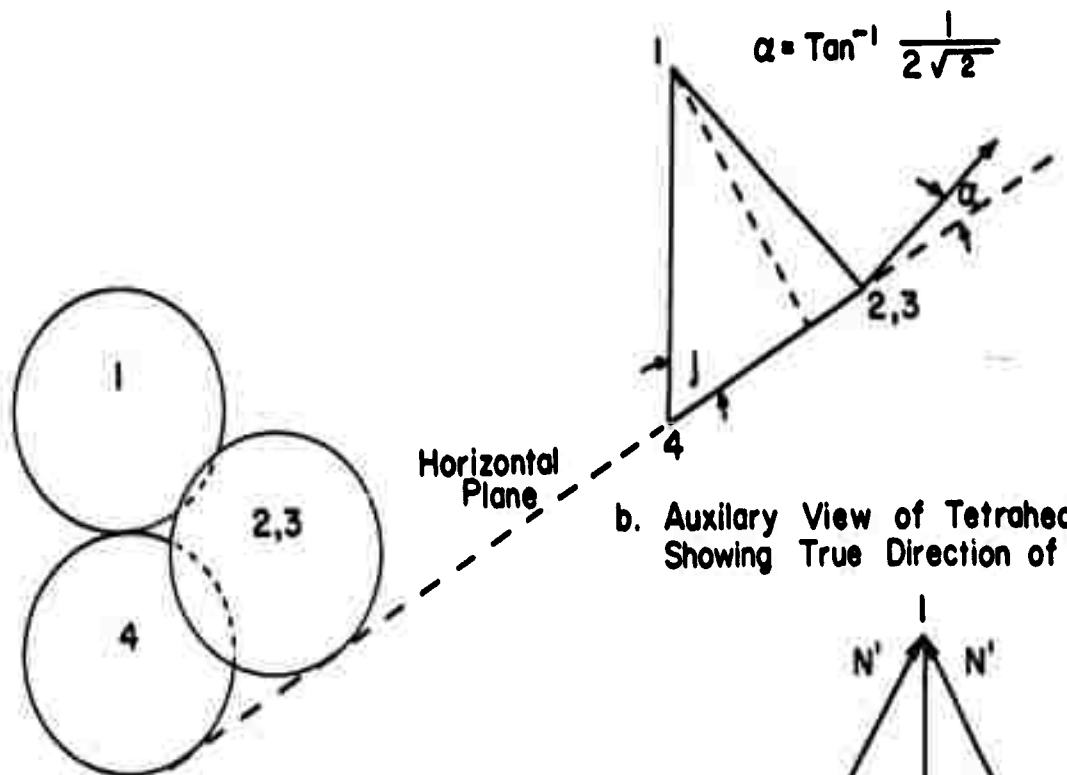
Thus the normal force N' , between spheres 1 and 2 and between spheres 1 and 3, due to S only, can be determined by summation of forces in the plane 1-2-3. A true shape view of plane 1-2-3, with force vectors superimposed, is shown in Figure 6d.

$$N' = \frac{S \sin \alpha}{2 \sin 60} \quad (5)$$

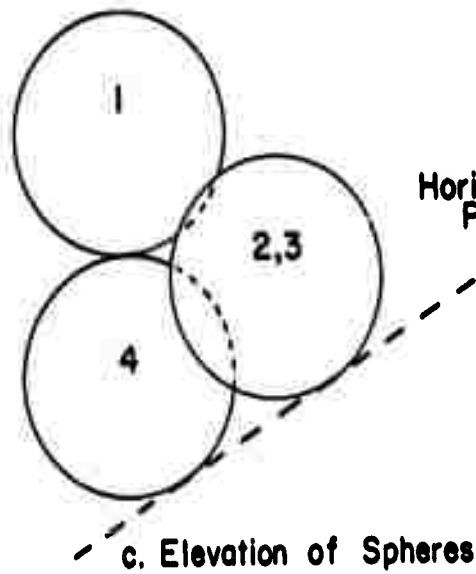
Summation of forces acting on sphere 1 in the



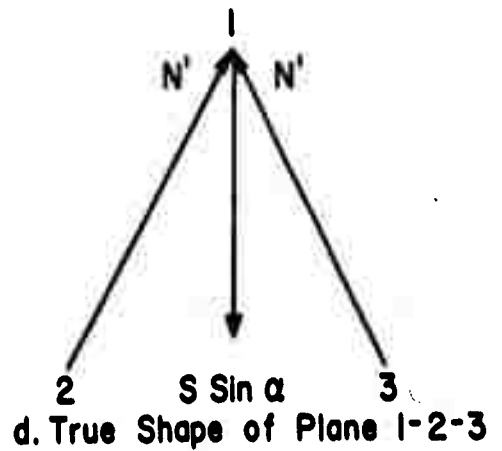
a. Plan View of Spheres and Tetrahedron



b. Auxiliary View of Tetrahedron Showing True Direction of Motion



c. Elevation of Spheres



d. True Shape of Plane 1-2-3

Geometry of Failure Path II

Figure 6

direction of initial motion gives,

$$S \cos \alpha = f \left[2N + \frac{S \sin \alpha}{\sin 60^\circ} \right] + P \sin \alpha .$$

This result can be used, as before, with equation (1) to determine the shearing resistance:

$$\tan \phi = \frac{S}{P} = \frac{\frac{2f}{3(\sin \theta + f \cos \theta)} + \sin \alpha}{\cos \alpha - \frac{f \sin \alpha}{\sin 60^\circ}} . \quad (6)$$

FAILURE PATH II, KINETIC CASE:

In this case the sliding sphere will be in contact with only two of the underlying spheres. The component of the external load P , acting in plane 1-2-3 is

$$P \cos \alpha .$$

Then the normal force N'' acting between spheres 1 and 2 and between spheres 1 and 3 due to P only can be written as

$$N'' = \frac{P \cos \alpha}{2 \sin 60^\circ} . \quad (7)$$

Upon application of the shear force S , one can again apply equation (5) to determine the normal load N' , between spheres, due to S alone. Summation of forces in the direction of initial motion,

together with equations (5) and (7) gives

$$S \cos \alpha = f \left[\frac{P \cos \alpha}{\sin 60^\circ} + \frac{S \sin \alpha}{\sin 60^\circ} \right] + P \sin \alpha$$

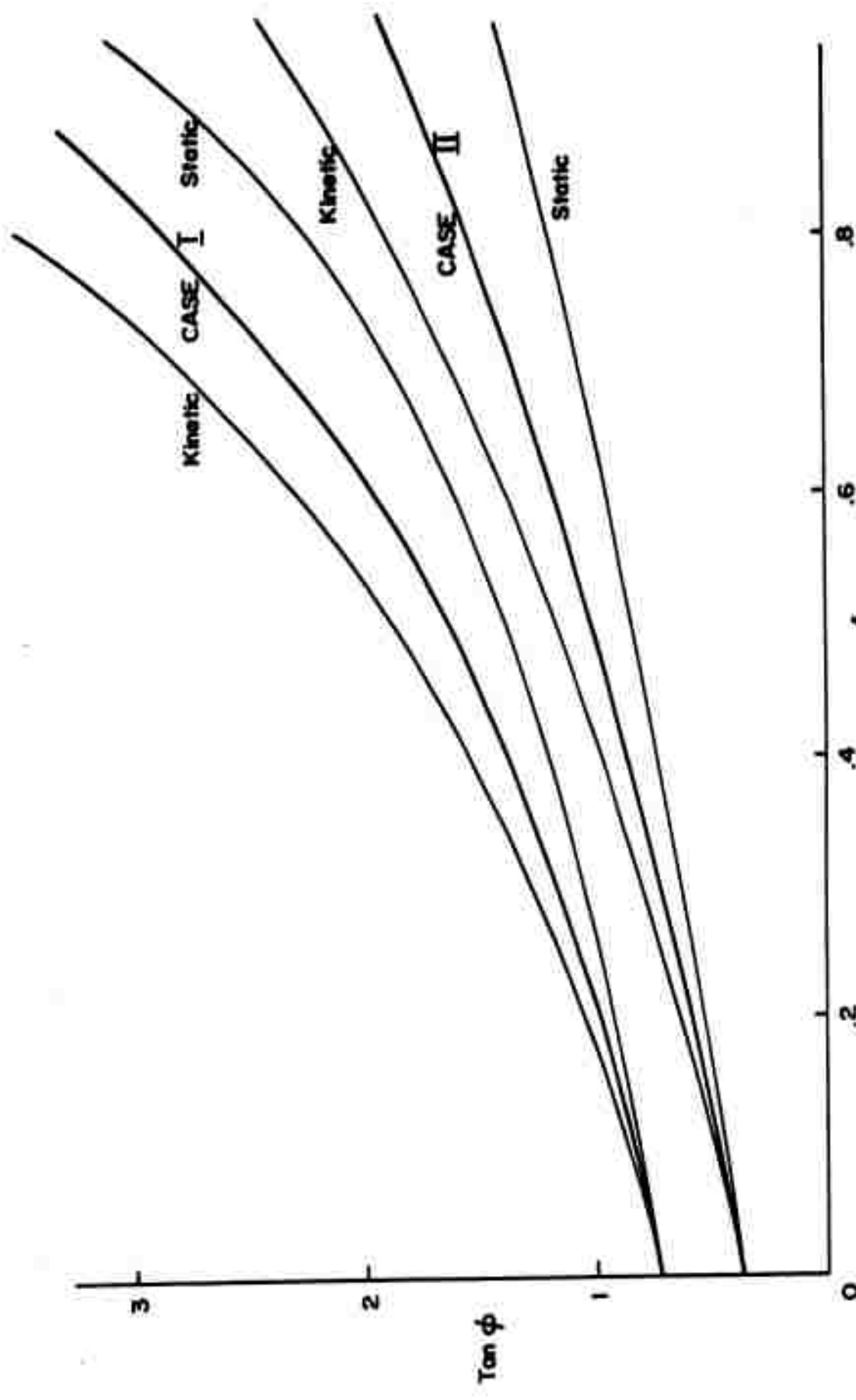
Rewriting to obtain an expression for shearing resistance,

$$\tan \phi = \frac{S}{P} = \frac{\sin \alpha \sin 60^\circ + f \cos \alpha}{\cos \alpha \sin 60^\circ - f \sin \alpha} \quad (8)$$

Equations (2), (4), (6) and (8) give the ratio of shear force to normal force acting on the sliding plane at the moment of impending motion for the various failure mechanisms. As failure proceeds in each case it can be seen that the angle Θ increases and the values of $\tan \phi$ given by these equations decrease. The equations then give the peak shearing resistance which occurs at the time of initial motion in the system under consideration. Values of $\tan \phi$ as a function of the coefficient of friction are plotted for the four cases in Figure 7.

Any number of methods could be applied to the four solutions to obtain a resultant relationship. The one which is followed here seems as reasonable as any when considered in view of the physical approach being taken to the overall problem.

First, a mean curve is taken for Case I and Case II by averaging the kinetic and static values. This results in the curves shown in Figure 7. Second, equal probability is assumed for the movement of any sphere along either



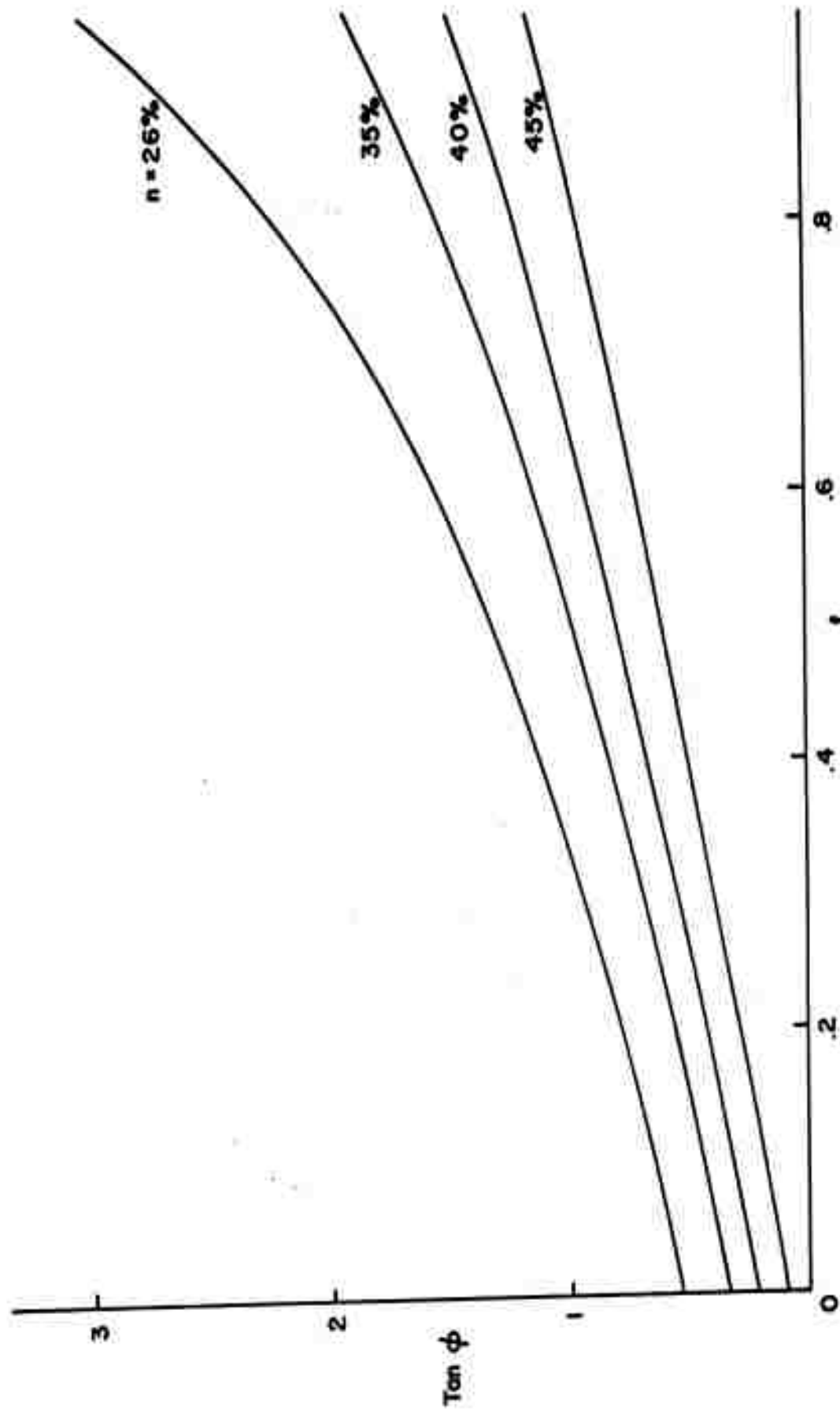
Tan ϕ vs f Relationships for Extreme Failure Paths

Figure 7

failure path. This results in the curve for a porosity of 26% given in Figure 8. The basis for this assumption can be seen by recalling that the assumed failure mechanism involves an entire layer of spheres moving as a sheet. The failure path taken by any sphere then depends upon the direction of the overall motion (applied shear force) relative to the axis of the failure paths here considered. Since no preferential orientation can be expected an equal probability exists for each failure path.

On the other hand one might argue that more spheres will tend to follow failure path II because it involves less energy and thus an equal probability does not exist. An assumption of equal partition of energy between two extreme failure mechanisms might be more realistic. Pursual of this reasoning beyond elementary approximations soon becomes more involved than the previously reviewed analysis. It is possible, however, to make a simple and reasonable approach to the concept of equal partition of energy in the following manner.

As an approximation of the energy required for a given horizontal displacement one can take the energy required for a virtual displacement at the point of initial motion. Thus, the ratio of energy per displacement for the two failure paths is the ratio of the peak shear forces. While this ratio is a function of the coefficient of friction f , an average value of 2:1



Tan ϕ vs f , Based on Equal Probability and Relative Density

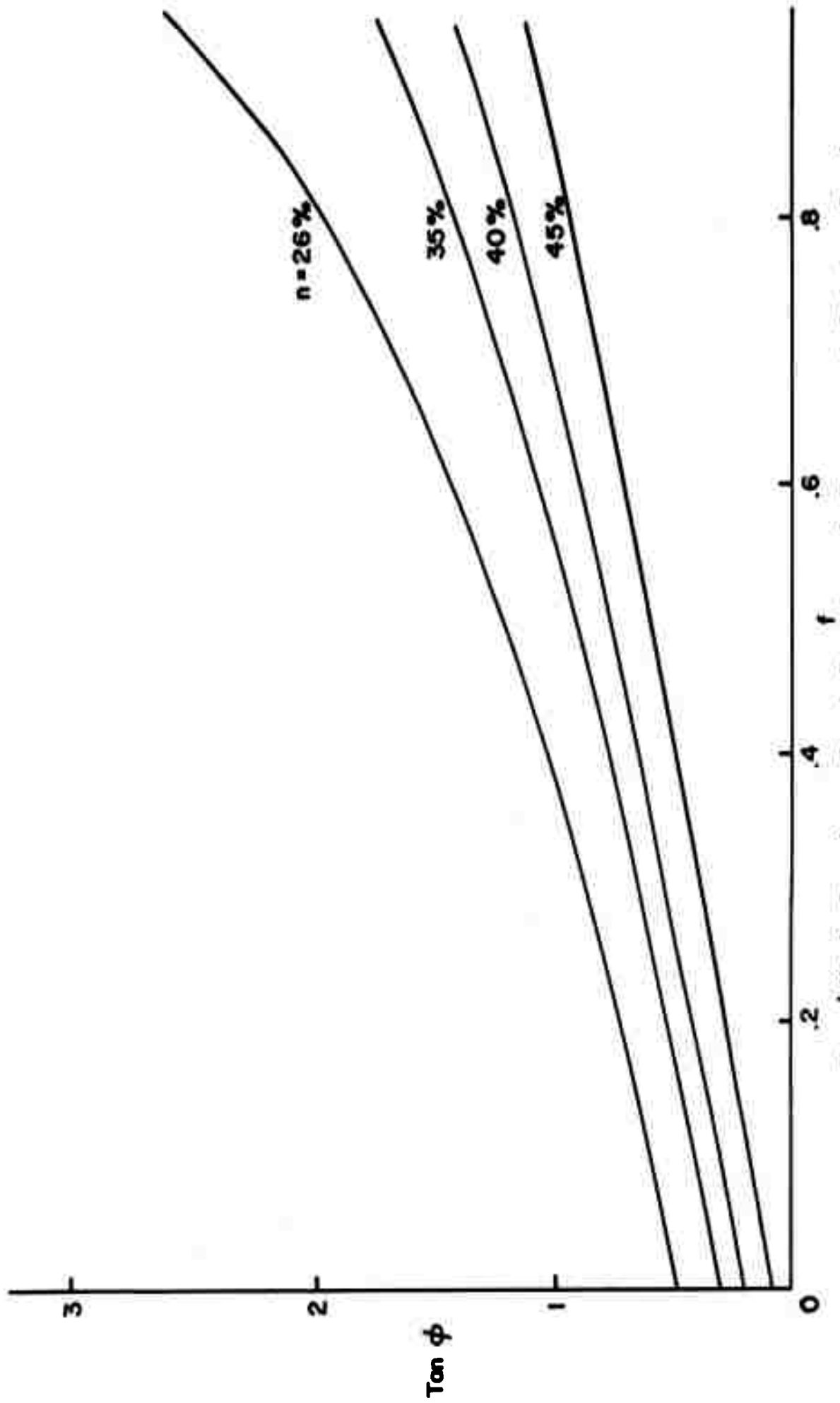
Figure 8

(Case I: Case II) can be taken over the range $0 \leq f \leq 1.2$. Then assuming a probability of 2:1, Case II over Case I, the limit curve (porosity of 26%) of Figure 9 is obtained.

A comparison of Figure 8 and 9 shows that very little difference exists between the equal probability and equal partition procedures as outlined in this analysis. This indicates the relatively small and dubious benefit gained by extensive refinements. It is interesting to note, however, that the upper limit curve of Figure 9, based on equal partition of energy agrees quite well with the more rigorous solution given by Scott (68) and shown in Figure 1.

LOOSEST PACKING

The cubic packing is taken as the lower limit case. Here the tangent of the angle of shearing resistance is taken as equal to the coefficient of sliding friction between the grains. While the rhombohedral and the cubic may be considered separate and distinct cases, each giving a limit to the range of porosities possible in packings of equal sized spheres, they are related in a manner shown by Idel (43). Taking his equation for porosity in terms of the previously defined angle j (see page 22) Idel has shown it to degenerate to the cubic case though the equation was formulated for a rhombohedral (hexagonal) packing. By maximizing the expression through differentiation Idel shows that the porosity equals 47.6% as j



Tan ϕ vs f , Based on Equal Partition of Energy and Relative Density

Figure 9

increases to its limit and the lattice expands. This porosity can only be obtained in the cubic packing, hence a relationship with continuity is shown.

VALUES AT INTERMEDIATE POROSITIES

If one applies directly an interpolation based on the concept of relative density, the intermediate curves shown in Figures 8 and 9 are obtained. Sample calculations for the 40% porosity curve of Figure 8 at a coefficient of friction of 0.8 are given in Figure 10.

A modification of this method involves application of a formula suggested by Winterkorn in analogy with liquid viscosity (89). The equation, written in the equivalent form,

$$\tan \phi = \frac{C}{e - e_{\min}} \quad (9)$$

has shown itself to be very accurate when compared with a wide range of experimental data (24). In addition the equation has been checked with samples of uniform sized glass spheres in connection with the work described in Chapter III. In this case a calculated value of $\tan \phi$ of 0.698 was closely confirmed by an average (10 tests) experimental value of .688. In applying equation (9) to the determination of the intermediate curves shown in Figure 11, C and e_{\min} , for a particular f , are calculated from the upper and lower limit curves. This allows one

$$\phi_{40-.8} = \phi_{\min-.8} + \left(\frac{e_{\max} - e_{40}}{e_{\max} - e_{\min}} \right) \Delta \phi_{.8}$$

$$e_{\max} = \frac{.476}{.524} = .912$$

$$e_{\min} = \frac{.26}{.74} = .350$$

$$e_{40} = \frac{.4}{.6} = .667$$

$$\frac{e_{\max} - e_{40}}{e_{\max} - e_{\min}} = \frac{.245}{.562} = .436$$

$$\Delta \phi_{.8} = \phi_{\max-.8} - \phi_{\min-.8} = 65.6^\circ - 38.6^\circ = 27.0^\circ$$

$$\phi_{40-.8} = 38.6 + (.436)(27) = 50.4^\circ, \text{ Tan } 50.4^\circ = \underline{1.21}$$

a. n = 40%, f = .8, Figure 8

$$\text{Tan } \phi = \frac{C}{e - e_{\min}}$$

$$2.2 = \frac{C_{.8}}{.350 - e_{\min-.8}} \quad C_{.8} = .708$$

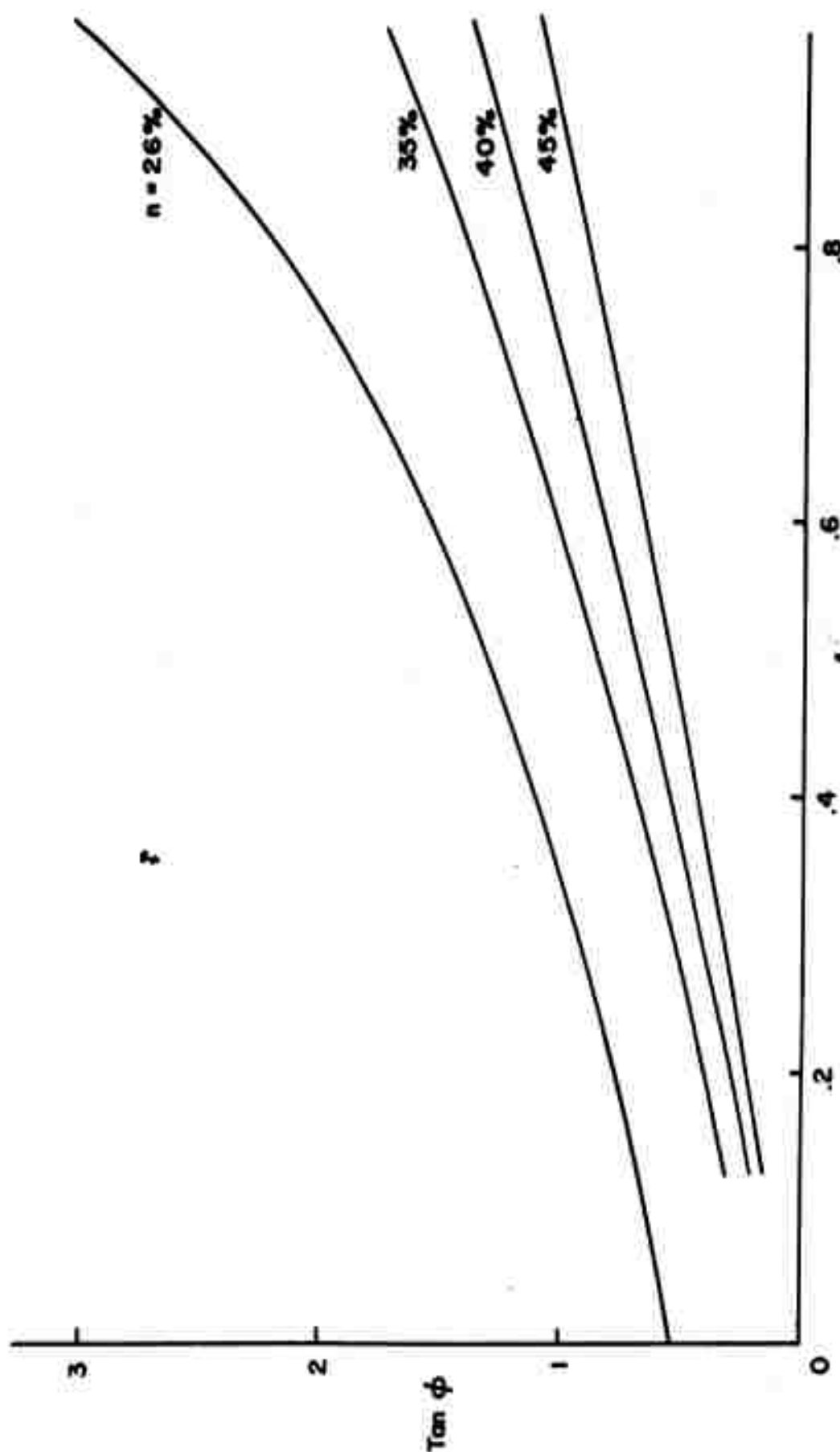
$$.8 = \frac{C_{.8}}{.912 - e_{\min-.8}} \quad e_{\min-.8} = .028$$

$$\text{Tan } \phi_{40-.8} = \frac{C_{.8}}{e_{40} - e_{\min-.8}} = \frac{.708}{.667 - .028} = \underline{\underline{1.11}}$$

b. n = 40%, f = .8, Figure 11

Sample Calculations

Figure 10



Tan ϕ vs f , Based on Equal Probability and Macromeritic Equation

Figure 11

to obtain $\tan \phi$ directly for any porosity. An example is shown in Figure 10b.

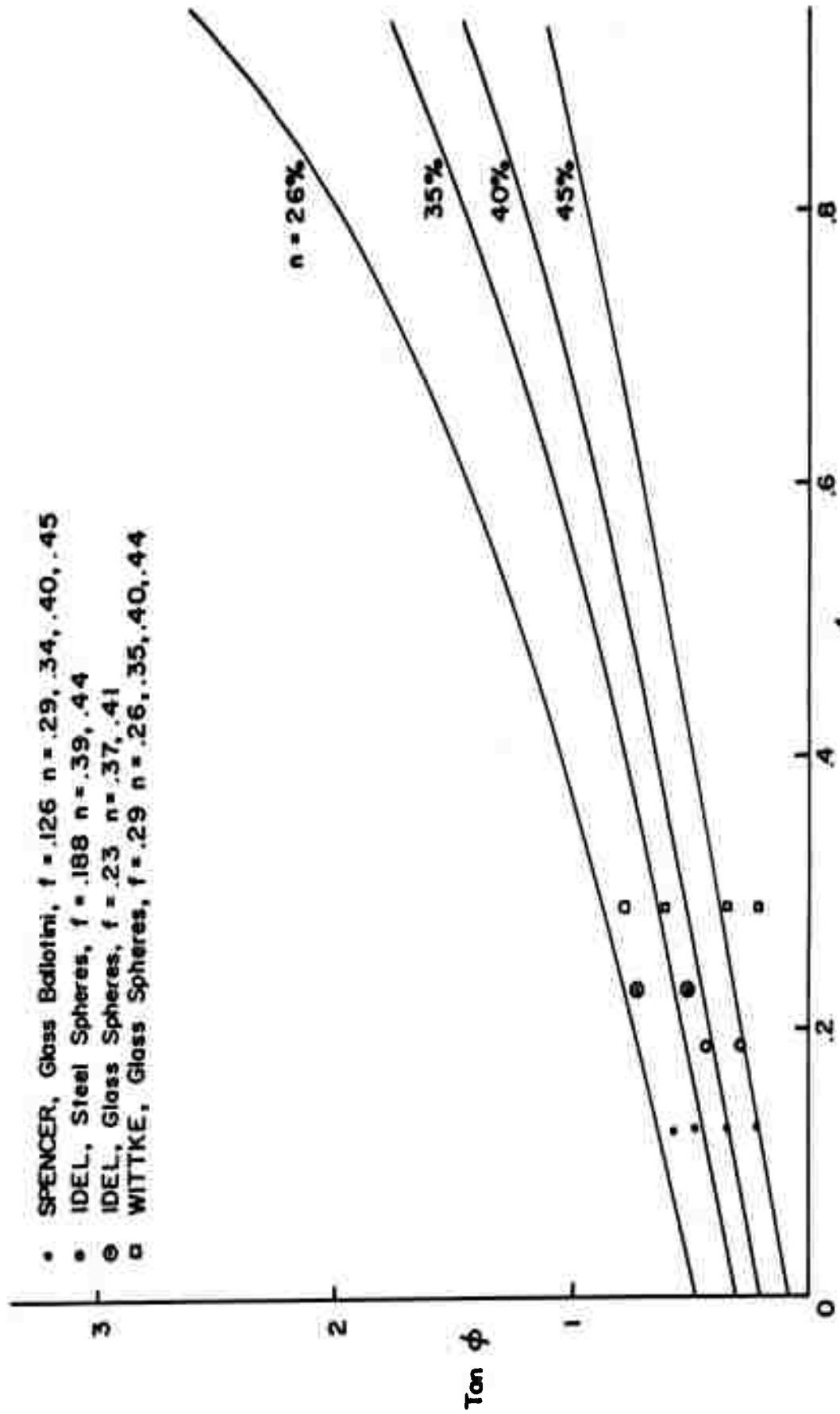
REVIEW OF EXISTING DATA

Since all of the analytic solutions relating $\tan \phi$ to f involve the assumption of an ideal system of equal sized spheres, only data which have been determined by use of such model materials will be considered here. Some attempts have been made to compare the various analytic solutions with results of tests on natural materials (4, 87). These have shown, to a greater or lesser degree, that in general the analytic solutions are approximately representative of actual performance at the low coefficients of friction of natural minerals. It is considered, however, more appropriate to survey the known data concerning tests on idealized systems. That data will be compared with those solutions which allow for a variation in porosity.

In tests on glass ballotini spheres Spencer (76) found that his solution, shown in Figure 4, was well confirmed at the coefficient of friction 0.13. Triaxial tests at porosities of 29, 34, 40 and 45% gave angles of shearing resistance of 29, 26, 19 and 12° respectively*. These values fall considerably away from Idel's solution and especially fail to agree with that of Wittke. The agreement with the Equal Partition Solution (Figure 9) is almost exact, however, as shown in Figure 12.

Idel (43) gives results for triaxial tests on steel and glass spheres. Steel, with a coefficient of friction of 0.19 gave values

* These values are not given in Spencer's publication but taken from a small scale drawing. See note on page 24.



- SPENCER, Glass Ballotini, $f = .126$ $n = .29, .34, .40, .45$
- IDEL, Steel Spheres, $f = .188$ $n = .39, .44$
- IDEL, Glass Spheres, $f = .23$ $n = .37, .41$
- WITTKÉ, Glass Spheres, $f = .29$ $n = .26, .35, .40, .44$

Comparison of Existing Data With Equal Partition Solution

Figure 12

of $\tan \phi$ of 0.44 and 0.29 at porosities of 39 and 44%. These data fit his solution (Figure 2) and that of Spencer (Figure 4) reasonably well but fail to support Wittke's solution (Figure 3). Again, as shown in Figure 12, the substantiation of the Equal Partition Solution is clear. In the tests on glass, with a coefficient of friction of 0.23, Idel found $\tan \phi$ values of 0.71 and 0.51 at porosities of 37 and 41%. These data fit Spencer's solution quite well but can not be fit to that of Idel or of Wittke. A marginal agreement can be seen for the Equal Partition Solution as shown in Figure 12.

Wittke's data (92) on glass spheres results from very careful tests in a special triaxial device. The individual particles (12 and 15 mm.) were packed in hexagonal forms to insure a rather precise rhombohedral arrangement. Great care was taken in determination of the coefficient of friction of the actual spheres used. These tests represent the most accurate known reproduction of the analytic model. With a coefficient of friction of 0.29, $\tan \phi$ values of 0.78, 0.61, 0.34 and 0.21 corresponded to porosities of 26, 35, 40 and 44%. These data do not seem to fall within a reasonable range of the various analytic solutions here reviewed, least of all perhaps that of Wittke himself. In general the analytic solutions lie well above these experimental points. The closest agreement is seen with the Equal Partition Solution as shown in Figure 12, which indicates a more gradual increase in $\tan \phi$ with coefficient of friction.

In summary one might conclude that while none of the analytic solutions can be considered as fully confirmed by existing data,

most of them are reasonable, at least at smaller values of coefficient of friction. Spencer's solution seems best to fit the data obtained with idealized materials at lower coefficient of friction. The Equal Partition Solution appears to give reasonable values over a wider range of f .

It is not the minor differences between the several solutions that should be emphasized, however, but rather the essential similarity. All the solutions reviewed, except that of Caquot, show an exponential increase in shearing resistance with increasing interparticle friction. This implies a shearing strength of the granular system approaching that of the individual particles at large values of interparticle friction. Why this result is not surprising might be illustrated for two spheres only by Figure 5b. Considering only the shear force S one can determine the forces acting in the direction of motion tangent to the spheres at the point of contact. The driving force can be expressed as

$$S \cos \beta ,$$

and the resisting force as

$$f S \sin \beta .$$

It can be seen that once a certain value of f is reached, the resisting force will increase more than the driving force for any addition to the applied shear force.

CHAPTER III

THE EFFECT OF PARTICLE SIZE ON THE STRENGTH
OF GRANULAR MATERIALSTHE SIGNIFICANCE OF PARTICLE SIZE IN THE ARGUMENT OF THIS THESIS

It should be noted that the analytic solution, presented in Chapter II, relating shear strength with grain to grain friction is independent of individual particle diameter*. This fact was considered as a logical and relatively easy qualified check on the validity of the solution. That is, actual independence in real physical situations is a necessary, though not sufficient, condition for confirmation of the solution. Accordingly, this factor has been reviewed in some detail. At the same time, it is believed that this question may hold general interest for some readers.

It must be stressed at this time that the absolute effect of grain size is the subject under consideration. This excludes those effects arising in the case of very small (micron range) particles where the ratio of surface to body forces becomes large. It notably excludes those secondary effects such as porosity, particle roughness, shape and size distribution which frequently accompany a given size in a particular material. In fact these secondary effects must be used to explain some of the data which have been offered from time to time as substantiation of a relationship between particle size and strength behavior. That these secondary effects sometimes regularly accompany a given series of materials has been well

* An examination of the solutions of other writers reviewed in Chapter II confirm that these also show an independence from grain size.

illustrated by Shockley and Garber (71). They found that in the case of natural sands of the lower Mississippi River Valley such factors as grain size distribution, and maximum and minimum dry densities follow directly from the most frequent particle size.

EXISTING BELIEFS CONCERNING THE RELATIONSHIP BETWEEN GRAIN SIZE AND SHEAR STRENGTH

The effect of change in particle size on shear strength of non-cohesive soils is not generally given much attention. This of course arises from the fact of its relative unimportance as a single decisive factor in natural soils. Changes in size are almost always accompanied by other, more significant factors. There exist however, general opinions that size itself has some effect on the shear strength (17).

Several rather positive statements concerning such a relationship appear in recent literature. Caquot and Kerisel (15) state that the angle of shearing resistance increases with increasing maximum grain size. Leonards (52) in discussing the importance of actual particle size states that coarser-grained soils will have higher shear strength, all other factors being equal. Lambe (51), while refraining from a direct statement, implies a similar increase in strength with increasing grain size. It should be noted, however, that Lambe partially qualifies his comments by mentioning generally compaction energy and density relationships. The other writers make no qualification.

The conclusion is then that at least several of the more prominent writers in soil mechanics imply that there is a definite

particle size effect in the shear strength of granular soils. While it would be unfair to state that this represents the opinion of all soils engineers, it seems safe to say that there is not a widespread acceptance of the case for independence of shear strength from particle size.

It seems that this failure is due primarily to the fact that particle size itself is seldom, if ever, varied singly. In the next section this fact will be used to show that most of the data purporting to substantiate a relationship between size and strength, actually fail to do so.

REVIEW OF EXISTING DATA FAVORING A PARTICLE SIZE EFFECT

Relatively little data has been published which lend themselves, even at casual observation, to the support of an argument for either an increase or a decrease of shear strength with increasing particle size. Such data as could be found, however, are critically reviewed in the following paragraphs.

Hennes (38) conducted a series of direct shear tests on gravels and on crushed rock. His results caused him to conclude that particle size has a strong influence on shear strength. Samples of near uniform size ($3/4$ " - $1/2$ ", $1/2$ " - $3/8$ ",#50-#100) were separated by sieving from a rounded particle river gravel and a crushed basalt. A plot of the results of direct shear tests indicated a sharp rise in strength with size up to a particle diameter of about $1/4$ inch. The rise in strength continues, at a more moderate rate for sizes greater than $1/4$ inch. Nearly parallel curves were obtained for the gravel and crushed rock. In this case no effort

was made to secure a constant void ratio; rather a uniform compactive effort was applied to each sample. Only a few values of void ratio, these in the case of individual tests, are given and no trend can be determined. The application of a uniform compactive effort is considered as at least a partial explanation for the results of these tests. When compaction energy (particularly vibratory as in this case) is applied to a granular system body forces act to aid and surface forces to hinder densification. Since body forces increase with the third power (volume) and surface forces with the square (surface) of the linear dimension, an increase in density with particle size can be postulated. This in fact was verified in the previously cited work by Shockley and Garber (71) where it was found that density at a given compactive effort increased significantly with particle size. This was confirmed further in a series of tests with ideal materials performed by the writer and described in a later section.

Parsons (57) reported the results of a large number of direct shear tests that indicated a size-strength relationship. In this case strength increased with decreasing particle size from about 0.6 mm. to 0.1 mm. Above 0.6 mm. strength increased with size through the range tested (maximum 2.8 mm.). Here again a uniform compactive effort rather than constant void ratio was used as a standard. In addition, as pointed out by the author, the possibility of increasing the number of fractured faces and angularity of particles with smaller sizes was present.

In his studies on relative density and shear strength of sands Wu (93) reported data that included shear strength and size for

comparable material. Although the author himself did not state any opinion in his paper regarding a size-strength relationship, he has been credited with two opposing conclusions (43)*. One reader in discussing the paper concludes that the addition of a logical implication allows one to interpret Wu's data as supporting an increase in strength with grain diameter. Actually, the only data given by Wu that implies the existence of a size-strength relationship is a figure showing a plot of initial void ratio versus ϕ for each of three different sands. Representative points (the plots are all straight lines) have been extracted and are shown in Table 1. A consistent decrease in strength with size is evident. In this

TABLE 1
EXTRACT OF SIZE AND STRENGTH DATA, WU (93)

<u>Sample</u>	<u>Mean Size</u>	<u>Standard Deviation (Idel, 43)</u>	<u>Coefficient of Uniformity</u>	ϕ° <u>(e = .45)**</u>
134	.15 mm.	1.4	1.4	46.3
121	.44	1.8	2.6	43.5
133	1.0	2.6	3.0	42

* On page 2 an increase of shear strength and on page 81 a decrease of shear strength with grain size.

** e = void ratio, see note on page 10.

case the increasing values of standard deviation* and coefficient of uniformity** are seen as a possible explanation of the change in strength. Larger values of these parameters indicate a wider or better graded material which should be expected to have lower strength. Since this fact is not generally accepted in civil engineering practice it is covered in more detail at the end of this Chapter.

A series of tests on granular material used in construction of a dam in Switzerland also indicated a decrease in shear strength with increasing particle size (94). In this case also the increase in uniformity with smaller sizes is pleaded as an explanation of this behavior. Table 2 shows pertinent information calculated from data given in the above cited reference.

TABLE 2
SIZE, UNIFORMITY AND STRENGTH DATA, ZELLER AND WULLIMAN (94)

Maximum Size, mm.	U	$\tan \phi$ at $n = 31\%$
1	17.1	1.25
10	53.5	.935
30	76.4	.855
100	145	.791

* Of particle size from the mean value. See Reference 81 for a discussion of standard deviation.

** Coefficient of Uniformity, $U = \frac{d_{60}}{d_{10}}$ where d_x is the diameter of particle for which x% of the particles are finer.

The results obtained by Kjellman and Jakobson (48) are not so easily explained. Here direct shear tests were run on four materials each in a loose and in a dense state. Table 3 summarizes the data concerning the size-strength relationship. It can be seen, as was concluded by the authors, that the coarser material gave

TABLE 3
RESULTS OF DIRECT SHEAR TESTS, KJELLMAN AND JAKOBSON (1955)

<u>Material</u>	<u>Size, mm.</u>	<u>Void Ratio</u>	<u>Average Angle of Int. Friction, deg.</u>
Fine Pebbles, loose	8-11	.685	36.2
" " , dense		.592	42.9
Coarse Pebbles, loose	38-53	.818	37.1
" " , dense.		.698	44.1
Fine Crushed Rock, loose	8-11	1.02	28.4
" " " , dense		.835	34.4
Coarse Crushed Rock, loose	38-53	1.06	31.3
" " " , dense		.835	40.5

higher average strengths in every case. Density obviously is not a factor in this situation as the finer material has a smaller or near equal void ratio when compared with its coarser counterpart. Insufficient information is given to allow a comparison of uniformity or grain size distribution characteristics. This later may be a factor even though the size range is small and sieving procedure

assumed similar. Another factor that may have been of importance is that each of the four materials was taken from a different source and had somewhat different, though similar, compositions. Resulting small differences in angularity or surface texture could cause significant strength changes. Also, only three tests, at different normal stresses, were run on each material. Data scatter was of course significant in so few tests. While actual values were not given, interpolation from graphical presentation indicated a scatter of several degrees (about 5° for the fine pebbles and 4° for the coarse pebbles for the dense material). This can in part be explained by the expected drop of friction angle with increasing normal pressure. Still a rather large deviation remains.

While this review cannot contain all reported cases involving size-strength comparisons, no known case has been left out. It seems that the tentative conclusion that no such relationship is substantiated or well justified.

REVIEW OF DATA SUPPORTING INDEPENDENCE OF STRENGTH FROM PARTICLE SIZE

It is realized that some of the uncertainties mentioned in the preceding section may be operating to a greater or lesser degree in one or more of the cases cited below. This of course must be considered as possibly mitigating the evidence here offered in support of general independence of strength from particle size.

Casagrande (16) commented on the very nearly equal shear strength of two similar sands though the size difference between

the two materials was of the range of one to two orders of magnitude. In this case the samples had similar uniformity and were of the same geologic origin. The porosity factor was reported only as loose or dense and no absolute values are given.

Bishop (3) commented on the very close similarity of shear strength versus porosity relationships for two river bank materials though the size ratio was 60:1. Both materials were rounded and exceedingly uniform. A series of tests over a range of porosities gave near identical angles of shearing resistance. It seems that this data is free of most of the secondary factors noted in other cases.

Work done by Holtz and Gibbs (40) on effect of gravel content on shear strength caused them to conclude that maximum particle size had no measurable effect on shear strength. This conclusion was tempered by the authors statement that the few numbers of large particles in a given sample was probably the decisive factor in these results.

Several series of triaxial tests on quartz sand and glass spheres have been performed recently at Karlsruhe in Germany by Idel (43). Here the author sought to establish the independence of shear strength from particle size in support of his analytic failure criteria referred to in Chapter II. Five sizes of rather uniform quartz sands, at various porosities, ranging from about 0.45 mm. to about 4.5 mm. were used in the first group of tests. The results given by Idel indicate that porosity rather than size governs shear strength. An absolute independence from grain size, however, was not shown. When plotted on a graph showing strength

versus porosity all the points fall within a relatively narrow range. Although Idel does not identify results for any particular grain size, he does state that there was no tendency for any size or size range to seek either limit line of this range. Further tests on glass spheres of 3, 5 and 35 mm. were reported to have given the same results. Idel also ran several tests on a pair of less uniform sands ($U=2.8$) with size ranges of 0.2 - 2.0 mm. and 0.5 - 5.0 mm.. There were so few tests reported that conclusions can not be drawn, but here again no relationship was found. Later work at Karlsruhe by Wittke (92) was also offered as evidence against the existence of a relationship between size and strength. These tests as reviewed in Chapter II were very closely controlled and the results can be assumed equally reliable. Unfortunately, however, only two sizes of glass spheres were used and these of near equal diameter (12 and 15 mm.). As a result no general conclusions can be reached from Wittke's work.

PARTICLE SIZE EXPERIMENTS PERFORMED AS A PART OF THIS RESEARCH PROJECT

While the trend of experimental evidence seems to indicate that individual particle size does not play a role in determining the shear strength of granular media, decisive data has not yet been published. As noted in the preceding paragraphs very few investigators have undertaken tests specifically to determine the particle size effect. Of these only Idel has produced data that can be considered as other than non-conclusive. Since his tests fail to find a definite relationship the situation has yet

to be cleared experimentally.

In order to provide further data on this subject two series of direct shear tests were run on ideal granular materials. These tests and their results are discussed in detail in the following paragraphs.

FIRST SERIES OF TESTS

MATERIALS AND APPARATUS

Direct shear tests were run on five samples of crown barium glass shot to obtain more data on the size effect. The material is described in more detail in Chapter IV. The samples were material taken as that passing a given U.S. Standard sieve and retained on the next smaller sieve. The mean size of the limiting sieve openings was taken as the particle size. Since a complete set of sieves was available and adjacent sieves in the series were used, a constant ratio of mean size to size range was obtained. Assuming a regular distribution of sizes as manufactured, each sample would be a scale reproduction of each of the others. Logic seemed to require that if the ratio d/D^* be kept constant, identical performance for all sizes could be expected. Since it was not feasible to vary the specimen diameter over an order of magnitude (the minimum grain size range to give significant results) it was sought to eliminate this effect by keeping the maximum d/D within safe limits.

* d - diameter of particle.
 D - diameter of sample or test apparatus.

Experience with the subject indicates that a ratio of d/D between $1/5$ and $1/12$ marks the upper limit to avoid the effects of sample size (40, 43, 94). The larger ratio ($1/5$) applies to graded systems that seem to be less sensitive to effect of sample size. A ratio of $1/20$ was selected as the maximum for this series of tests. It was desirable to insure elimination of all effects due to sample size. Further, as pointed out in Chapter IV, the larger sizes of glass balls possess a smaller degree of sphericity. At a size of about $3 - 3\frac{1}{2}$ mm. this loss of sphericity becomes notable. As a lower limit was taken a mean size of 0.46 mm.. This was dictated largely by static electricity effects that made it impossible to control density on smaller particles. Even with the 0.46 mm. size, tests were suspended on particularly dry, cool days that produced an increase in the surface electric effects.

A standard direct shear box with 2.5 inch (63.5 mm.) diameter sample container was used. The normal load was applied with air pressure by means of a calibrated bellows, loading yoke, and plate placed directly on the sample. The upper box was held fast while the lower box was drawn at a constant rate thereby shearing the sample. Normal load was determined from the bellows calibration, which was checked against a known proving ring before the tests. The shear force was measured with the proving ring and displacement dial gage

furnished by the manufacturer of the direct shear machine. Normal and shear displacement were measured with dial gages.

PERFORMANCE OF TESTS

The materials were placed in the shear cup with a void ratio of 0.62. Application of normal load reduced this to a fairly constant value (0.605 - 0.610) which was taken as the initial void ratio.

The selection of this placement void ratio (0.62) is worthy of a few words. Preliminary experiments were made applying a uniform compactive effort to each sample. The samples were placed in three layers. After each layer was in the box a five pound cylindrical weight was placed on the material and the entire assembly (upper and lower cup, sample and weight) was vibrated for one minute on the base plate of a sieve shaker*. The weight of material placed in the known volume of the cup was noted and the sample loaded and sheared. Twenty-one tests were run at a normal pressure of 40.7 psi. While there was a scatter of results two trends were evident. First, an increase in strength with sizes was noted, and second, void ratio increased (from 0.53 to 0.62) for the smaller particles. This result is considered similar to that of Hennes (38) which was reviewed earlier in this Chapter. These preliminary tests

* Trials showed that approximately one minute is the optimum time for the materials used. In more carefully controlled tests on similar materials (larger glass spheres) Leussink and Kutzner (53) found in all cases that 80%-95% of ultimate densification occurred within the first minute.

served to illustrate the effect of a standard compactive effort criterion and the resulting pattern of shear strength behavior. In addition, technique of running the tests was improved considerably and minor modifications to the shear machine were found to be required. The outcome was more consistent and reliable results in the main series of tests. Further work showed that a void ratio of 0.62 could be obtained readily with all materials and consequently this value was taken as the standard for future tests. As indicated above, the smaller material required a definite compactive effort, while larger sizes fell readily to this density with slow pouring and some shaking. The coarsest material was poured as rapidly as possible and settled easily to the required void ratio. Placement factors that affect the density of granular materials are discussed by Kolbuszewski (49).

During the preliminary tests it was noticed that the upper cup and its restraining collar tilted significantly as shearing progressed. This may have accounted for some degree of the data scatter obtained. In order to avoid this problem in the main series of tests the upper cup was secured to the collar and the collar in turn bolted to the fixed buttress of the machine. This insured that the upper cup remained perfectly rigid throughout a given test. A clearance of 0.015 inch (0.38 mm.) was set between the lips of the

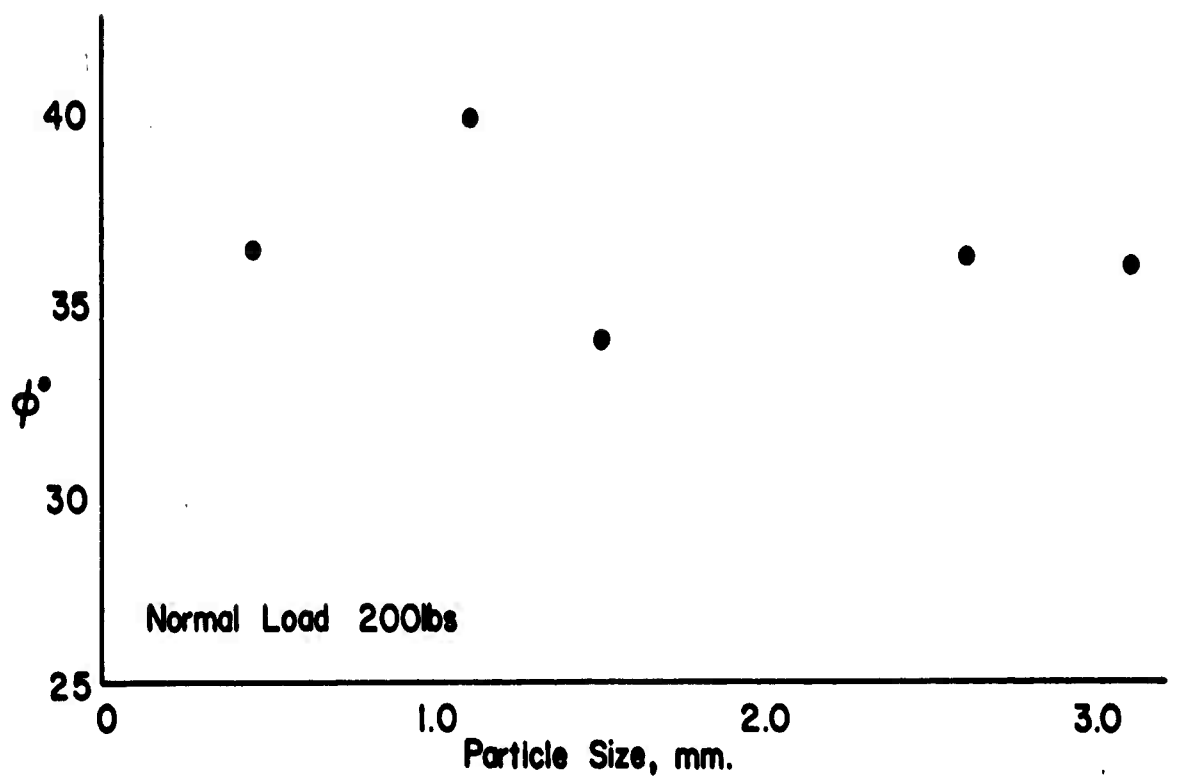
upper and lower cups. This distance was large enough to be easily maintained and small enough to prevent escape of the smallest size particles used in the tests. Rate of shearing was approximately 0.03 inch per minute.

DISCUSSION OF RESULTS

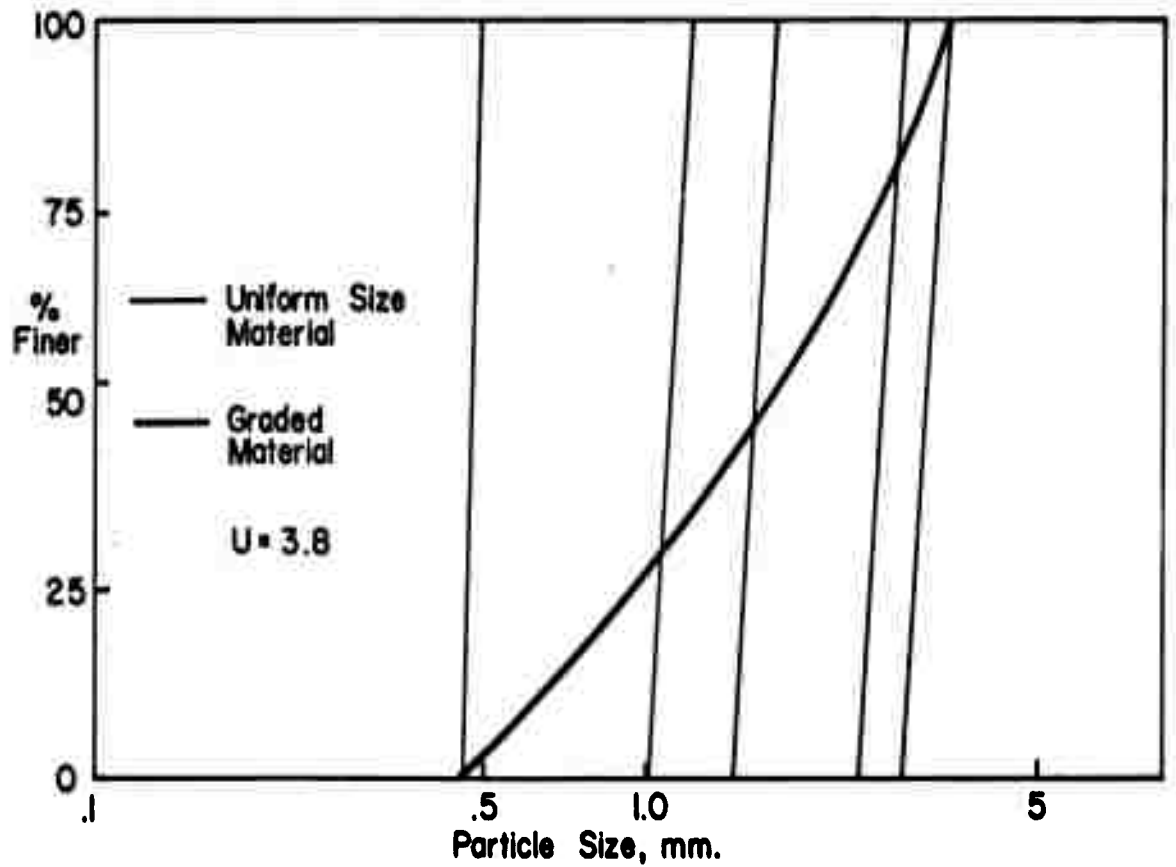
Tests were run on five distinctly sized samples of glass shot. These were designated by the mean particle size, taking as limits the openings of the pair of standard sieves bounding the sample. The sizes used were:

<u>Size, mm.</u>	U.S. Standard Sieve Number	
	<u>passed</u>	<u>retained</u>
.46	35	40
1.1	16	18
1.5	12	14
2.6	7	8
3.1	6	7

Results are shown in Table 4 and on Figure 13. Mean values are given. Most of the tests were run at a normal load of 200 lbs (40.7 p.s.i.). Additional tests at 350 lbs (71.2 p.s.i.) were run on the largest and smallest sized materials as a general verification. These tests gave slightly smaller angles of shearing resistance as is common for increasing normal loads (51).



a. Angle of Shearing Resistance ϕ° vs Particle Size



b. Grain Size Distribution

Size and Strength Relationships for Glass Spheres

Figure 13

TABLE 4

RESULTS OF DIRECT SHEAR TESTS ON GLASS SHOT

<u>Size</u>	<u>Normal Load</u>	<u>ϕ</u>	<u>Relative Standard Deviation*</u>	<u>Number of Tests</u>	<u>Initial Void Ratio</u>
0.46 mm.	200 lbs	36.4°	4.1 %	10	.608
1.1	200	40.3	5.9	5	.608
1.5	200	34.1	3.3	10	.608
2.6	200	36.2	4.0	10	.609
3.1	200	36.0	1.7	6	.608
0.46	350	35.8	4.2	6	.608
3.1	350	35.7	3.4	10	.607

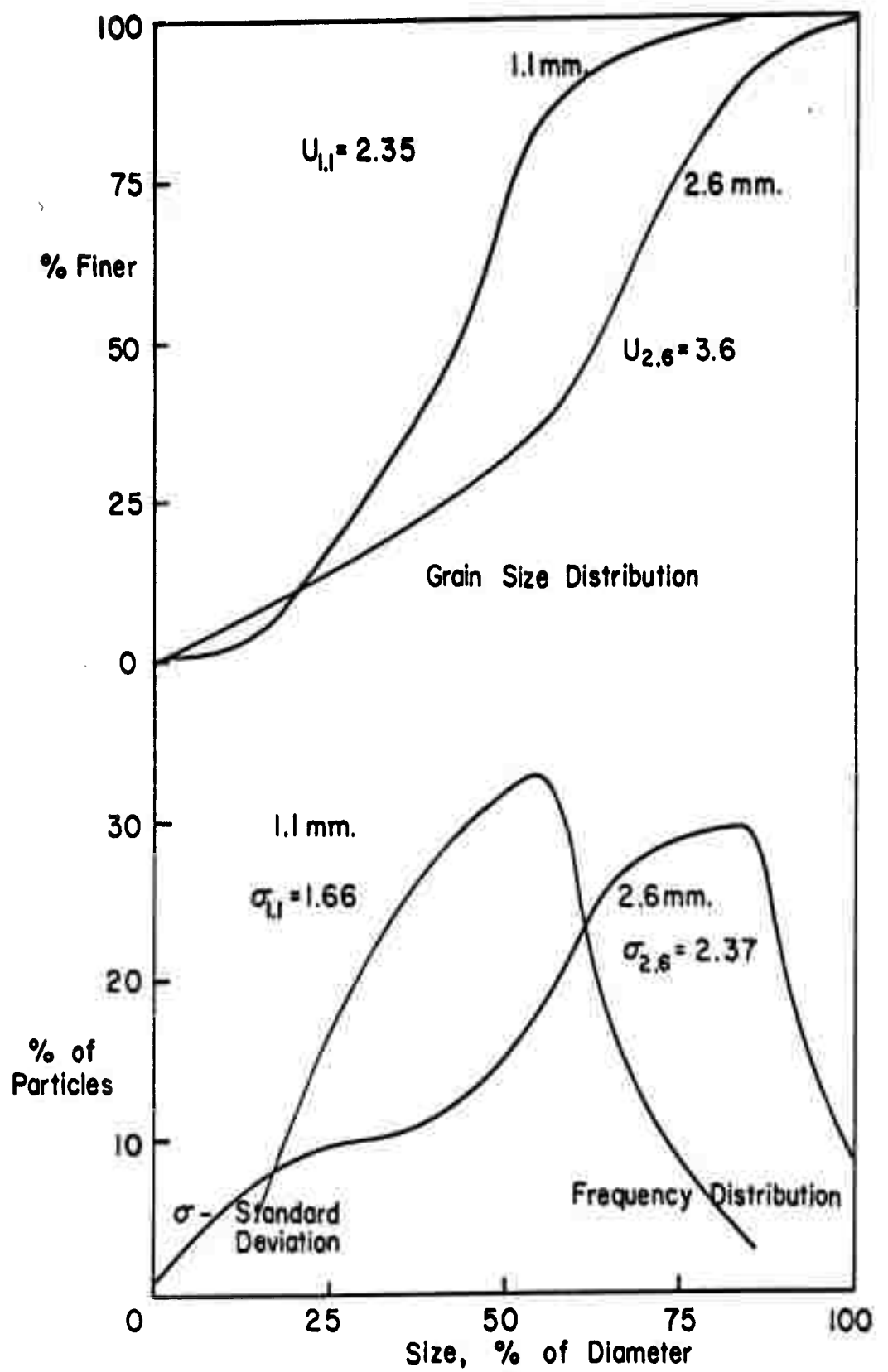
As can be seen from the data presented, a general relationship between shear strength and particle size can not be substantiated. It had been expected that each sample would show the same angle of shearing resistance as size was the only parameter intentionally varied. Since this did not prove to be the case an effort was made to determine a possible cause of the high shearing resistance found for the 1.1 mm. sample. It was initially suspected

* Of peak failure load from mean value. See Reference 81 for discussion of relative standard deviation.

that a variation in the gradation or particle size distribution may be a possible explanation. A more uniform gradation (lower coefficient of uniformity or lower standard deviation of particle size) should result in greater strength as ascertained earlier and discussed more fully at the end of this Chapter. Accordingly an optical particle size distribution analysis was performed on the 1.1 mm. sample and on the 2.6 mm. sample so that a comparison might be made. A binocular microscope with stage micrometers was used to measure the diameter of several hundred particles of each sample. This allowed construction of the size frequency distribution and grain size (summation) distribution curves and calculation of the coefficient of uniformity and the standard deviation. The results are shown on Figure 14. In the Figure the data shown have been reduced to a common unit diameter so that curves could be superimposed for comparison. The greater uniformity of the 1.1 mm. material is offered as a probable explanation for its greater strength.

SECOND SERIES OF TESTS

As indicated previously it was hoped that each sample in the first series of tests would yield the same angle of shearing resistance. A probable reason for the only significant variation has been offered in the preceding paragraph and thus the tests can be considered at least moderately successful. Since the variations are assumed to be due to



Grain Size Analysis, 1.1 and 2.6 mm. Glass Spheres

Figure 14

the fact that the glass shot used is not actually a uniform ideal material, an attempt was made to further limit this shortcoming by use of another model. Accordingly, low grade carbon steel precision bearing balls were selected for the next series of tests. Sizes used were limited by the cost and the previously discussed d/D ratio and were $1/8$, $3/32$ and $1/16$ inch (3.18, 2.38 and 1.59 mm.) balls.

In selecting a void ratio which could be readily obtained for all three size balls two interesting factors were noted. First, the void ratio obtained easily by the glass shot could not be duplicated with the bearing balls. A higher initial void ratio (0.66) had to be used. This is what one should expect in the case of the more uniform precision balls. This will become more clear after the discussion on gradation effects at the end of this Chapter. Second, the ease of obtaining the selected void ratio increased as the size decreased. This is contrary to what one should expect from normal experience and from the results with the glass spheres reported earlier in this Chapter. This situation proved to be a preview of the rather unexpected results of the subsequent direct shear tests.

The balls were treated as uniformly as possible. They were washed first in benzene and then in acetone, dried with compressed air and stored in a warm (70°C) oven until just before use. All tests were run at the same void ratio, normal load and rate of loading and procedure was as described previously for the glass shot. Contrary to the expected

results, however, shear strength was greatest for the largest balls, least for the smallest balls, and an intermediate value for the middle sized balls (33', 31' and 25'). While only three tests were run on each sample there was very little deviation and no reason to expect that additional tests would alter the obvious trend.

A binocular microscopic examination of the balls indicated a definite increase in surface roughness with size. This would account for a higher shear strength and for the increased difficulty of packing the larger sizes. This seems very similar to the experience reported by Jakobson which was mentioned in Chapter II. The second series of tests, therefore, were considered non-conclusive as regards the effect of size in shear strength determination. The series is not, however, considered to be a failure as it illustrates the extreme difficulty involved in controlling test variables. If precision bearing balls, even though low quality, differ so radically due to uncontrolled surface differences one can expect even greater problems with natural materials. The shear test results obtained with the steel balls could easily be taken as strong evidence for a direct size-strength relationship in the absence of the other data given here.

EFFECT OF GRADATION ON SHEAR STRENGTH OF GRANULAR MATERIALS

It has been pointed out by Winterkorn (89) that a system of uniform particles, at a given density, can be expected to have more resistance to deformation than a well graded material at

similar density. A general belief exists, however, among civil engineers that, all other factors being equal, well graded granular materials will give greater shearing resistance than those with a more uniform particle size. This belief is illustrated and reinforced by statements to that effect in recent text and handbooks (47, 51, 52, 77). Existing data, however, do not substantiate such an ascertainment and in fact indicate the contrary. Such published data which lends itself to analysis in this regard will be reviewed in the following paragraphs. In addition, an attempt will be made to show that confusion on this point originates primarily from a failure to differentiate clearly between absolute and relative densities.

The commonly accepted civil engineering measure of uniformity is the previously* defined uniformity coefficient U . In general, the larger the value of U , the less uniform is a material. A material with all particles identically the same size would have a uniformity coefficient of 1.0. Since the uniformity coefficient considers only the ratio of diameters for two arbitrary percentage points in a normal gradation curve it is not necessarily representative of the sample as a whole. Possibly standard deviation or relative standard deviation* is a more satisfactory parameter for describing the uniformity of particle size for a given material. It seems obvious that larger deviations from the mean particle size will indicate less uniform material. It should be made clear again that increasing values of the uniformity coefficient (U) also mean a

* See notes on page 45 and page 55.

less uniform material. In general the uniformity coefficient will be given for the materials covered in the following cases. This is, of course, because it is most frequently reported by engineers and is easily computed from the gradation curve.

The data shown in Table 5 was given by Bishop (3) and concerns generally similar river sands and gravels. It illustrates well the increase in strength with uniformity. The grain size distribution curves of two uniform materials, 4 and 5, bound the curves of others.

TABLE 5

STRENGTH AND UNIFORMITY DATA ON RIVER SANDS AND GRAVELS, BISHOP (3)

<u>Material</u>	<u>Maximum Size, mm.</u>	<u>Minimum Size, mm.</u>	<u>U</u>	<u>n = 36</u>	ϕ° <u>n = 38</u>
1	25	0.2	29.2	38	36.6*
2	43	0.2	2.1	37	----
3	6.4	0.2	2.6	39	35.7
4	0.6	.2	1.5	44*	41.1
5	38	15	1.2	46	41.8

* projected

Because of the shape of the curves, only material #1 is well graded in spite of the low values of U for #2 and #3.

Chen (18) has reported considerable data concerning the shearing resistance of various aggregates. Only a very limited number of his results, however, lend themselves to an evaluation of the strength versus gradation problem. These are given in Table 6.

TABLE 6

STRENGTH AND UNIFORMITY DATA ON NATURAL AGGREGATES, CHEN (18)

<u>Material</u>	<u>Particle Shape</u>	<u>Size, mm.</u>	<u>U</u>	<u>ϕ° at $e = 0.3$</u>
A Well graded gravel	subangular	11	40	44
B Gravel	subangular	11	10	47.5
C Gravelly Sand	subangular	4	10	49
D Well graded sand	subangular	2	10	49

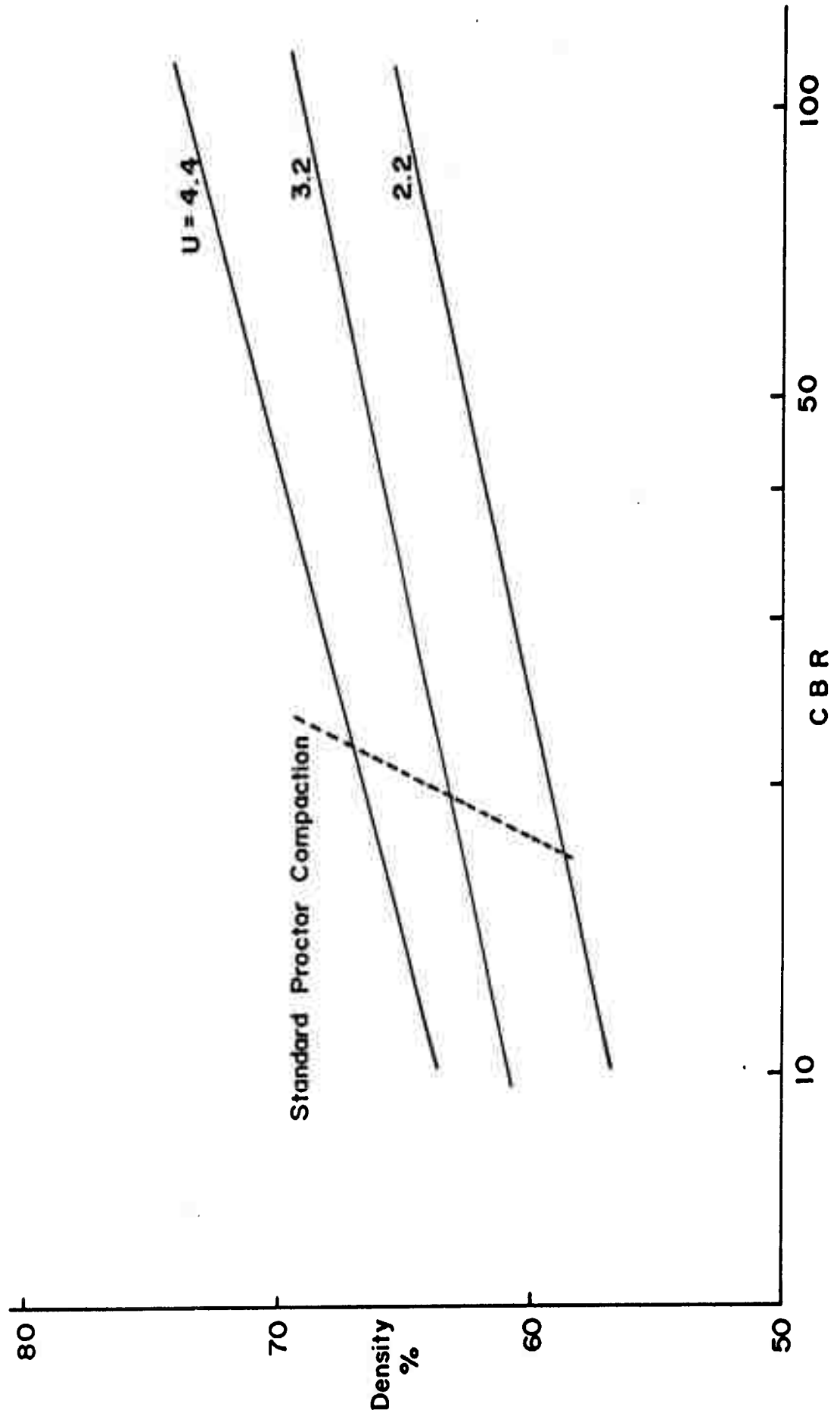
In spite of the results shown, Chen concludes that shearing strength increases with increasing coefficient of uniformity. It must be assumed that this conclusion was formed on the basis of the performance of materials with different initial void ratio and particle shape. The only data which can properly be compared leads to precisely the opposite conclusion.

Computations made from data given by Hennes (38) also show an increasing shear strength with uniformity (decreasing uniformity coefficient). Four river gravels, $\frac{1}{2}$ " maximum particle size, with computed U of 392, 36, 13 and 1 gave $\tan \phi$ values of 0.86, 0.93, 1.07 and 1.17 respectively. Initial void ratios were not given, but the test procedure involved a uniform compactive effort for each aggregate. This would mean a larger void ratio for the more uniform material, other things being equal, hence magnifying the effect of the results given above.

An interesting case evolves from a critical review of Idel's comments on the work of Siedek and Voss (73). Idel reports that these authors found an increase in resistance with increasing uniformity coefficient*. A review of the cited paper indicates that in fact this conclusion was reached by Siedek and Voss. A closer scrutiny of the data, however, shows that CBR** increases with uniformity for a given dry density. Figure 15 is based on data taken from Siedek and Voss with an assumed specific gravity of 2.65 for the material. This apparent discrepancy results from a use of a different standard for comparison. If one makes the comparison on the basis of absolute density, the more uniform material shows a greater strength. On the other hand if one uses the Standard Proctor (51) compactive effort as a basis, the less uniform material has a greater strength. Siedek and Voss, writing in a highway research publication, obviously intended the Proctor test with a uniform compactive effort as the standard for comparison. Idel, though his report deals exclusively with absolute densities fails to point this out.

* Page 5, Reference 43.

** California Bearing Ratio, a strength or bearing parameter. Larger values of CBR indicate a more resistant material. See Reference 51.



Density, CBR Relationships, Siedek and Voss

Figure 15

Idel makes a similar error of omission in referring to the work of Jahn (44). In pointing out that Jahn found greater shear strength with material graded in accordance with Fuller's criteria (26) he fails to indicate that a uniform compactive effort was applied to each of the materials. If one does not recall that the Fuller criteria establishes a gradation with maximum workability (the opposite of shear strength) he may be misled. If he does recall this fact he may be confused by Idel's statements.

In both of these cases, as in many others, a dense well graded aggregate is compared with a loose uniform material and misleading general conclusions are drawn. The well graded aggregates were found to possess greater workability with maximum density in both the concrete construction and highway fields. They have come to be generally favored for these applications, but for workability rather than shear strength (89).

To further illustrate the validity of the ascertions outlined herein, some tests were performed on a graded mixture of the five uniform samples mentioned earlier in this Chapter. The grain size distribution curve of the graded mixture is shown in Figure 13b where it is compared with the uniform materials. Each of the uniform materials has an angle of shearing resistance of 34° - 36° (except the 1.1 mm. size which was discussed previously). The question of shear strength as a function of gradation then might be answered by comparing strength values of the graded mix with this value. Attempts to place the graded material at a comparable (0.608) initial void ratio were completely unsuccessful. The graded material settled naturally to an initial void ratio of

0.511. Using procedures as close as possible to those of previous tests, an angle of shearing resistance of 32° was found. Although it is almost axiomatic that an even smaller angle would be found at a higher void ratio such as 0.608, a further comparison was made. The graded mixture was subjected to a compactive effort similar to that applied to the smaller sizes of uniform material. In this case a void ratio of 0.439 and a shearing angle of 36.4° were obtained. If these values are applied to equation (9)

$$\tan \phi = \frac{C}{e - e_{\min}}$$

which was discussed in Chapter II, the parameters e_{\min} and C can be computed. This allows one to compute an angle of shearing resistance of 27.5° for an initial void ratio of 0.608. As mentioned in Chapter II this equation has been checked in a large number of cases of natural granular materials and with uniform glass spheres with very good results. Although it is applicable to systems with uniform sized particles it seems reasonable to permit its use in a qualitative manner, at least, in this case. Even allowing a large margin of error, 25% or more, a lower shear strength of the graded material at equal initial void ratios is shown.

SUMMARY

It appears clear that particle size as such does not influence the shearing resistance of a granular material. On the other hand it is nearly impossible to vary particle size alone while holding all other variables constant. So in effect there is in real

materials a secondary particle size effect that results from changes in other variables such as surface roughness, density and gradation which alters shear strength with size. Confusion on this point results from a failure to recognize the change in strength as issuing from the secondary variables.

It is also clear that, at a given absolute density, a uniform material has in general a greater shearing resistance than a well graded material. Confusion on this point has resulted from a failure to consider the questions of absolute and relative density. Because of their tendency toward easier densification well graded aggregates may be more resistant to shear than uniform materials, after densification at a standard compactive effort.

CHAPTER IV

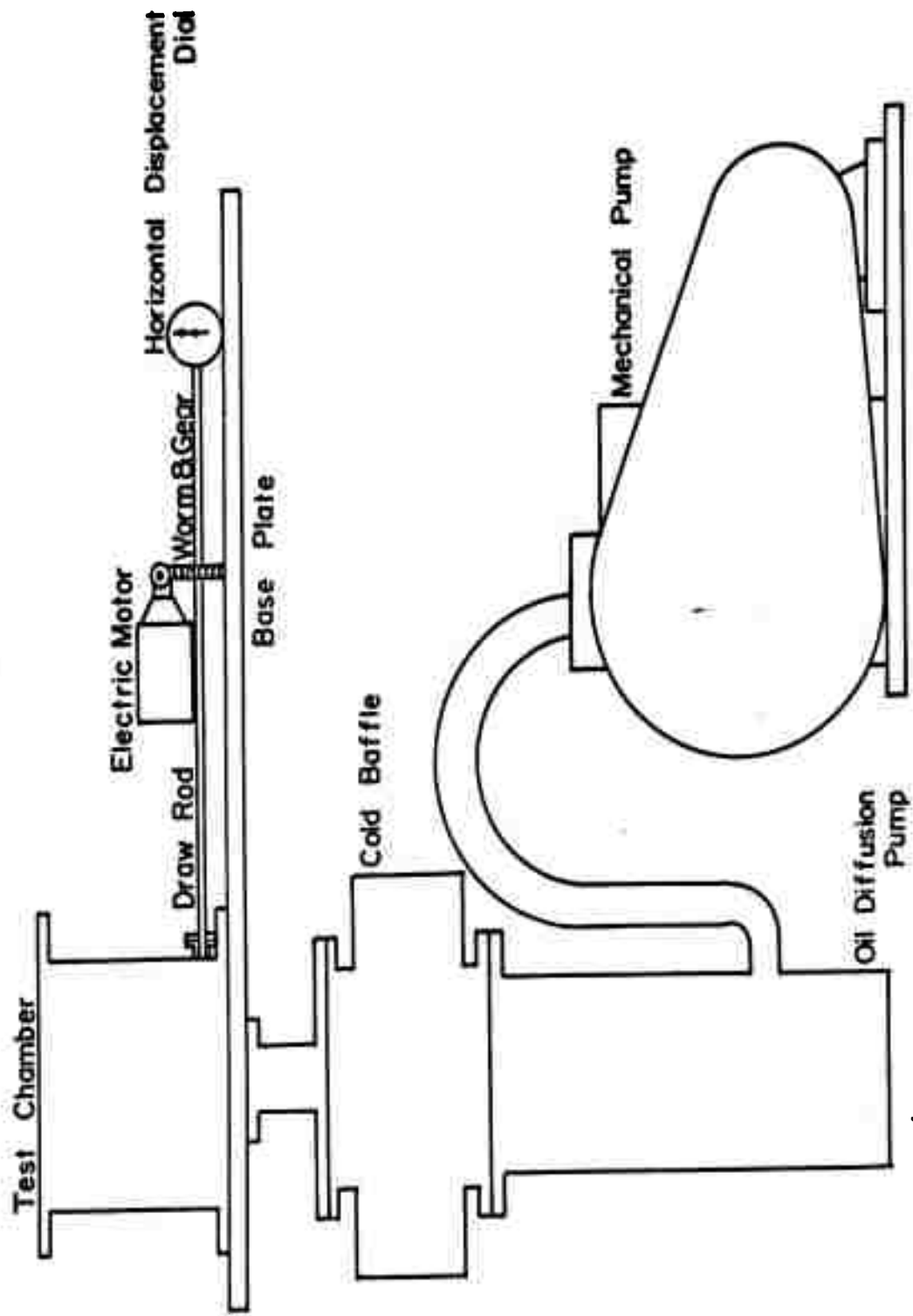
APPARATUS, TESTS AND RESULTS OF EXPERIMENTAL PROGRAM

In order to test the basic premise of this thesis and to meet the other objectives of the project which are outlined on page 13, a series of direct shear tests on ideal granular materials have been performed. These tests, the apparatus used and the results obtained will be discussed in this Chapter.

APPARATUS

The apparatus consists of a direct shear device operating within a vacuum test chamber. The test chamber is an eight inch diameter by six inch stainless steel cylinder resting on an aluminum base plate which is bolted to the supporting framework. A photograph of the apparatus is given as Plate I and a schematic diagram is shown in Figure 16.

The sample is placed in a two and one-half inch diameter by one and one-half inch aluminum shear box. The shear box consists of a fixed upper cup and a moveable lower cup. The bottom cup of the shear box moves on 52100 chrome steel balls in a brass ball track attached to the bottom of the cell. The ball track and the ball contact surface of the cup are coated with a dry film molybdenum disulfide lubricant (Molykote X-15). The upper cup is held firmly by a brass collar attached to the floor of the cell by means of a fixed buttress. The height of the upper cup, hence the spacing



Schematic Diagram of Apparatus

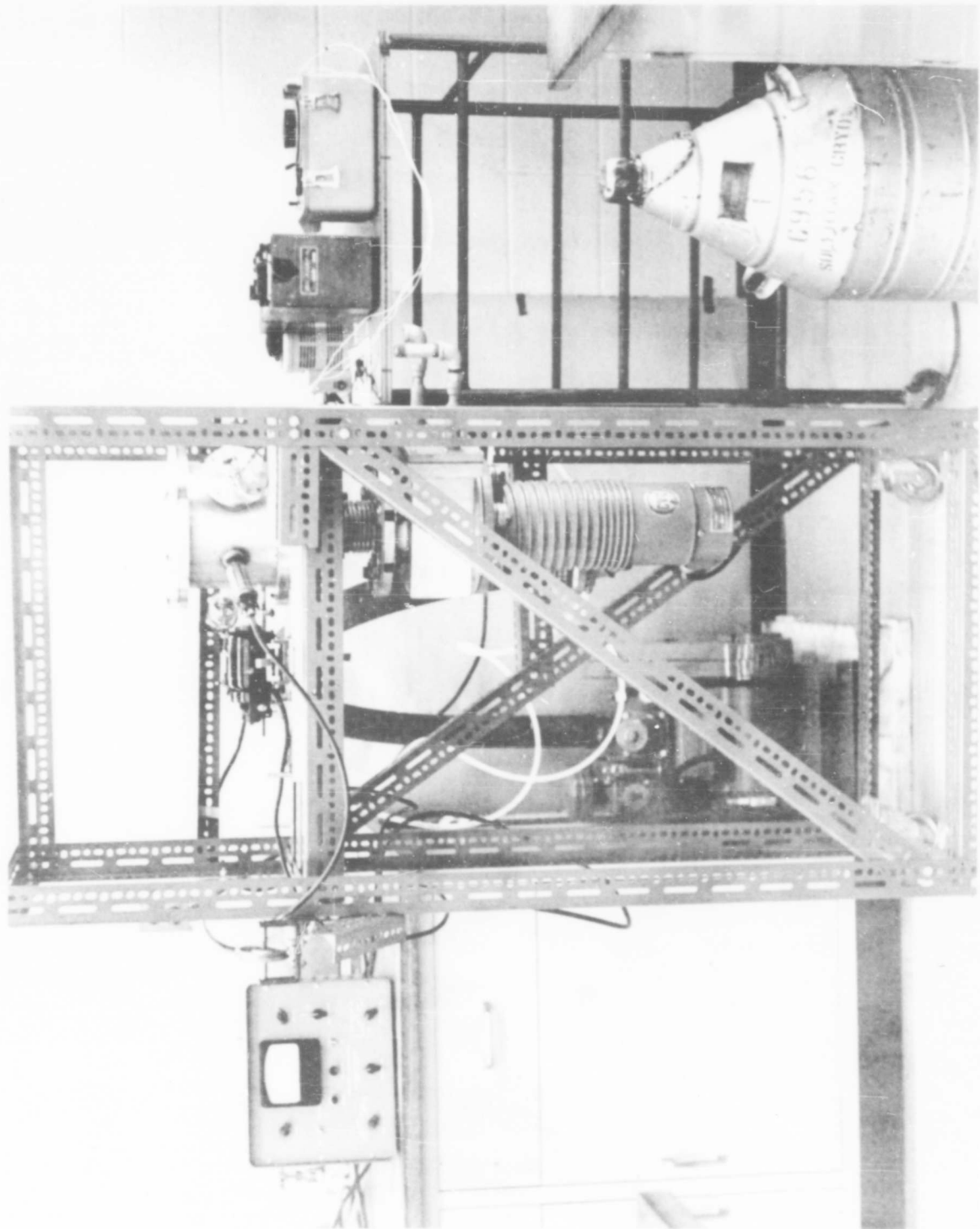


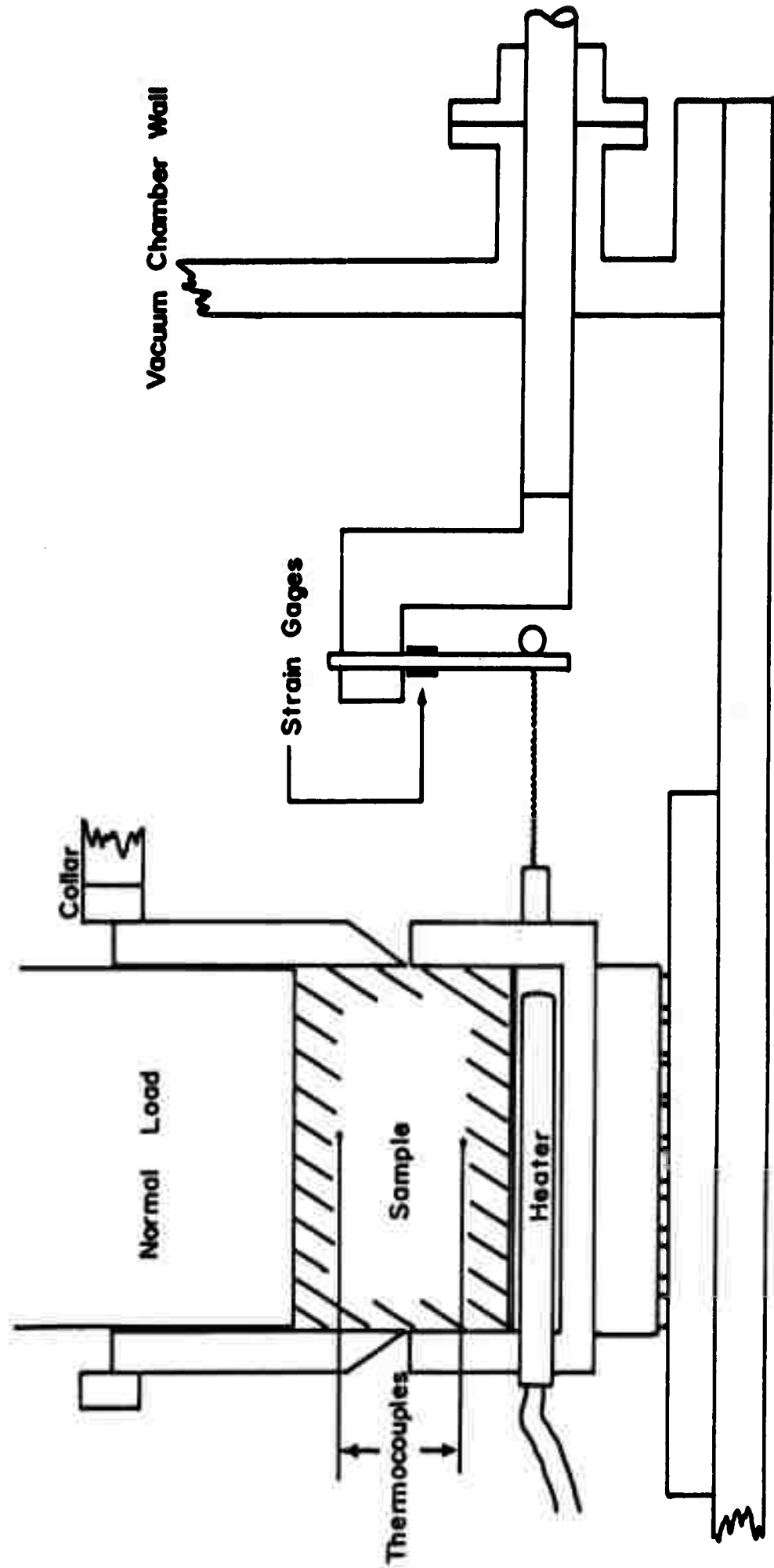
PLATE 1

between upper and lower cup lips, can be varied.

Normal load is applied by means of a 2 3/8 inch diameter steel cylinder placed directly on the sample. Shear force is measured by means of electric resistance strain gages cemented to a metal load cell (bending strip) mounted in an aluminum Z bar as shown in Figure 17. The Z bar is fixed on the draw rod which transmits horizontal displacement into the test cell. The motion is transferred to the lower shear cup by means of a short piece of fine wire clamped to a fitting which screws onto the cup. The wire passes through a hole in the metal bending strip and is secured by a silver solder ball thus making a moment free connection. The force is determined by comparing strain gage readings with a calibration curve previously determined by applying known loads.

A constant shear displacement of 0.067 inches/minute is applied through the draw rod by means of a 1/150 h.p. electric motor mounted outside the test cell. Horizontal displacement is measured with a dial indicator at the end of the draw rod.

Access to the test cell is obtained by removing the eight inch diameter cover plate which is secured by means of an aluminum collar bolted to the test cell. One-half inch plate glass and aluminum have been used alternately for the cover plate. Glass has the advantage of allowing visual inspection of the shear device during the test. An electric access port with eight studs and a one-eighth inch pipe thread nipple are attached to the wall of the test cell. The draw rod passes through a standard access flange. Connection to the pumping system is made with a two inch (I.D.) standard flange on the bottom of the test chamber. Neoprene O-rings



Detail of Shear Device

Figure 17

with Apiezon "L" grease are used with all flanges and plates while Glyptal varnish is used with threaded connections.

Certain components of the apparatus merit a more detailed discussion which is given in the following paragraphs.

LOAD CELL

The bending load cell, shown in Figure 17, was selected after attempts to use a simple tension strip failed. In order to attain the sensitivity required (0.10 lb or less) a straight metal tension strip must have a very small cross-section, resulting in a very flexible and insecure load cell. The bending strip arrangement, however, provides two basic advantages that allows a much thicker and more stable cross-section and a more easily handled load cell. The first advantage follows immediately from the great increase in stress which results from application of a given load in bending, over that which results from direct (tension or compression) loading. Second, the bending load cell can be used with the temperature-humidity compensating (dummy) gage as an additional active unit thereby doubling the strain for any given load. This is true because one strain gage is in tension and one in compression since they are on opposite sides of the neutral axis of the bending strip. This can be seen in Figure 17.

Four different metal strips have been used in conjunction with the Z bar to make up a working load cell. The strips are one and three-quarters inches in length. This gives an average one inch moment arm, measured from the previously mentioned

fine wire, the line of force application, to the center of the strain gages. Thickness of the strips varies from 0.032 inch to 0.064 inch depending upon the sensitivity desired. For most purposes a sensitivity of 300 microinches per inch per pound was considered adequate. One cell, constructed of stainless steel, gave a sensitivity of 1200 microinches per inch per pound. This was used in some of the coefficient of friction measurements where total shear force was of the order of approximately one pound. Small SR-4 strain gages, both wire grid and metal foil type, have been used. Teflon insulated lead wires are used to connect the gages, by means of soft solder, to studs in the electric access port of the test chamber.

Beryllium-copper was used first as a metal bending strip because its ratio of yield stress to modulus of elasticity is unusually high. While the material varies widely depending upon processing details, an assumed value for modulus of elasticity of 18,000,000 p.s.i. is reasonable (42, 75). The strip actually used in the load cell was stressed to 90,000 p.s.i. during calibration without loss of linearity of the stress-strain curve. Because of the known sensitivity of beryllium-copper the load cell was recalibrated after each exposure to elevated temperature; the test chamber being cooled to room temperature before each measurement. Paper backed wire grid strain gages, Type A-13, were used with the beryllium-copper strip. Because of uncertainties regarding the vapor pressure of normal strain gage cements an epoxy

resin, Hysol R8-2038 with hardener TH2-3520, was used. In addition the strain gages were coated with a thin film of epoxy to avoid possible evaporation of the paper cement which forms a part of the gages. Although the epoxy used is designated as a type which cures at room temperature, the load cell was heat treated for one day at 180° F.

Two Type 305 stainless steel load strips were constructed in an effort to obtain a material free of the temperature sensitivity of beryllium-copper. One strip, approximately 0.032 inches thick was used to measure tangential force in determination of coefficient of sliding friction as indicated previously. This strip performed reasonably well. The other steel strip, however, did not maintain a constant force-strain ratio for all the tests. The reason for this behavior is not known, but very possibly it is due to the failure to heat treat the cell after application of the epoxy as was done with the other strips. In general the strip became less sensitive with age, indicating the possible hardening of the epoxy located at a maximum distance from the neutral axis. The results obtained with this load cell were not always in harmony with other test results and the expected trend. This will be mentioned briefly in the discussion of the test results.

The last bending strip used is made of Inconel X with bakelite backed foil strain gages. Inconel X is relatively insensitive to temperature, has a reasonable modulus of elasticity ($25-32 \times 10^6$ p.s.i.) and a high proof (yield) strength; 82,000 p.s.i. at room temperature, and 77,000 p.s.i.

at 425°C (75). The bakelite backed gages are secure in the 200°C temperature range when applied with EPY-400 cement and properly heat treated. This cement was used with a four hour temperature cure (2 hours at 400°F, 2 hours at 450°F) as recommended by the manufacturer for 200°C use. This cell gave the most consistent load-strain relationship and showed almost no zero drift of the strain readings upon removal of load. A zero drift of 2-4% was common for the other cells.

Strains were read manually by means of a battery operated strain gage indicator (Strainert). Direct readings to 10 microinches per inch are possible, with interpolation to 5 microinches per inch. In the direct shear tests performed in this project readings of that accuracy were impossible because the load was constantly changing. Between 20 and 30 microinches per inch were easily read, however, and load cell thickness was determined on this basis. The strain readings were compared with previously calibrated curves to give shear force in pounds directly. Calibration was performed by means of a fine wire with a detachable hook and silver solder ball similar to that used for connecting the load cell to the lower shear cup. The load cell, including the Z bar, was clamped in a vice, the wire passed over a low friction pulley and known weights applied to the hook, hence to the load cell. The pulley and a platform for the vice were attached directly to the framework of the apparatus facilitating frequent calibration of the load cell.

HEATING AND HEAT CONTROL EQUIPMENT

Desorption or outgassing of adsorbed surface molecules is a chemical rate process which varies exponentially with absolute temperature (29). In order to expedite the desired effect, or perhaps even to cause it to occur to a measureable degree, heat must be applied to the surface involved. In this apparatus heat is supplied direct to the sample by means of a small ($3/8$ " x $1\frac{1}{2}$ ") 85 watt incoloy sheath heater (Chromalox CI-201C). The heater is placed under a false bottom in the lower shear cup as shown in Figure 17. Lead wires are glass insulated and soft soldered to studs in the electric access port. The proximity of the studs dictated the use of ceramic hollow bead insulators around the inside connections and thin sheet mica isolating the external power connections. Power is controlled by means of a hand operated variable transformer (Powerstat 3PN-116). Because of the constant danger of shorting out the line voltage power supply the transformer is fused and furnished with a ground wire. In addition the apparatus framework is grounded to a water service line by means of heavy braided copper wire.

Temperature is measured manually by means of two iron-constantan thermocouples operated by a portable potentiometer (Wheelco 310). The thermocouple wires are fibre glass insulated with the welded tips covered with a thin protective coat of sodium silicate. The hot junctions may be placed at two levels in the sample, as shown in Figure 17, or elsewhere within the test cell. The thermocouple wires are soft soldered to each

side of the studs in the electric access port and taken directly to the potentiometer terminals. Calibration to 100°C has shown that this results in an error of less than 2°C. Although each thermocouple is composed of two wires, both are installed using only three studs in the electric access port. The negative (constantan) wires are soldered to a common stud.

VACUUM EQUIPMENT

The vacuum producing equipment consists of an oil diffusion pump, mechanical pump and baffle with thermocouple and ionization gages for measuring pressure. These are standard components for vacuum systems. Reference (67) contains a short general discussion of current vacuum practice. The initial testing was performed in a vacuum produced by equipment which was temporarily excess in another department and thus available for use on this project. After initial favorable results were obtained, properly sized pumps and a baffle were acquired for continuing use in the Program, the initial phase of which is described in this thesis.

The initial equipment centered on a 60 liter per second (Consolidated MCF-60) fractionating oil diffusion pump*. This was backed by a 5 cubic feet per minute two stage rotary mechanical pump (Welch Duoseal 1402B). Between the pump and chamber a 2 inch diameter by 24 inch optical baffle was installed. A two compartment cooling jacket allowed the use of water and/or liquid nitrogen to lower the temperature of the baffle plates and further reduce the possibility of

* See References 23 and 59 for a detailed description of vacuum equipment and technology.

backstreaming of the pump oil molecules into the test chamber. Pressure gages used include a thermocouple (National Research Corporation 501) and ionization gage (NRC 507) operated by a combined gage control (NRC 710B). The gages are attached, by means of pipe threads, directly to the test chamber. Ultimate pressure reached in the test chamber, with sample, using this equipment and liquid nitrogen was 1.5×10^{-5} torr*.

The permanent replacement equipment was selected on the basis of an operating pressure of 10^{-7} torr. Pressures below this range are, in general, best achieved by applying heat (baking out) to the entire apparatus to expedite outgassing. Without bake-out, 10^{-7} torr is a minimum pressure that can be reasonably expected with moderately priced (\$1000) pumping equipment. Based on this pressure, and an approximate interior chamber surface area of 300 square inches, a required diffusion pump capacity of 500 liters per second was determined (67). The pump which was selected is a Consolidated Vacuum PMC-720. This is a four inch nominal diameter pump rated at 720 liters per second without a baffle. A matching chevron baffle is used with the pump reducing the rated speed to 300 liters per second. A 27 cubic feet per minute mechanical pump is recommended for maximum capacity operation. On the other hand, pumps rated as low as 5 cubic feet per minute can be used with the PMC-720. In an attempt to balance cost with desired performance a 13 cubic feet per minute (Welch Duoseal 1397B) was acquired for use with the diffusion pump.

* torr = 1 mm. Hg.

The NRC gages and control described above are installed on the permanent system.

MODIFICATIONS

Experience with the apparatus indicates a need for two major modifications or additions that should result in considerably lower ultimate pressure and ease of operation.

First a refractory lined hood or oven or heating cover for baking out the entire test cell should be installed. This would allow application of heat to all parts of the apparatus which are exposed to low pressure, thereby expediting out-gassing and yielding lower ultimate pressure. Associated with this modification would be the replacement of the brass portions (collar, ball track, buttress) of the apparatus with steel or aluminum. This would avoid the now present problem of the relatively high vapor pressure (10^{-5} torr at 210°C) of zinc. Early experience with the apparatus showed that the temperature of the brass portions was considerable below that of the sample during normal heating. Until this was determined, however, the vapor pressure-temperature curve of zinc controlled the operation. Heating of the entire apparatus will again present this problem unless the brass elements are removed. Incident to such a bake-out process would be replacement of the neoprene O-rings with viton (to 200°C) or teflon (over 200°C). These are both commercially available. The Inconel X load cell with bakelite strain gages, which was previously described, should be adequate to withstand 200°C temperatures.

Another major advantage of installation of a bake-out hood would be the removal of the sheath heater in the base of the lower shear cup. Operation of this heater involves placing electric power (10 - 85 watts) into the chamber with an accompanying degree of hazard.

A second major recommended addition is the installation of a small two channel recorder. The present method of operation requires two people, one to adjust and read the strain gage null bridge and one to read horizontal displacement and record the data. This procedure has proven to be reasonably effective, and reliable results are regularly obtained. A degree of skill and experience is required, however, to insure that data which plot to a characteristic stress-strain curve are obtained.

MATERIALS

Two materials have been used successfully as ideal soil models in the experimental phase of this project. While these materials fall short of an exact portrayal of the analytic model of precise uniform sized spheres, they were selected as reasonably meeting this criterion.

Crown barium glass spheres (ballotini) manufactured by Potters Brothers, Incorporated, Carlstadt, New Jersey, were selected for initial tests as having the following characteristics:

1. High degree of uniformity in chemical composition and physical properties with expected uniformity of surface properties.
2. Very good regarding uniformity of shape with a high

percentage of near perfect spheres. Shape becomes less spherical with increasing size, however, thereby favoring use of smaller (≤ 2.5 mm.) sizes.

3. Available in a wide range of sizes, 5.66 mm. to less than 100 micron.
4. Reasonably good outgassing characteristics expected (23).
5. Convenient, inexpensive source of supply.

Carbonyl nickel shot, furnished by the International Nickel Company, Incorporated, was also selected primarily because the frictional behavior of nickel at low pressures has been previously studied (7, 39, 70) and seems to be reasonably well established. While the sphericity of the nickel shot is not extremely high, this was in part overcome by hand selection to remove obviously non-spherical material.

TESTS AND TEST RESULTS

TESTS ON GLASS SPHERES

Direct shear tests, in normal atmosphere and in vacuum, were performed on a sample of glass ballotini composed of spheres of 2.2 mm. in diameter. The sample was selected for roundness by the manufacturer, resulting in significantly greater sphericity of the particles. This size was selected as a reasonable balance between the need to keep the ratio of sample to grain size large, sample pores large and total particle surface small. Even at 2.2 mm. the surface area of the sample is approximately 400 square inches. This more than

doubles the total surface area exposed to vacuum. All tests were performed at an initial void ratio of 0.614. The void ratio was controlled by placing a known weight of the material (specific gravity measured as 2.51) into a known volume. Before each test the sample was washed in benzene followed by an acetone rinse, air drying and storage in a warm (70°C) oven until use. If two or three tests were run consecutively, within an hour's time, the cleaning process was not repeated between each test.

Ten tests at normal atmosphere were performed in the special shear device described earlier in this Chapter. The mean value of $\tan \phi$ was 0.622 (31.9°) with a relative standard deviation (81) of 1.4%. Tests were run at slightly varying normal loads of 3.58, 4.63 and 4.82 pounds. All glass sphere tests in vacuum were performed at a normal load of 3.58 pounds. The reduction in angle of shearing resistance at constant initial void ratio, from 34° - 36° for the material described in Chapter III to 32° for the 2.2 mm. sample can be explained by the increased sphericity of the particles of the latter.

Five tests were performed under vacuum conditions, each following one of two basic procedures. In the first procedure the sample was placed in the test chamber which was then reduced to the lowest pressure (approximately 5×10^{-5} torr) attainable in about 12 hours. Heat was applied slowly raising the temperature of the specimen to the desired value. Pressure fluctuated throughout the 10^{-5} torr range while heating because of variations in the gas desorption. The desired

temperature was held, while maintaining the vacuum, for 4 to 6 hours. The sample was allowed to cool to room temperature resulting in a pressure decrease to the very low 10^{-5} torr or high 10^{-6} torr range, and the sample was sheared. The entire process took from 48 to 56 hours. The second procedure involved holding the maximum temperature for 24 to 36 hours, giving the same length of time at low pressure, but shearing the sample without cooling. The heating power was cut immediately before the test to avoid actuating a short circuit through movement of the lower shear cup and heater. The results for these tests, 1 through 5, are shown in Table 7.

TABLE 7
RESULTS OF DIRECT SHEAR TESTS ON GLASS SPHERES IN VACUUM

<u>Test</u>	<u>Shear Pressure, torr</u>	<u>Bake-out Temperature, °C</u>	<u>Shear Temperature, °C</u>	<u>Tan ϕ</u>
1	2.5×10^{-5}	250	room	.911
2	2.2×10^{-5}	190	room	.825
3	3×10^{-6}	250	room	.780
4	8×10^{-6}	200	200	.860
5	6×10^{-6}	200	200	1.040
6	1.5×10^{-5}	200	200	.805

A sixth test was performed upon reaching high temperature after only 12 hours exposure to vacuum conditions and is shown as Test 6 in Table 7. This result shows the smallest increase (30%) over the well established value of 0.622 for $\tan\phi$ obtained for the same material in normal atmosphere. It is assumed that the short duration of exposure to low pressure explains this smaller increase. At least, such an explanation is compatible with the test results.

Dushman (23) shows a peak outgassing rate for glass lying between 150 and 200°C. It is postulated that a majority of adsorbed surface gases are driven off at these temperatures. Gas evolved at higher temperatures is considered as originating within the solid glass. This temperature range was therefore selected as the minimum for sample bake-out in the tests with glass spheres.

While there is insufficient data to allow formulation of any general conclusion regarding the differences between the various test results, one observation seems reasonable. The average increase for samples sheared at room temperature is 35% (to 0.84) while the increase for those sheared at high temperature, excluding Test 6, is 53% (to 0.95). This difference is probably due to a recontamination of the surfaces which occurred as they cooled to room temperature. Even at moderately high vacuum as used in these tests a monomolecular film forms on a clean surface in 2 or 3 seconds. The recontamination of clean surfaces when allowed to stand in a vacuum has been well illustrated by Bowden and Tabor (7).

Tests 1 and 2 might show the advantage of somewhat higher heat in the sample bake-out. These tests were performed consecutively using the same beryllium-copper load cell. Test 3 was performed later using the stainless steel load cell which was shown to be less reliable on successive calibrations. No conclusions are justified in this regard, but further tests might substantiate this speculation.

The relative unimportance of an order of magnitude in ultimate pressure under these general test conditions seems evident. One might conclude that within this vacuum range, 10^{-5} - 10^{-6} torr, at 200°C temperatures, the coefficient of friction of the glass used here varies little if at all with a decade change in pressure.

These results show clearly an increase in $\tan \phi$ with vacuum for the ideal systems of glass spheres which was used in the experiments. From this a substantial increase in the coefficient of friction f can be postulated if any of the various analytic solutions of Chapter II are valid. Assuming the validity of the Equal Partition Solution one can anticipate a 300 - 400% increase in the coefficient of friction under the vacuum conditions used in the shear tests.

To further investigate this factor the coefficient of friction of the glass used was measured. Measurements were performed on small flat plates of the glass which were specially made by the manufacturer to duplicate as nearly as possible the surfaces of the glass spheres.

Friction measurements were made in normal atmosphere by

three different methods with the results agreeing within the limits of experimental error. Two methods involved the use of plaster casts to mount the specially prepared surfaces which were furnished by the manufacturer. In one method the surfaces were placed together on a horizontal platform, the bottom plaster cast fixed and the upper cast supporting a known normal load. A slowly increasing tangential force was applied to the upper surface and plaster cast by means of a line, pulley, small cup and fine sand. The ratio of the force required to cause motion to the normal force, including the weight of the upper surface and cast, was taken as the coefficient of friction. A second method involved measurement of the angle at which sliding of one surface over the other just begins. The tangent of this angle is the coefficient of friction of the surfaces. These tests were performed several times using two mounted plates and also substituting a plaster cast of spheres for the upper surface with an average result of 0.12. The glass plate surfaces were also mounted in aluminum chucks for use in the special shear device. The shear box, ball track, collar and buttress were removed and one chuck was secured to the floor of the test chamber. A special ceramic cement (RCA 33-C-312) was used to hold the glass surfaces in the chucks which were recessed for that purpose. The chuck holding the upper plate was drilled and tapped to receive the fixture which holds the wire for connection to the load cell. The top of the upper chuck is recessed to take the normal load cylinder which is used in the direct shear test. Results with

this apparatus agreed with those obtained in the previously described tests.

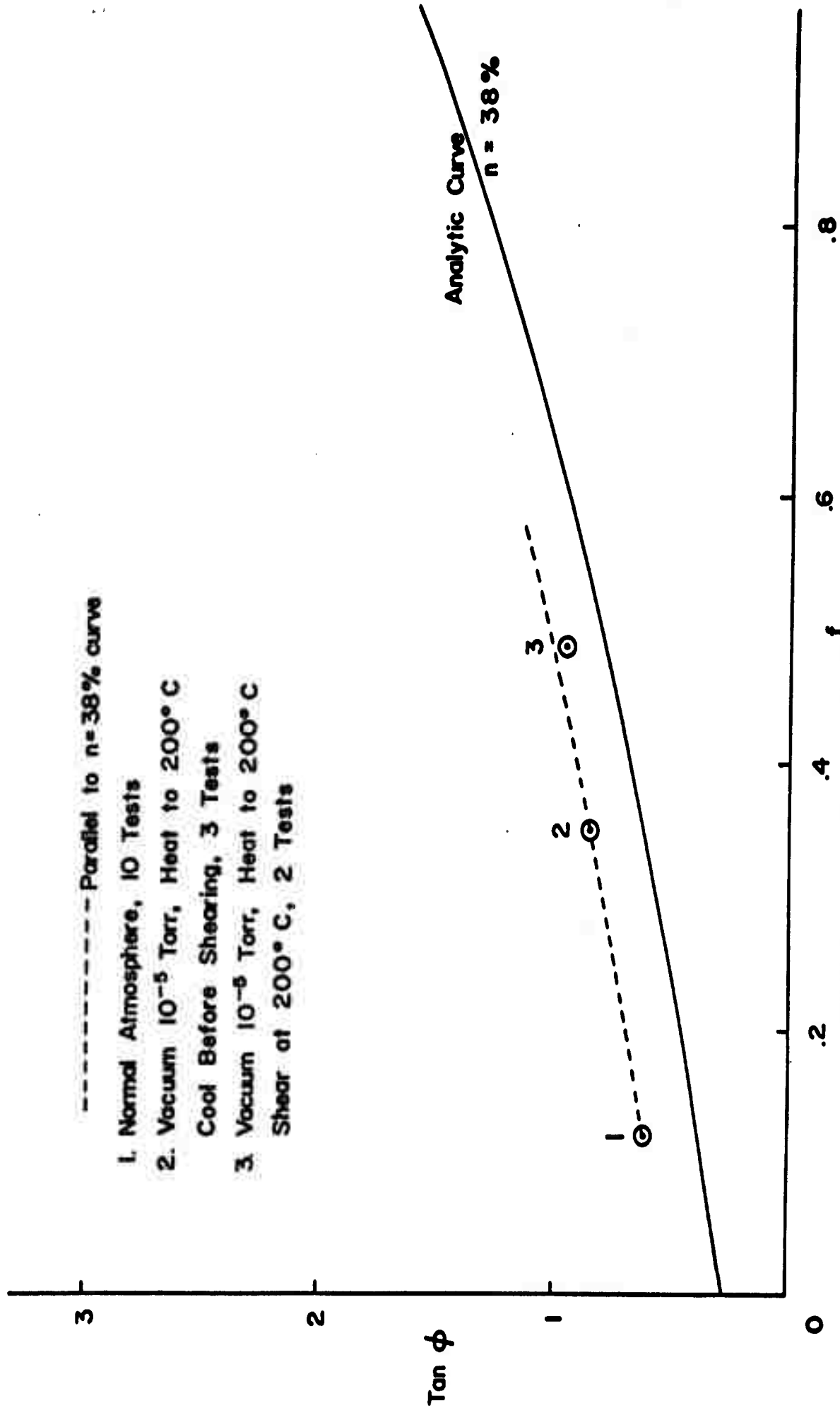
The aluminum chucks were used to measure the coefficient of friction of the glass plates under vacuum conditions similar to those used for the tests on glass sphere aggregates. The lower chuck is drilled to receive the sheath heater and thermocouples were mounted in the ceramic cement which holds the plates. The results are summarized and compared with the appropriate average $\tan \phi$ values in Table 8.

TABLE 8

COMPARISON OF f AND $\tan \phi$ VALUES FOR GLASS

<u>Condition</u>	<u>f</u>	<u>$\tan \phi$</u>
Normal atmosphere.	0.12	0.622
Vacuum 10^{-5} - 10^{-6} torr, Heat to 200°C , Cool, then test.	0.36	0.840
Vacuum 10^{-5} - 10^{-6} torr, Heat to 200°C , Test while hot.	0.49	0.950

These data are plotted in Figure 18 where they can be compared with the Equal Partition Solution developed in Chapter II. The analytic curve for a porosity of 38% (void



Results of Vacuum Tests on Glass Spheres

Figure 18

ratio 0.614) is shown as a solid line in Figure 18. Since Point 1 is the average of numerous tests and considered well established it is used as an origin for the dashed curve which is drawn parallel to the analytic curve. Point 1 lies above the analytic curve partly because the sample tested fails to duplicate the ideal model, and possibly also because of the simplifying assumption which reduce the accuracy of such a solution. The rather close agreement of Points 2 and 3 with the adjusted analytic curve, however, partially substantiates the general validity of the Equal Partition Solution within the range covered, $0.1 < f < 0.5$.

TESTS ON NICKEL SHOT

Tests on nickel shot, 4.4 mm., under conditions similar to those described above for glass spheres, have also been performed. The initial void ratio for each test was maintained at 0.614. Normal load on the failure plane was slightly more than in the case of the glass spheres, 4.1 pounds rather than 3.58 pounds, due to the greater specific gravity of nickel.

Two tests under normal atmospheric conditions in the special shear device gave a value for $\tan \Phi$ of 1.01 with practically no deviation. This value has been confirmed with a number of tests at various normal loads (100 - 500 pounds) in the conventional direct shear machine described in Chapter III. Two shear tests at high vacuum were performed on the nickel shot. One test involved heating to 110°C, cooling and

shearing at room temperature. The other was heated to 250°C, held at that temperature and sheared while the sample was hot. Pressure at time of shearing was very similar, 1.2×10^{-5} and 6.5×10^{-6} , respectively. Total time under vacuum was the same, 48 to 50 hours, for both tests. Unexpectedly, both tests gave almost the same value of $\tan \phi$, 1.46 and 1.47. It was anticipated that the test performed at high temperature would give a significantly higher shear strength. Although the outgassing characteristics of nickel are not perfectly known enough information is available to justify the anticipation of different results. Nickel continues to outgas at very high temperatures and does in fact desorb water vapor at several hundred degrees C (20). This indicates that one should expect a continuing reduction in thickness of the adsorbed surface films throughout the 250° heating range of the second test. The apparent failure of the nickel surfaces to recontaminate significantly on cooling is also not readily understood. Clearly, not enough shear test data are available to warrant speculation. One can only conclude that reduction of the adsorbed surface films of nickel shot aggregate results in a significant increase in shearing resistance. The data are shown in Figure 19 in a form similar to that used for the glass spheres in Figure 18. In this case, however, the coefficient of friction of nickel under the vacuum conditions applied can only be anticipated as no ready means for measurement were available.

Another attempt was made with nickel shot based upon

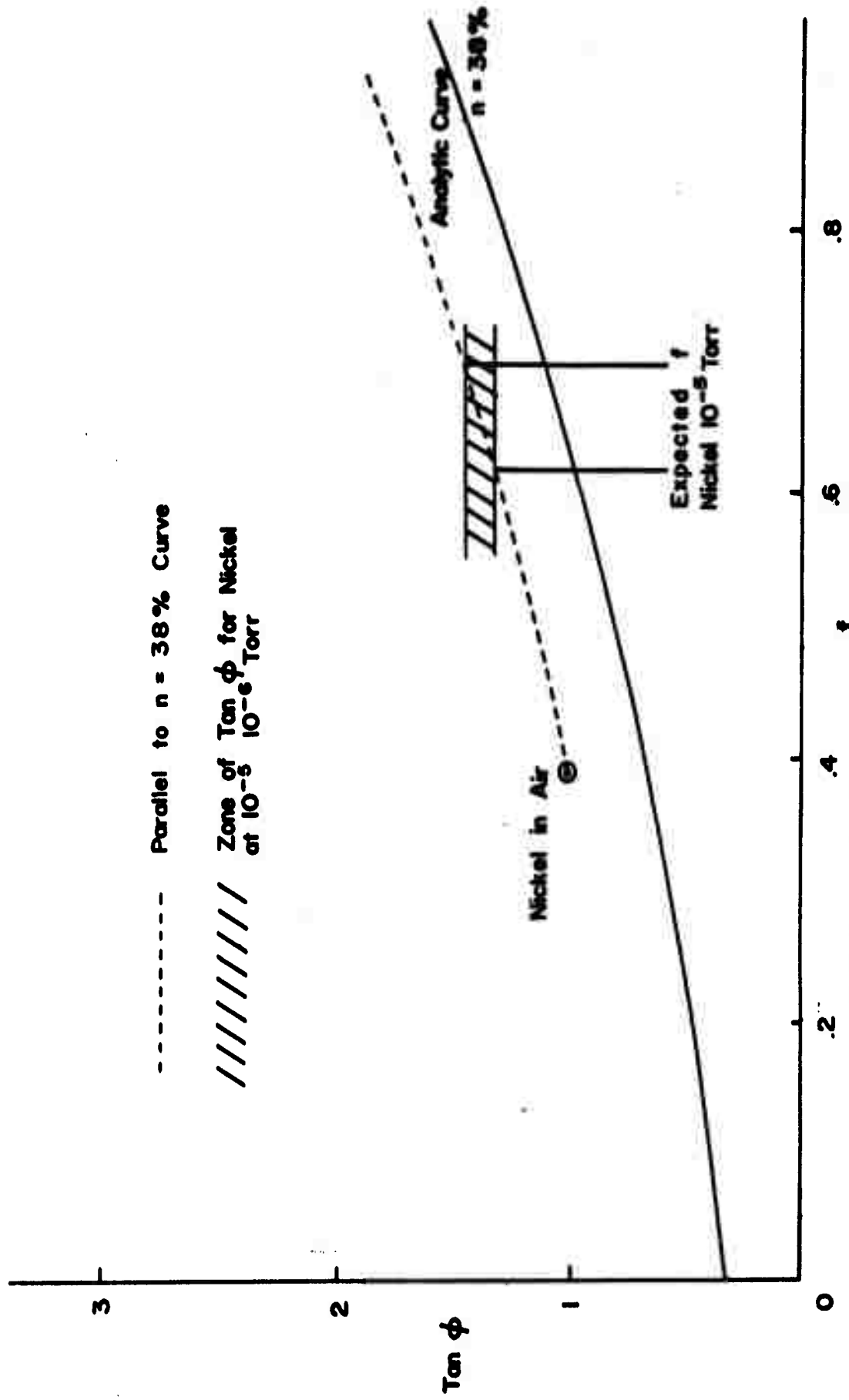


Figure 19

previously published data of Shaw and Leavey (70). By heating to 350°C and cooling to room temperature at 10^{-2} torr a value 1.1 was determined by these investigators for the coefficient of friction of nickel. It was anticipated that a $\tan \phi$ of approximately 2.0 could be obtained by following the procedure given by Shaw and Leavey. In the one test performed with this object however, a $\tan \phi$ of only 1.15 was measured. It is probable that the precise conditions varied significantly from those imposed in the earlier work.

Bowden and Tabor (7) show very high values of coefficient of friction under more severe pressure and temperature conditions. It is expected that a correspondingly high shearing resistance could be obtained under similar conditions. The tests on nickel should be repeated after provisions to bake-out the test chamber are made. Other metals, such as aluminum with a 'clean surface' coefficient of friction of 1.4 (8), should be used in an attempt to establish the validity of a $\tan \phi$ versus f relationship at high values of these parameters.

TESTS IN ATMOSPHERE

The nickel shot and copper coated lead shot (4 mm.) were also used in a series of unsuccessful tests in normal atmosphere. It has been established that nickel and copper each exhibit two distinct values of coefficient of friction depending upon whether or not the relatively soft normal atmospheric oxide layer is penetrated (7, 8). The coefficients of friction of the metal on metal case for both nickel and copper is in the range 1.2 to 1.4.

In the case of oxide on oxide the value is approximately 0.4. The point load values at which the oxide layer is penetrated differs for the two metals; 1-100 grams for copper, and something less than 4000 grams for nickel. A series of direct shear tests were run over a wide range of normal load. No change in $\tan \phi$ for the copper shot was found. A constant value of 1.01 was measured for each of several tests ranging from 4.1 to 200 pounds (12 to 600 grams, point to point contact). Similar results were obtained with the nickel shot (over a wider range of point to point loads) except for the last test at 700 pounds (2100 grams per contact). In this case the value of $\tan \phi$ rose from the previously constant value of 1.1 to 1.8. Since this represented the linear stress-strain limit of the force measuring device available for the shear machine used additional tests at higher loads were not made. Since all tests were performed at a porosity of 38%, an expected $\tan \phi$ of approximately 2.5 could be anticipated at final or complete penetration of the oxide layer. Whether the last test, at a value of 2100 grams per contact, represents a partial penetration or not is open to question. Additional tests in the 2-3000 gram range should be performed with a higher capacity machine. In this way it might be possible to establish two specific widespread points on the $\tan \phi$ versus f curves.

TEST ON MINERAL FRICTION

One test was made to determine the effect of vacuum conditions on the coefficient of friction of quartz. Two small quartz plates were polished with fine pumice and secured in the aluminum chucks and the tests were performed as described earlier for glass plates.

The quartz was prepared by washing with benzene and acetone followed by air drying and was stored in a warm (70°C) oven until used. Prior to the vacuum test the coefficient of friction in air was determined as 0.33. This value is similar to that obtained in numerous tests (41, 58, 79) for saturated or damp surfaces. It was expected that the lower value of 0.15 associated with dry quartz surfaces would be measured. It is probable, however, that the solvent wash and 70°C temperature were not sufficient to remove surface moisture.

The quartz plates were then exposed to vacuum, 10^{-5} - 10^{-6} torr, and slowly heated to 200°C. The high temperature was held for approximately 30 hours with a total time under vacuum of 50 hours. A coefficient of friction of 0.60 was measured under these conditions.

CHAPTER V

SUMMARY AND CONCLUSIONS

The preceding Chapters have described in detail a research project on one phase of the frictional behavior of granular soils. The work was primarily motivated by the apparent need for a soil mechanics study of some of the factors which may influence the performance of postulated lunar surface materials.

Previous work on the mechanical properties of possible lunar soils has been largely of a speculative nature with only a few experimental studies being recorded. These few experimental efforts have not been complemented by parallel analytic studies, either qualitative or quantitative, and the results have, in general, been difficult to evaluate. The several experimental works have been confined to static and dynamic impact tests on postulated lunar soil models. The results have, in most cases, been strictly limited by the method of test and the model selected.

In order to improve upon these previous efforts in this area a program supported by an analytic study and having specific limitations and objectives was developed. This program involved a study into the effect of atmosphere, specifically very low air pressure, on the shear strength on an ideal granular material.

An analytic study of the problem indicated that shear strength of an ideal granular material can be expected to vary with atmosphere in a rather generally predictable manner.

Specifically, the action of high temperature and low pressure in reducing the adsorbed surface films of individual particles can be expected to increase grain to grain friction with a resulting gain in shearing resistance of the aggregate. A series of test on idealized granular systems has been performed to determine the validity of this ascertainment. In addition existing data were critically reviewed and tests were performed to determine the effects of grain size and of grain size distribution (gradation) on the shearing resistance of granular materials.

CONCLUSIONS

The frictional behavior of ideal individual particle media was investigated in connection with lunar soil applications.

While the data obtained are somewhat limited and considerably more investigation is needed in this area several conclusions seem ~~to be reasonably well~~ justified. These are:

- (1) The shear strength of an ideal granular system is a function of the atmosphere. Specifically, it is concluded that very low air pressure causes a decrease in thickness of the adsorbed surface films resulting in increased grain to grain friction and shearing resistance.
- (2) The relationship between interparticle friction and shearing resistance is subject to theoretical analysis that can be reasonably substantiated over a moderate range of values.
- (3) It is reasonable to expect that very high vacuum conditions will cause a significant increase in coefficient of friction of some, if not all, rock forming minerals.
- (4) Size, as such, has no effect on the shear strength of

↓
granular materials. It is almost impossible, however to vary particle size alone while holding all other variables constant. The result is, in real materials, a secondary size effect such as a change in surface roughness, density or gradation which alters shear strength with size. These conclusions are limited to particle sizes larger than 0.5 mm. which is the approximate upper limit of significant surface force effects such as static electricity.

- (5). At a given absolute density, a uniform material has, in general, a greater shearing resistance than a well graded material.

CHAPTER VI

ADDITIONAL CONSIDERATIONS AND SUGGESTIONS FOR FURTHER RESEARCH

The preceding Chapters are involved with the objectives, approach, methods, results and conclusions associated with the initial phase of the research program in granular soils being conducted at Princeton University. In this Chapter several factors which fall outside the scope of the work described will be discussed. Some of these factors arise from consideration of the lunar surface problems, others may have a wider basis of interest. Implicit in portions of the following paragraphs is an invitation of the reader's attention to areas needing further study. Some of these areas are specifically recommended for study within the continuing research effort of which this thesis represents an early phase.

SOIL COHESION IN THE LUNAR ENVIRONMENT

This study dealing with the frictional behavior of granular soils ignores possible contributions to total shearing resistance which might arise from cohesion. The Coulomb equation for the shearing resistance of soils taken in its more general form is:

$$S = C + \bar{N} \tan \phi$$

where \bar{N} = the effective normal load on the failure plane,

and C = the cohesion.

ϕ is precisely as in earlier Chapters. \bar{N} can be considered as N , differing only by pore fluid force which is absent under vacuum conditions. C , the cohesion, results from molecular attraction and is assumed independent of normal force. In the case of terrestrial soils this attraction is due to the adsorbed moisture films. Because of the very high ratio of body to surface forces in a granular soil in the normal atmosphere the cohesive effects are negligible. In the case of the anticipated lunar environment, however, the role of cohesive forces in soil behavior may exceed that of frictional forces. With the removal of all adsorbed surface films direct molecular attraction between surfaces of contacting particles becomes a major factor. This is the case for clean metal surfaces as has been well established primarily through the work of Bowden and Tabor and their associates. That the same conditions exists for rock and mineral powders under high vacuum conditions is being illustrated in current research aimed at the lunar surface problem*. Any conclusions therefore, which may be drawn as regards possible behavior of lunar soils, should be considered with these concepts in mind.

In the extreme limit case, however, of absolutely clean surfaces in contact it is likely that little distinction could be made between cohesion and friction. As ultimate cleanliness of surfaces is reached both friction and cohesion will increase, limited only by the strength of the material itself. In addition,

* See Salisbury, Stein, et al in Lunar Surface Materials, Academic Press, to be published late 1963.

the adhesive component of friction* will increase greatly, possibly eliminating the distinction as made in the Coulomb equation.

Incidentally, most of the $\tan \phi$ versus f solutions mentioned in Chapter II provide for the absolute limit case of vacuum welding, in the practical case at least, by allowing ϕ to approach 90° at high values of f . This implies that a very small normal load, even the weight of a single grain, will give a large shearing resistance.

POROSITY

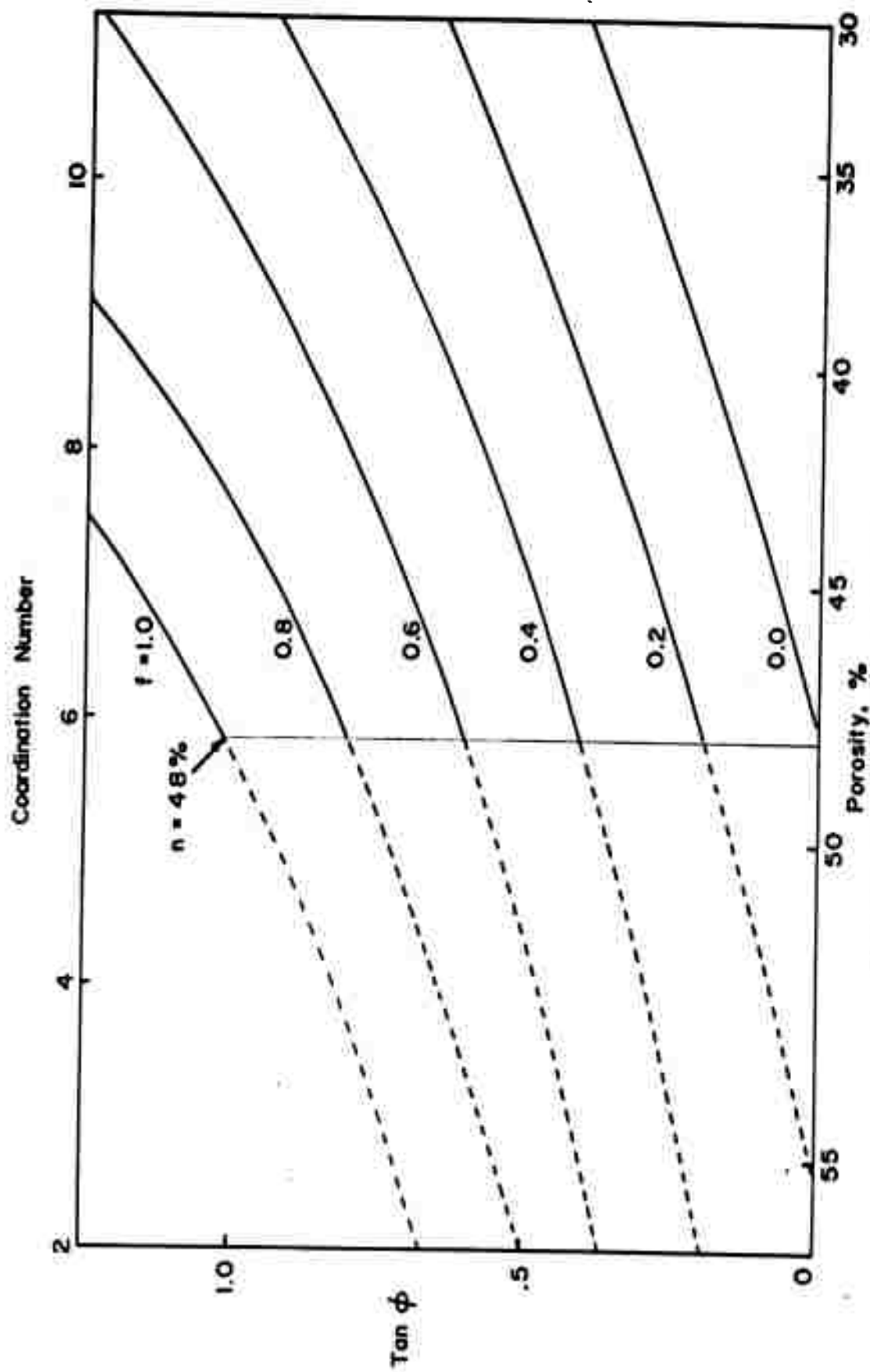
The possible effect of a very high porosity on the frictional behavior of a lunar soil has been briefly discussed in some of the previously cited literature (63, 83). This effect is partially illustrated by the considerable decrease in slope with porosity of the curves in Figures 7-9. This then is why one might expect the greater increases in strength at higher densities as was reported concerning the Armour Tests (62) described in Chapter I.

All of the analytic solutions which are based upon a model system composed of uniform spheres are nominally limited by the values obtained in the most dense and least dense packing as previously described. It is possible, however, to extend the solutions a limited amount in the following manner. One may expect that the shear strength of a granular material will be a function of the coordination number of the system, that is the average

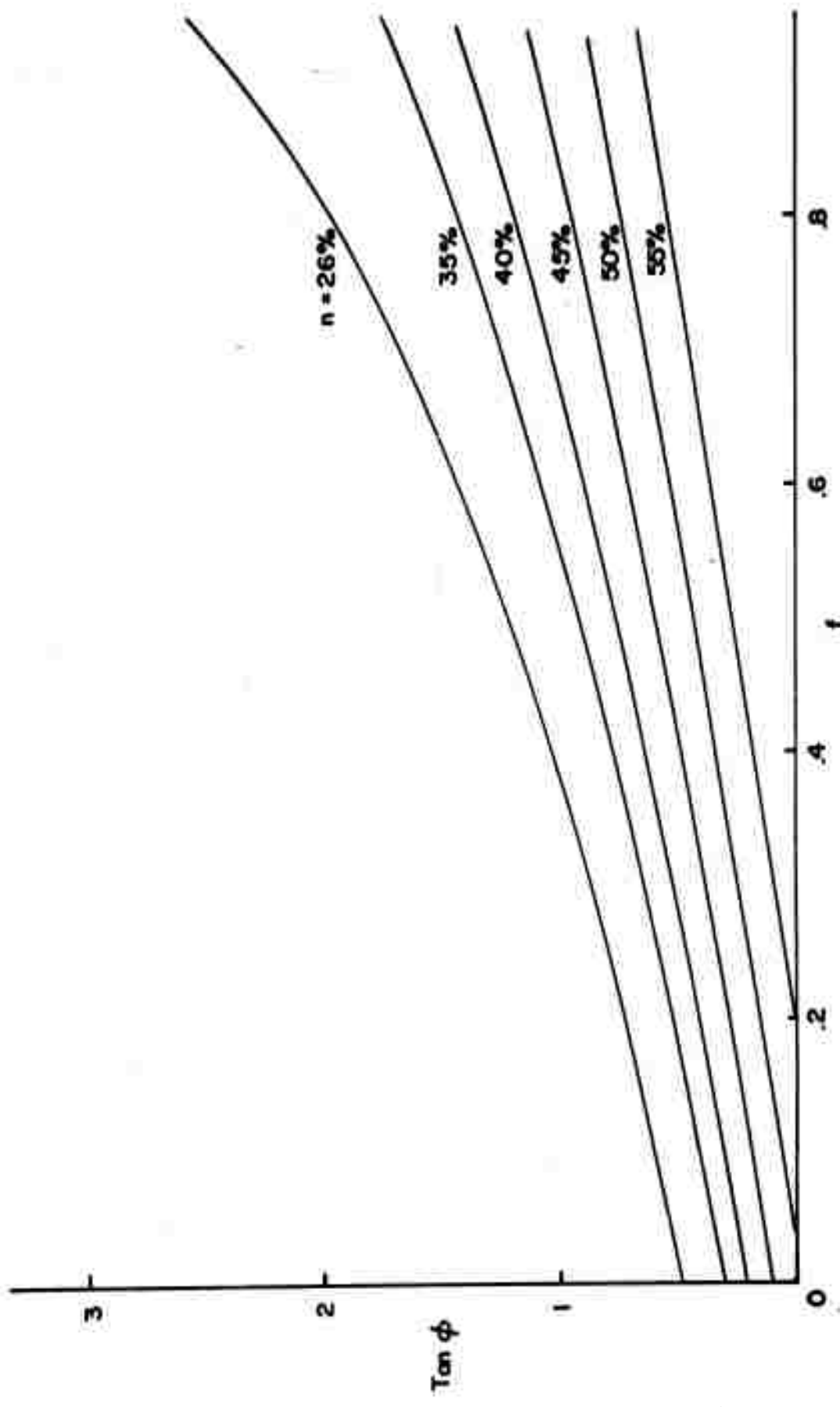
* Considering energy loss in friction due to: (1) deformation of asperities, (2) lifting one body over the asperities of the other and (3) overcoming molecular bonds formed as one body slides over the other (adhesion).

number of contacts per sphere. Deresiewicz (21) has developed an analytic expression relating the coordination number to the porosity for a system of equal spheres. This relationship has been verified within an average of 3% by the experimental data of Smith, Foote and Busang (74) which was obtained with lead shot packings. One is able to plot a series of curves showing shearing resistance as a function of porosity for various values of coefficient of friction. This is done for the Equal Partition Solution of Chapter II in Figure 20. The solid portions of the curves are taken directly from Figure 9 and are limited by the vertical line at a porosity of 48%. The curves have been extended as dashed lines in Figure 20 to include a porosity of 55%. These extended curves then provide the basis for expanding the range of the Equal Partition Solution through this porosity as shown in Figure 21. This porosity represents the approximate extreme limit of applicability of solutions based upon systems of uniform spheres. A porosity of 58%, represents, according to the Deresiewicz relationship, a coordination number of 1, clearly an impossible situation. These considerations, coupled with rather widespread speculation of very high porosities (80 - 90%) of the lunar surface material, favor the case for extreme non-spherical particle shapes.

The importance of porosity is generally recognized by the civil engineer, the concept of relative density being almost universally accepted. Its possible effect toward offsetting the potential gain in shear strength resulting from increase in coefficient of friction is shown clearly in Figure 21. Taking the



Shearing Resistance γ_3 Porosity
Figure 20



Extended Equal Partition Solution

Figure 21

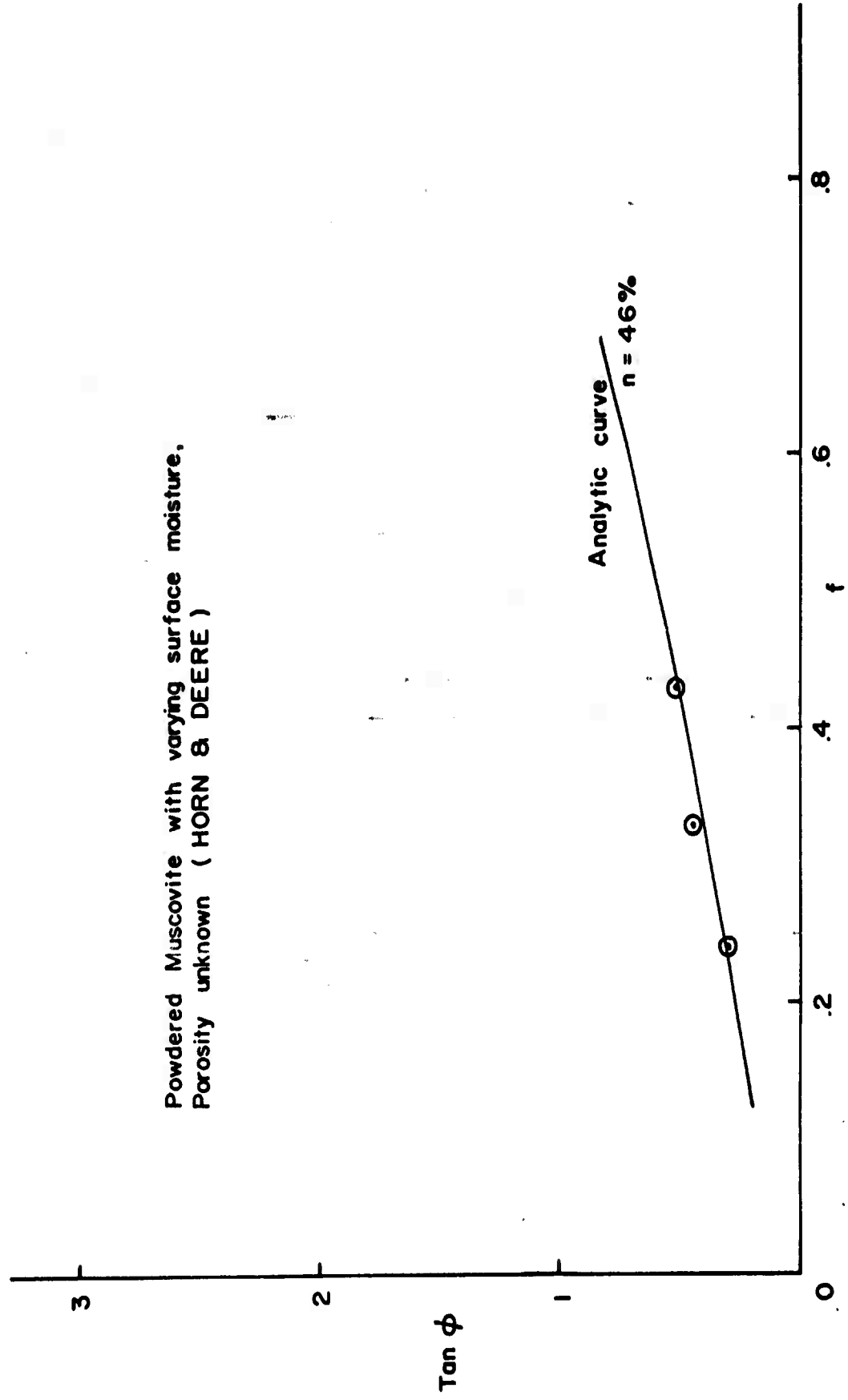
commonly experienced porosity of 35% with a coefficient of friction of 0.2, one can see that the shear strength gain produced by a four fold increase in f is lost if the porosity increases to 55%. One can only speculate on the effects of a porosity of the order of 80 or 90%.

PARTICLE SHAPE

The importance of particle shape in shearing resistance seems obvious. It appears equally evident that the sphere, with the lowest ratio of surface to volume, will represent the extreme low as regards shape effects on strength. This is in part due to its lack of angularity, hence reduced opportunity for interlock, and partly on its tendency for a low ratio of surface to body forces.

This subject has been considered only in a superficial manner and no data exist that would allow formulation of more than very general conclusions. Data obtained by Horn and Deere (41) on powdered and sheet muscovite are plotted in Figure 22. While plate-like particles of muscovite can not be expected to closely follow an analytic relationship derived for spherical grains, the Equal Partition curve for a porosity of 46% is shown for comparison. The porosity of the powdered muscovite was not given but probably exceeded 46% by a considerable margin. One might expect that the surface area to volume ratio would cause a loose assembly of plate-like particles to exhibit frictional behavior similar to a more dense packing of spherical particles. It seems that these few data support such a contention. In the case of non-spherical particles then the effects of high porosity might be somewhat dampened.

Powdered Muscovite with varying surface moisture.
Porosity unknown (HORN & DEERE)



Tan ϕ vs f Relationship for Plate-like Particles

Figure 22

Another factor that may be expected to enter into the behavior of extreme non-spherical shapes, such as plates and needles, is that of preferred orientation. This would manifest itself primarily in anisotropy.

GRADATION

Gradation or particle size distribution has been well covered in Chapter III as regards its direct effect on shear strength. Interrelationships between gradation and friction may prove to have some bearing on the problem considered in this thesis. It appears that aggregates with a high degree of uniformity may be less sensitive to changes in particle shape or roughness than well graded particles (38, 73). This may be true also for changes in the interparticle coefficient of friction. Some evidence exists also which indicates that effects of porosity may be somewhat greater in a well graded or non-uniform aggregate (43, 73). In concrete technology the greater effect of increased water content (porosity) in altering the slump of a well graded aggregate mix is widely known.

If cohesion proves to be a major factor in the behavior of lunar surface materials, soils may handle as clods of smaller adhesive particles. In such a situation workability may be a major problem. The effect of reducing friction* for the purpose of improving workability for various gradations would be interesting.

THEORETICAL METHOD FOR DETERMINATION OF STRESS-STRAIN DIAGRAM FOR GRANULAR MATERIALS

A logical extension of the analytic relationship between the

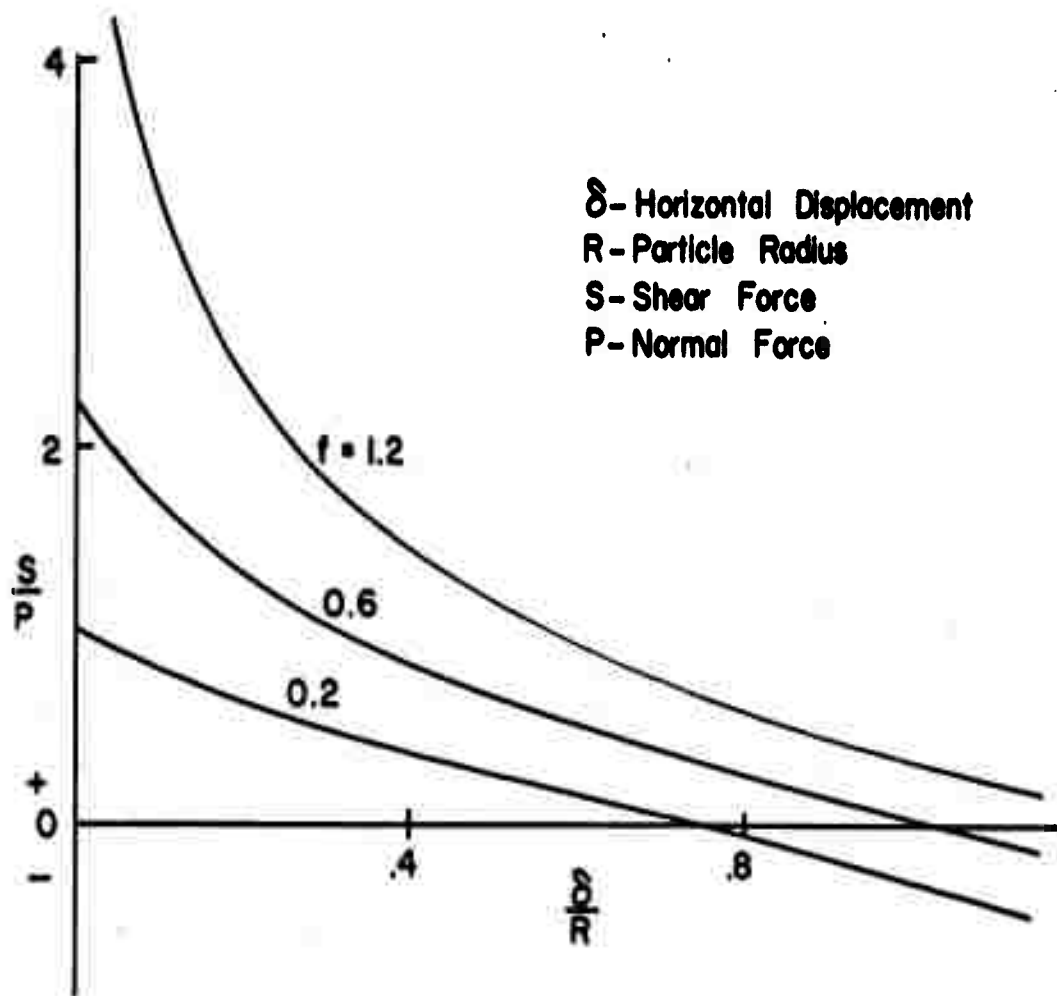
* For instance, by a compressed gas spray with resulting partial reduction of free surface energy.

$\tan \phi$ and f which was developed in Chapter II allows one to outline a general method for determination of the stress-strain diagram for ideal granular materials. Specifically it seems apparent that the appropriate diagram could be determined for a given porosity and interparticle coefficient of friction for a given system of uniform spheres. The specific details of such a theory have not yet been worked out, but it seems that all of the elements are available.

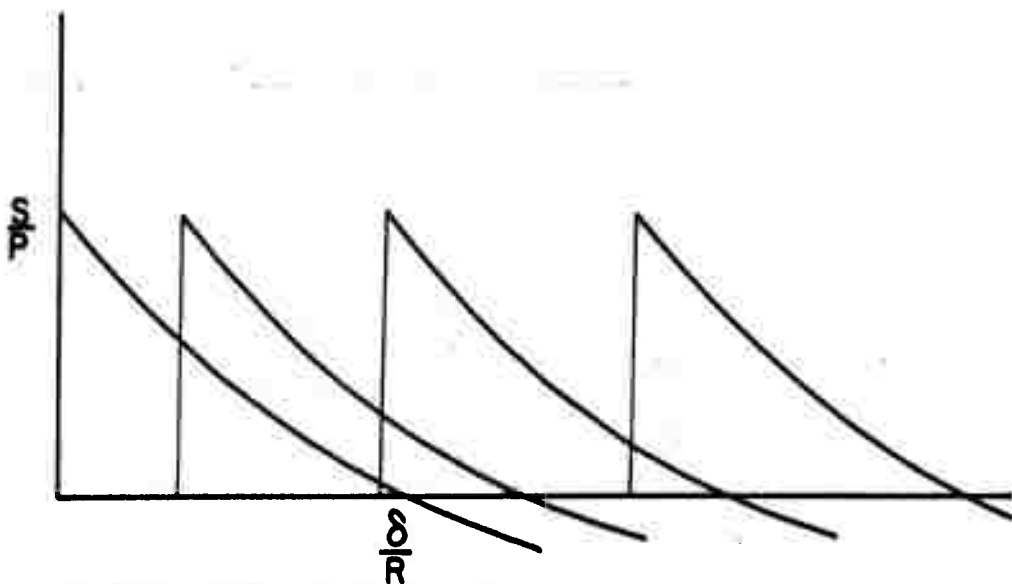
If equation (4) of Chapter II for the kinetic case of failure path I is solved for various increasing values of Θ as the moving sphere slides up and over the one upon which it rests, the equilibrium force for each of several horizontal displacements can be determined. The resulting relationship, expressed in dimensionless terms of shear (equilibrium) force to normal force and horizontal displacement to particle radius is shown in Figure 23a for several values of coefficient of friction. Solution of equation (8) will yield similar, but subdued, curves.

By a straight or weighted mean procedure, identical or similar to the equal probability or equal partition of energy concepts, a curve for the average or representative particle can be established.

If each particle were in direct contact with an adjacent particle in the direction of motion, the curve for the representative particle just mentioned would be the stress-strain or load-deformation diagram for the system. It is assumed, however, that only a portion of the individual spheres have such contact. The remainder of the particles must travel a free path, primarily



a. Curve for Failure Path I



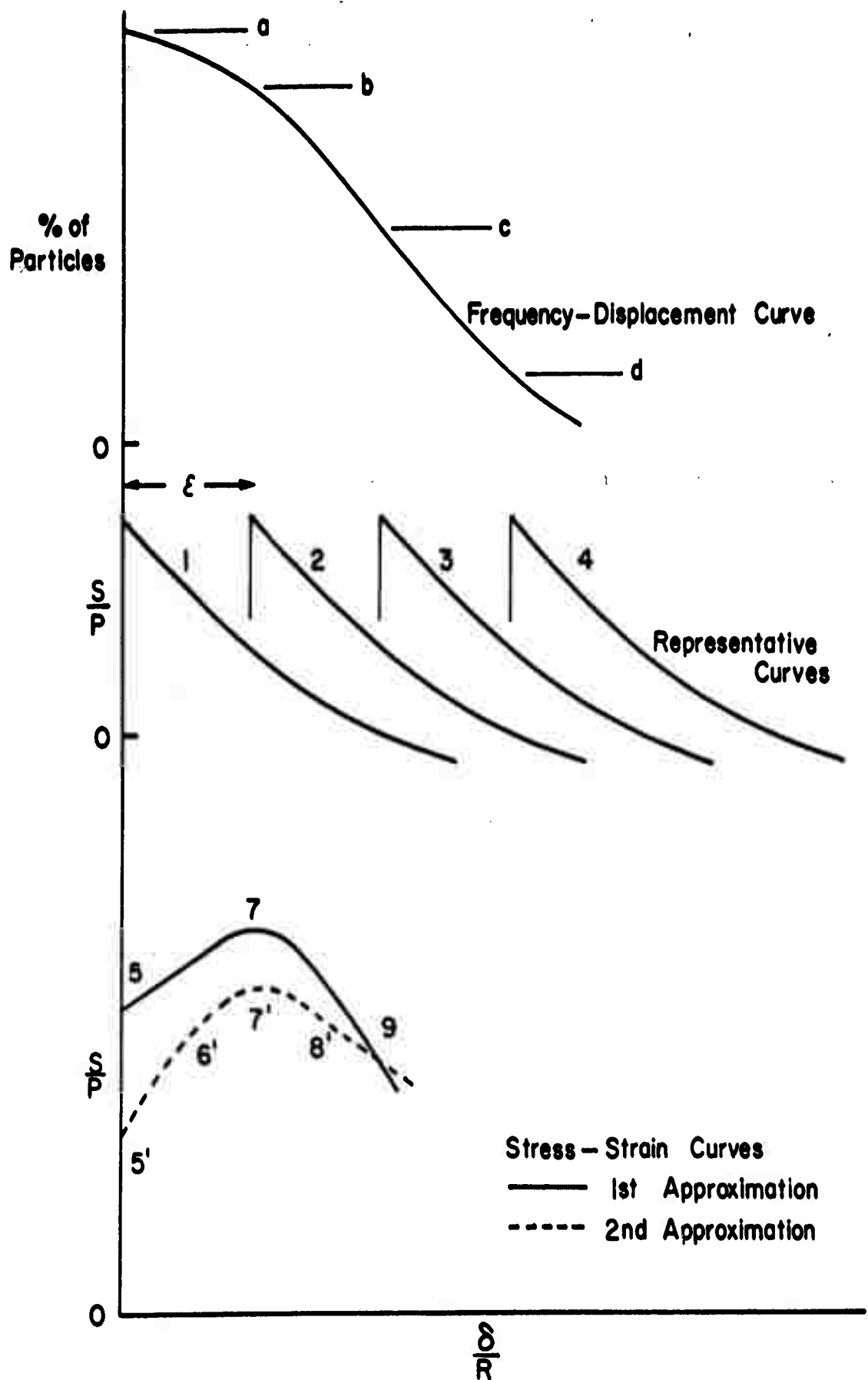
b. Representative Particle Curves

Load-Deformation Diagrams

Figure 23

unhindered, before making such contact and then can be considered to follow the representative curve. The mean of N such curves, each representing one particle and displaced to the right of the origin a distance equal to the length of the free path of the particle, would give the load-deformation diagram of the aggregate. A few such curves for a given value of f are shown in Figure 23b. These curves are shown at random displacement from the origin. Actual displacement of the curves will be as the free path of the particles and can be represented by a frequency distribution diagram. It seems likely that at porosities ordinarily encountered in granular materials, the most frequent free path length will be zero. The frequency-free path diagram will probably take the general shape shown at the top of Figure 24. In this sketch the ordinates a , b , c and d are taken at whole units of the distance ϵ from the origin. The second drawing shows previously discussed representative curves spaced a distance ϵ apart. Curve 1 represents a total of a particles, curve 2 a total of b particles and so on, where $a + b + c + d = N_1$.

The total force associated with the initial motion is the product of the ordinate a and the ordinate of curve 1 at $\frac{\delta}{R} = 0$. The mean force per particle then is obtained by dividing the total force by N_1 . This is represented by point 5 on the lower sketch of Figure 24. The total force at a horizontal displacement of ϵ is the sum of the product of ordinate a and the ordinate of curve 1 at $\frac{\delta}{R} = \epsilon$ and the product of ordinate b and the ordinate of curve 2 at $\frac{\delta}{R} = \epsilon$. The mean force per particle is obtained as before by dividing the total force by N_1 . This is shown as point 7.



Development of Stress-Strain Curve

Figure 24

Point 9 is obtained in an identical manner.

The resulting curve, 5-7-9, will approximate the true stress-strain diagram to a greater degree as the number of representative curves (1, 2, 3, 4....) is increased. The true stress-strain diagram will result when a representative curve is formed for each of the total of N particles in the system. It can be seen that as N increases without limit, point 5 will approach the origin. Curves 5'-6'-7'-8-9 results from taking twice as many representative curves, that is at a spacing of $\frac{\epsilon}{2}$. The trend toward the typical stress-strain diagram for a granular soil can be seen by comparing these two approximations.

It should be noted that the entire stress-strain diagram can not be determined in this manner. At deformations of the same order as the particle radius the failure mechanism described in Chapter II no longer approximates the true physical situation.

This approach seems to merit further research to determine whether or not it might allow establishment of the stress-strain diagram. The primary deficiency in the procedure seems to involve the determination of the frequency-displacement curve. This might be established as a function of the porosity by analytic and/or experimental methods.

CONDUCTIVITY RELATIONSHIPS

Study of thermal and electrical conductivity is recognized as applicable to the lunar surface problem in a variety of ways. Attenuation of radiation and required depth of cover can be computed from such data. Rather extensive estimates of lunar thermal and electro-magnetic properties have been made by radar,

radio and optical measurements. Additional data on conductivity properties of granular media may help to further diagnose actual lunar surface materials. Further, a relation between shear strength and thermal or electrical conductivity of granular systems seems feasible since both depend on the number and nature of the point to point contacts.

Thermal conductivity will decrease with atmospheric pressure as gaseous phase conduction and convection are replaced by radiation as the primary agent. It is likely, however, that a partial compensation might be made by increased solid phase conduction resulting from more intimate grain to grain contact. This increased solid phase conduction should be subject to analysis, theoretical and experimental, and thus relatable to increased shear strength.

Electrical conductivity-shear strength relationships would be somewhat easier to study though possibly not as directly applicable to the lunar problem. The electrical resistance of a metal to metal contact is related directly to the true area of such a contact (7, 39). As indicated in Chapter I the frictional resistance of such a contact is a reasonably known function of the true area and the yield strength of the material. The shear strength can be determined as a function of the point to point frictional resistance, at least in the case of ideal materials, as is established in Chapter II. The problem then becomes one of determining the point to point electrical resistance for individual particles in a granular system. The problem can be seen as a three dimensional field of N points bounded on all sides by a known surface; for instance a non-conducting shear box with

conducting top and bottom plates. Each point is joined to K other points by means of a resistance of unknown value r , where K is the coordination number or average number of point to point contacts of the system. If one is able to determine the individual resistance r knowing the resistance of the entire system R , then it appears that the shear strength may be predicted.

Solution of the electrical conductivity-shear strength relationship may facilitate the similar thermal problem.

BEHAVIOR OF FLOCCULATED OR DENDRITIC STRUCTURES

Based upon previously published thermal conductivity data (lunar and other), experience with attempted viscosity measurements mentioned earlier in this thesis, and phenomena well known in soil science, Winterkorn proposed a flocculent structure as a possible lunar surface model (90). This proposed structure is considered similar in form but of course different in origin from the flocculated clays known in soil mechanics (77).

Additional support to this proposal is given by recent work of Gold and his associates at Cornell University (35). Based on light scattering experiments he proposes a "fairy castle" structure of fine powders deposited in a vacuum, each particle sticking upon contact with another. This is analogous to the formation of flocculated clays in a marine environment. Something of value might be gained by a further study of these terrestrial soils.

Experiments on material deposited by vacuum sedimentation such as those proposed in the above cited report and recently accomplished in part by Gold seem to lie in a very promising area.

In addition, some thought should be given to a possible analogy with dendrites known in mineralogy and crystal physics.

Dendritic and flocculated structure are somewhat similar and either concept could fit the data of Winterkorn and Gold. While theory of dendritic crystal formation is not yet a closed subject certain aspects of this theory fit a lunar environment (12, 80). First, a homogeneity of the deposition medium seems to favor dendritic growth. Second, low thermal conductivity of the medium is a favorable factor in such crystal formation.

It is interesting to note that a consideration of geomorphology will indicate that the dendritic stream pattern is a perfectly random development on rocks of uniform resistance.

ADDENDUM

Details concerning a series of static and dynamic penetration tests on simulated lunar soils under vacuum conditions have become known since completion of the final draft of Chapter I.* In this case several samples of crushed olivine basalt with maximum particle sizes ranging from 100 to 600 microns were used as laboratory models. Pressures for the vacuum tests were in the 10^{-5} to 10^{-6} torr range. Moderate heating, to 115°C , was applied to facilitate outgassing in some of the tests. Heat was generally not used, however, because the observed effects on outgassing rate were small. Density was measured and controlled throughout the tests. In the case of the static penetration or bearing capacity tests on loosely packed soil some increase in resistance was noted for vacuum conditions when compared with the results obtained in normal atmosphere. No vacuum effect was observed for the more densely packed material. In the dynamic penetration tests the least resistance was found for loose material in air. The greatest resistance was observed for dense material in air. Dynamic penetration resistance for all vacuum tests fell between these two limits. It seems clear that these rather nonconclusive results stem from a failure to achieve significant outgassing

* See Jaffe, L.D., "Mechanical and Thermal Measurements on Simulated Lunar Surface Materials", in Lunar Surface Materials, to be published by Academic Press late in 1963. This work also has been reported by Roddy, D.J., Rittenhouse, J.B. and Scott, R.F., A.I.A.A. Paper Number 2713-62.

of adsorbed particle surface films. While the chamber pressures were reduced to the range of 10^{-5} to 10^{-6} torr the pressures within the very small soil voids were probably several orders of magnitude larger. This contention is supported by the failure of moderate heating to significantly increase the gas load.

VITA

Gerald Don Sjaastad [REDACTED]

[REDACTED] After attending elementary and secondary school at Minot, North Dakota he was appointed to the United States Naval Academy. Upon graduation from the Naval Academy with the Class of 1952 he was commissioned in the United States Air Force.

His Air Force service has involved base level engineering duties at several bases in the United States and at Thule, Greenland. Immediately before entering Princeton University he was on the faculty of the United States Air Force Academy as an Instructor in Mechanics. He holds the degree Master of Science in Civil Engineering from Purdue University and has done additional part-time graduate work at the University of Colorado.

BIBLIOGRAPHY

1. Baraboshov, N.P. and Chekirda, A.T., "A Study of the Rocks Most Closely Resembling the Surface Constituents of the Moon", Soviet Astronomy AJ, 3:5, 827, 1960.
2. Bekker, M.G., "Mechanics of Locomotion and Lunar Surface Vehicle Concepts", Soc. of Automotive Engineers, Automotive Engineering Congress, Detroit, Michigan, 1963.
3. Bishop, A.W., "A Large Shear Box for Testing Sands and Gravels", Proc. 2nd Int. Conf. on Soil Mech. and Found. Eng., 1:207, Rotterdam, 1948.
4. Bishop, A.W., Correspondence on Reference 58, Geotechnique, IV:1, 43, London, 1954.
5. Bowden, F.P. and Hughes, T.P., "Friction of Clean Metals and Influence of Surface Films", Nature, 142, 1039, 1938.
6. Bowden, F.P. and Hughes, T.P., "The Friction of Clean Metals and the Influence of Adsorbed Gases. The Temperature Coefficient of Friction", Proc. Royal Soc., A172, 263, 1939.
7. Bowden, F.P. and Tabor, D., The Friction and Lubrication of Solids, Oxford, 1950.
8. Bowden, F.P. and Tabor, D., Friction and Lubrication, Methuen, London, 1956.
9. Bowen, D., Discussion of Reference 31, Proc. Lunar and Planetary Exploration Coll., 1:1, 12, 1958.
10. Brunsichwig, M., Fensler, W.E., Knott, E., Olte, A., Siegel, K.M., Ahrens, T.J., Dunn, J.R., Gerhard, F.B. Jr., Katz, S. and Rosenholtz, J.L., "Estimation of Physical Constants of Lunar Surface", Univ. of Mich. Report, Subcontract 133-S-101, Contract DA 49-018 eng-2133(E), Army Map Service, 1960.
11. Buckley, D.H., Swikert, M. and Johnson, R.L., "Friction, Wear and Evaporation Rates of Various Materials in Vacuum to 10⁻⁷ mm. Hg.", Trans. Am. Soc. Lub. Eng., 5:1, 8, 1962.
12. Buckley, H.E., Crystal Growth, Wiley, 1951.
13. Burmister, D.M., "The Importance and Practical Use of Relative Density in Soil Mechanics", Proc. A.S.T.M., 48, 1249, 1948.
14. Burmister, D.M., "The Place of the Direct Shear Test in Soil Mechanics", Symposium on Direct Shear Testing of Soils, A.S.T.M., 1953.

15. Caquot, A. and Kerisel, J., Traité de Mécanique des Sols, 3rd Ed., Chapter X, Gauthier-Villars, Paris, 1956.
16. Casagrande, A., "Notes on the Shearing Resistance and the Stability of Cohesionless Soils and their Relation to the Design of Earth Dams", Discussion, Proc. Int. Conf. on Soil Mech. and Found. Eng., III, 58, Harvard, 1936.
17. Casagrande, A., "Characteristics of Cohesionless Soils Affecting the Stability of Slopes and Earth Fills", Contributions to Soil Mechanics, 1925-1940, Boston Society of Civil Engineers, 1940.
18. Chen, L-S, "An Investigation of Stress-Strain and Strength Characteristics of Cohesionless Soils by Triaxial Compression Tests, Proc. 2nd Int. Conf. on Soil Mech. and Found. Eng., V, 43, Rotterdam, 1948.
19. Dantu, P., "Etude mecanique d'un milieu pulverulent forme de spheres egales de compacite maxima", Proc. 5th Int. Conf. on Soil Mech. and Found. Eng., 1, 61, Paris, 1961.
20. Dayton, B.J., "Outgassing Rate of Contaminated Metal Surfaces", Trans. 8th Vacuum Symp. and 2nd Int. Conf., 1, 42, Pergamon, 1962.
21. Deresiewicz, H., "Mechanics of Granular Matter", Columbia Univ. Report, Contract Nonr-266(09), Technical Report No. 25, Project NR-064-388, Office of Naval Research, 1957.
22. DeLeonardo, G., "Lunar Construction", J. Am. Rocket Soc. 32:6, 973, 1962.
23. Dushman, S., Scientific Foundations of Vacuum Technique, Revised, Wiley, 1962.
24. Farouki, O.T., "A Comparison of Experimental Data with Values Calculated on the Basis of the Concept of the Solid and Liquid States of Macromeritic Systems", Unpublished Report, Soil Physics Laboratory, Princeton University, 1963.
25. Fielder, G., The Structure of the Moon's Surface, Pergamon, 1961.
26. Fuller, W.B. and Thompson, S.E., "The Laws of Proportioning Concrete", Trans. Am. Soc. Civil Eng., 59, 67, 1907.
27. Gemant, A., Frictional Phenomena, Chapter XX, Chemical Publishing Company, Brooklyn, 1950.
28. Gilvarry, J.J., "Nature of the Lunar Surface", Nature, 180: 4595, 911, 1957.
29. Glasstone, S., Laidler, K.J. and Eyring, H., The Theory of Rate Processes, McGraw-Hill, 1941.

30. Graton, L.C. and Fraser, H.J., "Systematic Packing of Spheres-
With Particular Relation to Porosity and Permeability",
J. Geol., XLIII:8:1, 785, 1935.
31. Green, J., "The Physical Characteristics of the Lunar Surface",
Includ. Discussion, Proc. Lunar and Planetary Exploration
Coll., 1:1, 11, 1958.
32. Greer, R.L., "Impact Studies on Lunar Dust Models at Various
Vacuums", Aeronautical Systems Division Technical Report,
61-595, AFSC, USAF, Wright-Patterson AF Base, 1962.
33. Gregg, S.J., The Surface Chemistry of Solids, 2nd Ed., Chapters
3,4 and 7, Reinhold, 1961.
34. Gold, T., "The Moon", Space Astrophysics, Edited by W. Liller,
Chapter 8, McGraw-Hill, 1961.
35. Gold, T., "The Surface of the Moon", Lecture, Am. Rocket Soc.,
Princeton University, 1962.
36. Halajian, J.D., "Laboratory Investigation of 'Moon-Soils'",
IAS Paper 62-123, N.Y., 1962.
37. Hanson, S., "Final Report, Research Program on High Vacuum
Friction", Hdq. Air Research and Development Command,
Contract No. AF 49(638)-343, Office of Scientific Research,
1959.
38. Hennes, R.G., "The Strength of Gravel in Direct Shear",
Symposium on Direct Shear Testing of Soils, A.S.T.M., 1953.
39. Holm, R., Electric Contacts, Part II, Almqvist and Wiksells,
Uppsala, 1946.
40. Holtz, W.G. and Gibbs, H.J., "Triaxial Tests on Previous
Gravelly Soils", Proc. Am. Soc. Civil Engineers, 82:SM1,
Paper 867, Jan. 1956.
41. Horn, H.M. and Deere, D.U., "Frictional Characteristics of
Minerals", Geotechnique, XII:4, 319, 1962.
42. Hoyt, S.L., Metals and Alloys Data Book, Reinhold, 1943.
43. Idel, K.H., "Die Scherfestigkeit rolliger Erdstoffe",
Veröffentlichungen des Inst. für Bodenmechanik und Grundbau,
Technischen Hochschule Fridericiana, Heft 2, Karlsruhe, 1960.
44. Jahn, A., "Erfahrungen und Beobachtungen beim Rüttelunterbau",
Strasse und Autobahn, IX, 3, 87, 1958.
45. Jakobson, B., "Some Fundamental Properties of Sand", Proc.
4th Int. Conf. on Soil Mech. and Found. Eng., 167, London,
1957.

46. Jenny, H., Factors of Soil Formation, McGraw-Hill, 1941.
47. Karol, R.H., Soils and Soil Engineering, Prentice-Hall, 1960.
48. Kjellman, W. and Jakobson, B., "Some Relations Between Stress and Strain in Coarse Grained Cohesionless Materials", Proc. Royal Swedish Geotechnical Institute, No. 9, Stockholm, 1955.
49. Kolbuszewski, J.J., "An Experimental Study of the Maximum and Minimum Porosities of Sands", Proc. 2nd Int. Conf. on Soil Mech. and Found. Eng., 1, 158, Rotterdam, 1948.
50. Kuiper, G.P., "The Surface Structure and the History of the Moon", Lecture Space Technology Laboratories, 1, 9, Redondo Beach, California, 1961.
51. Lambe, T.W., Soil Testing for Engineers, Wiley, 1951.
52. Leonards, G.A., "Engineering Properties of Soils", Foundation Engineering, Edited by G.A. Leonards, Chapter 2, McGraw-Hill, 1962.
53. Leussink, H. and Kutzner, C., "Laboratoriumsversuch zur Feststellung der dichtesten Lagerung korniger Erdstoffe", Veröffentlichungen des Inst. für Bodenmechanik und Grundbau, Technischen Hochschule Fridericiana, Heft 8, Karlsruhe, 1962.
54. Markov, A.V., "The Moon- A Russian View", Univ. Chicago Press, 1962.
55. Muurinen, E., Theoretical and Practical Aspects of the Workability of Granular Mixtures, Master's Thesis, Princeton University, 1961.
56. Opik, E.J., "Surface Properties of the Moon", Progress in the Astronautical Sciences, Edited by S.F. Singer, 1, Chapter 5, North-Holland, 1962.
57. Parsons, J.D., "Progress Report on an Investigation of the Shearing Resistance of Cohesionless Soils", Proc. Int. Conf. on Soil Mech. and Found. Eng., II, 133, Harvard, 1936.
58. Penman, A.D.M., "Shear Characteristics of a Saturated Silt Measured in Triaxial Compression", Geotechnique, III:8, 312, 1953.
59. Pirani, M. and Yarwood, J., Principles of Vacuum Engineering, Reinhold, 1961.
60. Rowe, G.W., "Vapour Lubrication and the Friction of Clean Surfaces", Proc. Conf. Lubrication and Wear, Institution of Mechanical Engineers, Paper No. 5, London, 1957.

61. Rowe, P.W., "The Stress- Dilatancy Relation for Static Equilibrium of an Assembly of Particles in Contact", Proc. Royal Soc., A269; 500, 1962.
62. Rowe, R.D. and Selig, E.T., "Penetration Studies of Simulated Lunar Dust", Armour Research Foundation, Chicago, Ill., 1962.
63. Ryan, J.A., "Some Predictions as to the Possible Nature and Behavior of Lunar Soils", Includ. Discussion, Proc. 1st Int. Conf. on the Mechanics of Soil-Vehicle Systems, Turin, Italy, 1961.
64. Salisbury, J.W., "The Lunar Environment", Space and Planetary Environments, Edited by S.L. Valley, Air Force Surveys in Geophysics No. 139, AFCRL, U.S. Air Force, Bedford, Mass., 1962.
65. Salisbury, J.W. and Campden, C.F. Jr., "Location of a Lunar Base", GRD Research Notes No. 70, AFCRL, U.S. Air Force, Bedford, Mass., 1961.
66. Salisbury, J.W. and Van Tassel, R.A., "State of the Lunar Dust", Pub. Ast. Soc. of the Pacific, 74:438, 245, 1962.
67. Santeler, D., "Vacuum Technology", International Science and Technology, 13, 46, 1963.
68. Scott, R.F., Principles of Soil Mechanics, Chapter 7, Addison-Wesley, 1963.
69. Sharonov, V.V., "Microrelief of the Lunar Surface and the Probable Ways of its Formation", The Moon, Symposium 14, IAU, Leningrad, 1960, Edited by Z. Kopal, 385, Academic Press, 1962.
70. Shaw, P.E. and Leavey, E.W.L., "Friction of Dry Solids in Vacuo", Phil. Mag., 7:10:66, 809, 1930.
71. Shockley, W.G. and Garber, P.K., "Correlation of Some Physical Properties of Sand", Proc. 3rd Int. Conf. on Soil Mech. and Found. Eng., 1, 203, Zurich, 1953.
72. Shoemaker, E.M., "Exploration of the Moon's Surface", American Scientist, 50:1, 99, 1962.
73. Siedek, P. and Voss, R., "Uber die Lagerungsdichte und den Verformungswiderstand von Korngemischen", Strasse und Autobahn, VI, 8, 273, 1955.
74. Smith, W.O., Foote, P.D. and Busang, P.F., "Packing of Homogeneous Spheres", Phys. Rev., 34:9, 1271, 1929.
75. Smithells, C.J., Metals Reference Book, Volume II, Butterworth, 1962.

76. Spencer, E., "The Relationship between Porosity and Angle of Internal Friction", Discussion, Proc. 5th Int. Conf. on Soil Mech. and Found. Eng., 111, 138, Paris, 1961.
77. Taylor, D.W., Fundamentals of Soil Mechanics, Wiley, 1948.
78. Thurston, C.W. and Deresiewicz, H., "Analysis of a Compression Test of a Model of a Granular Medium", J. of Applied Mechanics, Trans. A.S.M.E., 81:(3), 251, 1959.
79. Tschebotarioff, G.P. and Welch, J.D., "Lateral Earth Pressures and Friction Between Soil Minerals", Proc. 2nd Int. Conf. on Soil Mech. and Found. Eng., 1, 135, Rotterdam, 1948.
80. Van Hook, A., Crystallization, Theory and Practice, 139-145, Reinhold, 1961.
81. Wallis, W.A. and Roberts, H.V., Statistics- A New Approach, Section 8.5, Free Press, 1956.
82. Wehner, G.K., "Sputtering Effects on the Moon's Surface", J. Am. Rocket Soc., 31:3, 438, 1960.
83. Weil, N.A., "Probable Soil Conditions on the Moon and Terrestrial Planets", Includ. Discussion, Proc. 1st Int. Conf. on the Mechanics of Soil-Vehicle Systems, Turin, Italy, 1961.
84. Weiser, H.B., A Textbook of Colloid Chemistry, 2nd Ed., Chapter 5, Wiley, 1949.
85. Whipple, F.L., "On the Lunar Dust Layer", Vistas in Astro-nautics, II, 267, Pergamon, 1959.
86. Whitehead, J.R., "Surface Deformation and Friction of Metals at Light Loads", Proc. Royal Soc., A201, 109, 1950.
87. Wikramaratna, P.H.D.S., Discussion on Reference 19, Proc. 5th Int. Conf. on Soil Mech. and Found. Eng., III, 150, Paris.
88. Winterkorn, H.F., "Macromeritic Liquids", Symposium on Dynamic Testing of Soils, Am. Soc. for Testing Materials, 1953.
89. Winterkorn, H.F., The Scientific Foundations of Soil Engineering, Unpublished manuscript, XXX, 1960.
90. Winterkorn, H.F., "Soil Stabilization Methods and Techniques With a View Toward Lunar Soil Stabilization", Unpublished Reports, 1961-1962.

91. Winterkorn, H.F. and Johnson, R.W., "Consideration of Properties of Simulated Lunar Soil with Possible Stabilization Techniques", Proc. Lunar Surface Materials Conference, Air Force Cambridge Research Laboratories and Arthur D. Little, Inc., Boston, 1963.
92. Wittke, W., "Über die Scherfestigkeit, Rolliger, Erdstoffe", Veröffentlichungen des Inst. für Bodenmechanik und Grundbau, Heft II, Karlsruhe, 1962.
93. Wu, T.H., "Relative Density and Shear Strength of Sands", Includ. Discussion, Proc. Am. Soc. of Civil Engineers, 83:SM1, Paper 1161, Jan. 1957.
94. Zeller, J. and Wullimann, R., "The Shear Strength of Materials for the Goschenalp Dam, Switzerland, Proc. 4th Int. Conf. on Soil Mech. and Found. Eng., II, 399, London, 1957.

**THE EFFECT OF VACUUM ON
THE SHEARING RESISTANCE
OF IDEAL GRANULAR SYSTEMS**

by

**Gerald D. Sjaastad
Captain,
United States Air Force**

ABSTRACT

Recognizing the need for basic data to aid in the prediction of the possible behavior of lunar surface materials and to further understand terrestrial soils an experimental research project has been initiated in the Department of Civil Engineering at Princeton University.

Making a minimum number of assumptions concerning the nature of the lunar soil this study uses an ideal granular system as a laboratory model. This reduces the indeterminacy of the problem and allows the investigator to concentrate on the factors of immediate concern. Further, any results will apply, in a qualitative manner at least, to a wider variety of possible lunar and terrestrial soils. The vacuum effect on the shearing resistance of an ideal granular soil is chosen as the factor involving the lunar problem which is of most interest to and best studied by the civil engineer. The decrease in thickness of adsorbed surface films and the ensuing increase in interparticle friction is cited as the reason for expecting a change in shear strength with atmospheric pressure.

Several analytic solutions are reviewed and a new solution is presented relating the shearing resistance of an ideal granular system to the coefficient of friction between its individual particles. Existing data on idealized systems are reviewed and compared with the various solutions.

A review of existing data on the effects of grain size and grain size distribution on the shearing resistance of granular soils is presented. Additional data on these factors are given.

Apparatus, tests and test results for the determination of shearing resistance and coefficient of friction under high vacuum conditions are discussed.

The major conclusion is that the shearing resistance of an ideal granular soil increases with very low atmospheric pressure in a more or less predictable manner. The independence of shear strength from particle size is reaffirmed. The effects of soil cohesion, gradation, porosity and particle shape are anticipated in a general way, especially as they may bear on the lunar surface materials problem.

UNCLASSIFIED

UNCLASSIFIED